

UNIVERSIDADE FEDERAL DE MINAS GERAIS
INSTITUTO DE CIÊNCIAS BIOLÓGICAS
DEPARTAMENTO DE BIOLOGIA GERAL
PROGRAMA DE PÓS-GRADUAÇÃO EM GENÉTICA



TESE DE DOUTORADO

**Caracterização funcional de genes *PSTOL1* na
modulação do sistema radicular em milho e sorgo**

ORIENTADA: LAIANE SILVA MACIEL

ORIENTADOR: Dr. JURANDIR VIEIRA DE MAGALHÃES

BELO HORIZONTE

MARÇO – 2019

LAIANE SILVA MACIEL

**Caracterização funcional de genes *PSTOL1* na
modulação do sistema radicular em milho e sorgo**

Tese apresentada à Universidade Federal de Minas Gerais, como parte das exigências do Programa de Pós-Graduação em Genética, para obtenção do título de Doutora em Genética.

Orientador: Jurandir Vieira de Magalhães

BELO HORIZONTE

MARÇO – 2019

043 Maciel, Laiane Silva.

Caracterização funcional de genes *PSTOL1* na modulação do sistema radicular em milho e sorgo [manuscrito] / Laiane Silva Maciel. - 2019.

104 f. : il. ; 29,5 cm.

Orientador: Jurandir Vieira de Magalhães.

Tese (doutorado) - Universidade Federal de Minas Gerais, Instituto de Ciências Biológicas. Programa de Pós-Graduação em Genética.

1. Genética. 2. Raízes de Plantas - Morfologia. 3. Proteínas Serina-Treonina Quinases. 4. Fósforo. 5. Genes *PSTOL1-like*. I. Magalhães, Jurandir Vieira de. II. Universidade Federal de Minas Gerais. Instituto de Ciências Biológicas. III. Título.

CDU: 575

**"Caracterização funcional dos genes PSTOL1 envolvidos na
modulação do sistema radicular em milho e sorgo"**

Laiane Silva Mael

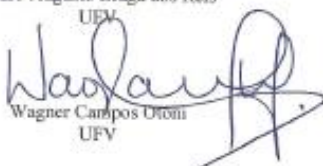
Tese aprovada pela banca examinadora constituída pelos Professores:


Jurandir Vieira de Magalhães - Orientador
EMBRAPA


Cláudia Teixeira Guimarães
EMBRAPA


Sylvia Moraes de Sousa Tinoco
EMBRAPA


Pedro Augusto Braga dos Reis
UEV


Wagner Campos Utom
UPV

Belo Horizonte, 29 de março de 2019.

Dedico este trabalho aos meus pais pelo exemplo de resistência e resiliência. Ao meu irmão pela amizade e cumplicidade. Ao meu parceiro de vida André pela dedicação e perseverança. Aos quatro pelo amor e incentivo pela busca ao conhecimento.

AGRADECIMENTOS

À Deus por sempre iluminar o meu caminho.

Ao programa de Pós-Graduação em Genética da UFMG pela oportunidade.

Ao Conselho Nacional de Desenvolvimento Científico e Tecnológico (CNPq) pela concessão da bolsa de estudos.

A Fundação de Amparo à Pesquisa do Estado de Minas Gerais (FAPEMIG) pelo apoio financeiro.

A Embrapa Milho e Sorgo pelo suporte científico e financeiro.

Ao meu orientador, Dr. Jurandir Vieira de Magalhães, pela oportunidade, incentivo e confiança depositada no meu trabalho. Muito obrigada por todas as contribuições durante esses quatro anos de convivência que proporcionaram a minha evolução profissional.

À Dra. Beatriz de Almeida Barros por todo apoio científico e participação efetiva na discussão dos experimentos conduzidos neste trabalho.

À Dra. Cláudia Teixeira Guimarães, Dra. Sylvia Morais de Sousa Tinoco, e a Bárbara França Negri pela parceria e apoio científico na construção do segundo capítulo.

À Karine Bernardino Costa e Vanessa de Almeida Barros pela valiosa ajuda durante a condução dos experimentos do terceiro capítulo.

À Dra. Andrea de Almeida Carneiro, Meire de Cássia Alves e a todos os amigos do Laboratório de Cultura de Tecidos pela ajuda constante na condução dos experimentos, e pela convivência agradável durante esses quatro anos.

Aos amigos do Laboratório de Biologia Molecular e aos amigos do Laboratório de Bioinformática, meu muito obrigada! Agradeço pelo companheirismo, paciência e por todos os momentos de descontração que tornaram essa caminhada mais leve e feliz.

Aos funcionários da Embrapa Milho e Sorgo por todo o apoio técnico no laboratório e na condução dos experimentos em casa de vegetação. Em especial à Gislene, Miguel, Célio, José Neto e Geraldo. Muito obrigada por todos os ensinamentos e experiências compartilhadas.

A todos os meus familiares por sempre incentivarem a minha busca pelo conhecimento. Em especial aos meus pais, Nelma e Geraldo, e ao meu irmão, Davisson, por sempre me acolherem e festejarem com orgulho as minhas conquistas.

Ao meu querido companheiro André, por todo o amor, pelo exemplo de perseverança e pela disponibilidade em compartilhar a vida comigo!

A todos aqueles que contribuíram para minha evolução profissional e pessoal nesses quatro anos de curso.

Muito obrigada!

“Ninguém é suficientemente perfeito, que não possa aprender com o outro e, ninguém é totalmente destituído de valores que não possa ensinar algo ao seu irmão.”

São Francisco de Assis

SUMÁRIO

LISTA DE TABELAS	X
LISTA DE FIGURAS	xi
RESUMO	13
DELINEAMENTO DA TESE	15
CAPÍTULO 1	16
Emerging Pleiotropic Mechanisms Underlying Aluminum Resistance and Phosphorus Acquisition on Acidic Soils	16
INTRODUCTION	18
OVERVIEW OF POSSIBLE PLEIOTROPIC MECHANISMS CONTROLLING BOTH AI RESISTANCE AND ROOT TRAITS THAT MAY LEAD TO ENHANCED PHOSPHORUS ACQUISITION UNDER LOW P CONDITIONS	19
POSSIBLE PLEIOTROPIC EFFECTS UNDERLYING AI RESISTANCE AND P ACQUISITION EFFICIENCY	21
CONCLUSION	24
REFERENCES	25
OBJETIVOS.....	29
Objetivo Geral	29
Objetivos Específicos.....	29
CAPÍTULO 2	30
Overexpression of <i>PSTOL1-like</i> genes increases root surface area and biomass accumulation for maize cultivated under low P availability	30
ABSTRACT.....	31
INTRODUCTION	32
MATERIALS AND METHODS	33
Maize transformation via <i>Agrobacterium tumefaciens</i> with rice, maize and sorghum <i>PSTOL1</i>	33
Phenotypic assessment of root morphology in hydroponics	34
Expression analysis of <i>PSTOL1</i> genes under low-P	35
Phenotypic assessment of maize biomass accumulation and plant height under low and high P concentrations in the soil	35
Statistical analyses	36
RESULTS.....	36
Root morphology of non-transgenic lines	36
Selection of transgenics events	37
Phenotypic characterization of maize events overexpressing <i>PSTOL1</i> for root morphology in nutrient solution with low-P.....	37

Overexpression of <i>PSTOL1</i> genes increases shoot dry matter accumulation in a low P soil...	38
DISCUSSION	39
SUPPLEMENTARY DATA	41
ACKNOWLEDGEMENTS	41
REFERENCE	42
TABLE	46
FIGURE LEGENDS.....	49
FIGURES.....	51
CAPÍTULO 3	56
O envolvimento de <i>Phosphorus Starvation Tolerance 1</i> sobre a morfologia do sistema radicular em sorgo	56
INTRODUÇÃO	57
MATERIAIS E MÉTODOS	60
Análise Filogenética.....	60
Estabelecimento da estrutura gênica dos genes <i>SbPSTOL1</i>	60
Amplificação da região 5'UTR.....	60
Análise <i>in silico</i> dos elementos <i>cis</i> regulatórios.....	61
Isolamento e clonagem da região promotora	61
Transformação de milho	62
Teste histoquímico do <i>GUS</i>	62
Análise da morfologia de raiz, acúmulo de biomassa e conteúdo de P em sistema de hidroponia em condições de baixo e alto P.....	62
Perfil de expressão dos genes <i>SbPSTOL1</i>	63
Localização subcelular	63
Análises estatísticas.....	64
RESULTADOS E DISCUSSÃO	65
As proteínas <i>SbPSTOL1</i> são RLKs/ <i>Pelle</i> membros da subfamília LRK10L-2	65
Confirmação dos modelos gênicos dos genes <i>SbPSTOL1</i>	66
Caracterização da região promotora.....	67
Caracterização fenotípica das linhagens de sorgo contrastantes para morfologia radicular em solução nutritiva com baixo e alto P	69
Perfil de expressão dos genes <i>SbPSTOL1</i>	69
Localização subcelular das proteínas <i>OsPSTOL1</i> e <i>SbPSTOL1</i>	70
REFERÊNCIAS.....	71
Tabelas	76
LEGENDAS DAS FIGURAS	79
CONCLUSÃO GERAL E PERSPECTIVAS FUTURAS	88

ANEXO.....	89
------------	----

LISTA DE TABELAS

Capítulo 2

Table 1: Analysis of variance for three quantitative traits of transgenic maize grown in greenhouse conditions with low and high P.....	46
Supplemental Table S1: Primers used for PCR and RT-qPCR assays.....	47
Supplemental Table S2: Description of maize transgenic events overexpressing <i>OsPSTOL1</i> , <i>SbPSTOL1</i> and <i>ZmPSTOL1</i> genes	48

Capítulo 3

Tabela 1: Lista de oligonucleotídeos utilizados nesse trabalho	77
Tabela 2 Análise <i>in silico</i> de putativos elementos <i>cis</i> regulatórios na região promotora dos genes <i>PSTOL1</i> preditos no <i>software MatInspector</i>	78
Tabela 3: Análise de variância (ANOVA) para características avaliadas em sorgo cultivado em sistema hidropônico com baixa e alta disponibilidade de P.....	79

LISTA DE FIGURAS

Capítulo 1

Figure 1: Structure and possible function of WAK, WAKL, and LRK10 members of the RLKs/Pelle superfamily..... 24

Capítulo 2

Figure 1: Phenotypic characterization of non-transgenic maize lines in low P conditions 52

Figure 2: Schematic structure of pMCG1005-*PSTOLI* cassette 53

Figure 3: Correlation analysis of root morphology traits, shoot dry weight and shoot P content traits and *PSTOLI* expression (ΔCt)..... 54

Figure 4: Phenotypic characterization of wild type B104 and transgenic lines *PSTOLI* (*OsPSTOLI*, *SbPSTOLI* and *ZmPSTOLI*) in nutrient solution with low-P 55

Figure 5: Phenotypic characterization of wild type B104 and transgenic lines *PSTOLI* (*OsPSTOLI*, *SbPSTOLI* and *ZmPSTOLI*) grown in a low P soil 56

Capítulo 3

Figura 1: Análise filogenética de proteínas da superfamília RLKs/*Pelle* 82

Figura 2: Comparação entre os modelos gênicos dos genes *SbPSTOLI* na versão 1.4 e 3.1.1 do genoma de sorgo..... 83

Figura 3: Análise *in silico* da distribuição dos possíveis elementos *cis* regulatórios na região promotora dos genes *OsPSTOLI*, *Sb07g002840*, *Sb03g031690* e *Sb03g006765*..... 84

Figura 4: Promotor pSb03g031690 direciona a expressão do gene *GUS* para as raízes laterais. 85

Figura 5: Caracterização fenotípica dos genótipos de sorgo SC103, BTx399, BTx635 e BTx623..... 86

Figura 6: Perfil de expressão dos genes *SbPSTOL1*..... 87

Figura 7: Localização subcelular das proteínas OsPSTOL1, Sb07g002840, Sb03g031690 e Sb03g006765 fusionadas a eGFP em células epidérmicas de *N. benthamiana* 88

RESUMO

A superfamília das proteínas *Receptor-like kinases* (RLKs/*Pelle*) é um grupo monofilético, cujos membros desempenham funções essenciais durante o desenvolvimento celular e na ativação de vias de sinalização em resposta a estímulos ambientais. Os genes *Phosphorus Starvation Tolerance 1* (PSTOL1) codificam proteínas serina/treonina quinase. Em arroz (*Oryza sativa*), a proteína OsPSTOL1 está relacionada ao crescimento inicial de raízes e à aquisição de fósforo (P). Genes homólogos ao gene *OsPSTOL1* em sorgo (*Sorghum bicolor*, *SbPSTOL1*) e em milho (*Zea mays*, *ZmPSTOL1*) foram associados, via mapeamento de QTL e mapeamento associativo, à modulação da morfologia e arquitetura do sistema radicular. Além disso, os genes *SbPSTOL1* também foram associados com aumento na aquisição de P e rendimento de grãos sob baixo P. Neste estudo, a superexpressão dos genes *OsPSTOL1*, *SbPSTOL1* e *ZmPSTOL1* em milho foi utilizada para avaliar o efeito desses genes na modulação do sistema radicular e no acúmulo de biomassa em solo tropicais com baixa disponibilidade de P. Demonstrou-se que a superexpressão dos genes *OsPSTOL1* e *SbPSTOL1*, sob o controle do promotor constitutivo ubiquitina, resulta no aumento da proliferação das raízes finas e aumento da biomassa da parte aérea de milho cultivado em solo com baixa disponibilidade de P. Eventos transgênicos de milho com superexpressão dos genes *ZmPSTOL1* não apresentaram diferenças significativas, para o acúmulo de biomassa da parte aérea, quando comparados ao controle não-transgênico. Uma análise filogenética indicou que as proteínas OsPSTOL1 e SbPSTOL1 são membros da subfamília LRK10L-2 e, portanto, provavelmente compartilham um ancestral comum. Em sorgo a expressão dos genes *Sb07g002840*, *Sb03g031690* e *Sb03g006765* é maior nas raízes do que na parte aérea. Resultados preliminares indicam que a região promotora do gene *SbPSTOL1*, *Sb03g031690*, direciona a expressão gênica para raízes laterais. Além disso, estudos de localização subcelular em folhas de *Nicotiana benthamiana* sugerem que as proteínas *Sb07g002840*, *Sb03g031690* e *Sb03g006765* podem associar-se a membrana plasmática e, possivelmente, atuarem como proteínas receptoras para estímulos extracelulares. Assim, o presente trabalho fornece informações iniciais para a compreensão dos mecanismos moleculares controlados pelas proteínas *Sb07g002840*, *Sb03g031690* e *Sb03g006765* em sorgo. O trabalho também demonstra que os genes *OsPSTOL1*, *Sb07g002840*, *Sb03g031690* e *Sb03g006765* modulam a morfologia do sistema radicular, que leva ao aumento no acúmulo de biomassa sob condições limitantes de P no solo. Assim, os resultados sugerem que os genes *PSTOL1* podem ser utilizados para aumentar a produção vegetal sob baixa disponibilidade de fósforo no solo.

Palavras-chaves: Aquisição de P, proteína quinase, morfologia do sistema radicular, genes *PSTOL1-like*

ABSTRACT

The RLKs / *Pelle* superfamily is a monophyletic group and its members play key roles during cellular development and in the activation of signaling pathways in response to environmental stimuli. *Phosphorus Starvation Tolerance 1 (PSTOL1)* genes encode serine/threonine kinase proteins. In rice, *Oryza sativa*, OsPSTOL1 is linked to enhanced early root growth and phosphorus (P) acquisition. Homologs of OsPSTOL1 in sorghum (*Sorghum bicolor*, *SbPSTOL1*) and maize (*Zea mays*, *ZmPSTOL1*) were implicated via QTL and association mapping in the modulation of root system morphology and architecture. In addition, *SbPSTOL1* genes were also associated with increased P acquisition and grain yield under low P. In the present study, overexpression *OsPSTOL1*, *SbPSTOL1* e *ZmPSTOL1* in maize was used to assess the effect of these genes on root system modulation and biomass accumulation in a tropical soil with low P availability. We demonstrate that ubiquitin-driven overexpression of *OsPSTOL1* and *SbPSTOL1* results in enhanced proliferation of fine roots and increased shoot biomass for maize cultivated in a soil with low P availability. Maize transgenic events harboring *ZmPSTOL1* did not show significant differences to the non-transgenic, B104, control for shoot biomass accumulation. Phylogenetic analysis supports that OsPSTOL1 and SbPSTOL1 are members of the LRK10L-2 subfamily and thereby are likely to share a common ancestry. In sorghum *Sb07g002840*, *Sb03g031690* and *Sb03g006765* are more highly expressed in the roots compared to the shoot. So far, we have been able to verify that the promoter region of the *SbPSTOL1* gene, *Sb03g031690*, drives gene expression to lateral roots. Moreover, sub-celular localization studies in *Nicotiana benthamiana* leaves suggest that *Sb07g002840*, *Sb03g031690*, and *Sb03g006765* are localized to the plasma membrane and could act as receptor proteins for extracellular stimuli. Thus, the present work provides initial information for understanding the molecular mechanisms controlled by *Sb07g002840*, *Sb03g031690* e *Sb03g006765* in sorghum. The work also demonstrates that the genes *OsPSTOL1* and *Sb07g002840*, *Sb03g031690* e *Sb03g006765* modulate root, which leads to increased biomass accumulation under low P availability in the soil. Therefore, PSTOL1 genes emerge as potential tools to increase crop yields under low P availability in the soil.

Keywords: Phosphorus acquisition, protein kinase, root system morphology, *PSTOL1-Like* genes

DELINEAMENTO DA TESE

Esta dissertação é constituída por três capítulos, seguidos por uma conclusão geral e perspectivas futuras, e um artigo publicado como co-autora em anexo. A dissertação está subdividida da seguinte maneira:

Resumo e Abstract

Capítulo 1: Corresponde ao artigo científico de revisão intitulado “Emerging Pleiotropic Mechanisms Underlying Aluminum Resistance and Phosphorus Acquisition on Acidic Soils”, e publicado na revista *Frontiers in Plant Science* (2018), com a minha co-autoria. Como o artigo contém uma revisão detalhada sobre temas relevantes da tese, ele será utilizado como o referencial teórico da tese.

Objetivo geral e objetivos específicos

Capítulo 2: Corresponde a um artigo científico que será submetido na revista *Journal of Experimental Botany*: “Overexpression of *PSTOL1*-like genes increases root surface area and biomass accumulation for maize cultivated under low P availability”.

Capítulo 3: Corresponde aos trabalhos conduzidos durante o doutorado que ainda estão em desenvolvimento, intitulado: “O envolvimento de *Phosphorus Starvation Tolerance 1* sobre a morfologia do sistema radicular em sorgo”.

Conclusão Geral e Perspectivas Futuras

Anexo, que contém o artigo científico de co-autoria publicado na revista *BMC Plant Biology* intitulado: “The genetic architecture of phosphorus efficiency in sorghum involves pleiotropic QTL for root morphology and grain yield under low phosphorus availability in the soil”.

CAPÍTULO 1

Emerging Pleiotropic Mechanisms Underlying Aluminum Resistance and Phosphorus Acquisition on Acidic Soils



Emerging Pleiotropic Mechanisms Underlying Aluminum Resistance and Phosphorus Acquisition on Acidic Soils

Jurandir V. Magalhaes^{1,2*}, Miguel A. Piñeros^{3*}, **Laiane S. Maciel**^{1,2} and Leon V. Kochian⁴

¹ Embrapa Maize and Sorghum, Sete Lagoas, Brazil, ² Departamento de Biologia Geral, Universidade Federal de Minas Gerais, Belo Horizonte, Brazil, ³ Robert W. Holley Center for Agriculture and Health, USDA-ARS, Cornell University, Ithaca, NY, United States, ⁴ Global Institute for Food Security, University of Saskatchewan, Saskatoon, SK, Canada

OPEN ACCESS

Edited by:
Peter Ryan,

Commonwealth Scientific
and Industrial Research Organisation
(CSIRO), Australia

Reviewed by:

Takayuki Sasaki,
Okayama University, Japan
Manny Delhaize,
Plant Industry (CSIRO), Australia

*Correspondence:

Jurandir V. Magalhaes
jurandir.magalhaes@embrapa.br
Miguel A. Piñeros
map25@cornell.edu

Specialty section:

This article was submitted to
Plant Abiotic Stress,
a section of the journal
Frontiers in Plant Science

Received: 01 March 2018

Accepted: 06 September 2018

Published: 26 September 2018

Citation:

Magalhaes JV, Piñeros MA, Maciel LS
and Kochian LV (2018) Emerging
Pleiotropic Mechanisms Underlying
Aluminum Resistance
and Phosphorus Acquisition on Acidic
Soils. *Front. Plant Sci.* 9:1420.
doi:10.3389/fpls.2018.01420

Aluminum (Al) toxicity on acidic soils significantly damages plant roots and inhibits root growth. Hence, crops intoxicated by Al become more sensitive to drought stress and mineral nutrient deficiencies, particularly phosphorus (P) deficiency, which is highly unavailable on tropical soils. Advances in our understanding of the physiological and genetic mechanisms that govern plant Al resistance have led to the identification of Al resistance genes, both in model systems and in crop species. It has long been known that Al resistance has a beneficial effect on crop adaptation to acidic soils. This positive effect happens because the root systems of Al resistant plants show better development in the presence of soil ionic Al³⁺ and are, consequently, more efficient in absorbing sub-soil water and mineral nutrients. This effect of Al resistance on crop production, by itself, warrants intensified efforts to develop and implement, on a breeding scale, modern selection strategies to profit from the knowledge of the molecular determinants of plant Al resistance. Recent studies now suggest that Al resistance can exert pleiotropic effects on P acquisition, potentially expanding the role of Al resistance on crop adaptation to acidic soils. This appears to occur *via* both organic acid (OA)- and non-OA transporters governing a joint, iron-dependent interplay between Al resistance and enhanced P uptake, *via* changes in root system architecture. Current research suggests this interplay to be part of a P stress response, suggesting that this mechanism could have evolved in crop species to improve adaptation to acidic soils. Should this pleiotropism prove functional in crop species grown on acidic soils, molecular breeding based on Al resistance genes may have a much broader impact on crop performance than previously anticipated. To explore this possibility, here we review the components of this putative effect of Al resistance genes on P stress responses and P nutrition to provide the foundation necessary to discuss the recent evidence suggesting pleiotropy as a genetic linkage between Al resistance and P efficiency. We conclude by exploring what may be needed to enhance the utilization of Al resistance genes to improve crop production on acidic soils.

Keywords: abiotic stress resistance, transporters, plant breeding, pleiotropy, aluminum tolerance, phosphorus acquisition, phosphorus efficiency

INTRODUCTION

Acidic soils are globally widespread, extending to more than half of the world arable lands (von Uexküll and Mutert, 1995). These low-pH soils, which are commonly found in tropical and subtropical regions, include areas where food production needs to be increased to cope with a continuously growing population (Godfray et al., 2010). For example, there have been a number of studies in the literature addressing the extent of Al-toxic acidic soils in Africa, with approximately 25% of the soils being highly acidic (FAO and ITPS, 2015; Tully et al., 2015). Two of the major constraints for crop production on acidic soils, including those in Sub-Saharan Africa (Doumbia et al., 1993, 1998), are aluminum (Al) toxicity and low phosphorus (P) availability.

Aluminum and iron (Fe) oxides, which are enriched in the clay fraction of acidic soils upon intensive weathering of primary minerals (Shaw, 2001), drive both types of abiotic stresses, causing a general coincidental occurrence of Al toxicity and low P availability on tropical soils (Sanches and Salinas, 1981). Phosphorus forms strong, covalent bonds with these oxides, becoming highly unavailable for uptake by the plants (Marschner, 1995; Lynch, 2011), due to restricted P diffusive fluxes from the soil toward the root surface. In addition, P diffusion on highly weathered soils is highly dependent on the soil water content (Novais and Smith, 1999), which varies during the crop season, making P supply to the plant and, consequently, P uptake, highly discontinuous. Under low pH, Al present in aluminosilicates and oxides is released as the rhizotoxic Al^{3+} ion into the soil solution, damaging the root system and inhibiting root growth (Delhaize and Ryan, 1995).

Aluminum resistance has long been associated with overall crop adaptation to acidic soils by indirectly enhancing mineral nutrient uptake and drought resistance (Foy et al., 1993). Accordingly, undamaged, “Al resistant” root systems are more effective in absorbing sub-soil water, and nutrients, particularly those that are highly unavailable on acidic soils, such as P. It is important to note that Al toxicity typically extends to sub-soil layers, where liming is highly ineffective in increasing soil pH, enhancing the deleterious effects of drought stress in reducing crop yields.

The widespread nature of Al toxicity and its global impact has spurred extensive research on the physiological, genetic, and molecular mechanisms that enable crops to withstand Al toxicity on acidic soils. Clearly, impressive progress has been made in the last two decades on the molecular underpinnings of crop Al resistance (reviewed by Kochian et al., 2015). These discoveries led to the isolation of a number of the previously anonymous molecular determinants of Al resistance in loci that had been identified previously *via* genetic mapping in crops such as wheat, barley, rye, sorghum, and maize, as well as in model systems such as *Arabidopsis thaliana*.

It is reasonable to expect that the identification of the molecular drivers of plant Al resistance can be instrumental in the development of novel strategies for improving crop performance

on acidic soils in a more efficient way. Marker-assisted backcross to improve Al resistance based on single major loci has been a feasible approach long before major Al resistance genes were cloned. Beyond that, these genes now offer opportunities for large scale germplasm screening approaches based on functional markers, which can streamline the utilization of large germplasm banks in favor of plant breeding (Tanksley and McCouch, 1997; Hufnagel et al., 2018). Most importantly, it is possible that the value of Al resistance for crop production in the context of the multiple stress scenario on acidic soil regions (Bahia Filho et al., 1997) has been somewhat underappreciated. Some possible reasons for that are the lack of systematic efforts to map Al saturation both in the surface and below ground soils and a rather incomplete quantification of the grain yield effect of known Al resistance genes *in soil*, which is to some extent understandable due to the highly complex chemical nature of acidic soils.

There is now an interesting body of emerging evidence suggesting that Al resistance genes may have an additional, pleiotropic effect on acidic soils, which involves enhancement of P acquisition. In conjunction with the known effect of Al resistance in enhancing water and mineral uptake, by promoting better root growth on acidic soils, this would further justify deliberate efforts to design novel, gene-based molecular breeding strategies aimed at developing cultivars adapted to acidic soil regions. These strategies can help in realizing the great potential there is in expanding the world’s agricultural frontier, by exploring the vast areas under acidic soils in the tropics and subtropics, which show in general a favorable topography for agriculture (Sanches and Salinas, 1981).

Here, our objective is not to review the current available information on plant Al resistance or P efficiency, which is defined here as improved performance in soils with low P availability. For that, readers are directed to many available comprehensive reviews (Delhaize and Ryan, 1995; Kochian, 1995; Ma et al., 2001; Kochian et al., 2004; Delhaize et al., 2007, 2012; López-Arredondo et al., 2014; Eekhout et al., 2017). Our goal here is to explore the emerging connections between Al resistance genes and P deficiency responses that help maintain favorable P nutrition, which happens possibly *via* alterations in root system architecture. We recognize these studies are just emerging and are still found largely in the realm of model species, in this case, *Arabidopsis*. This makes some of the crop-related implications drawn in this paper somewhat speculative in nature. However, due to the efficacy and breeding potential of common mechanisms underlying two important abiotic stress factors on acidic soils, taking advantage of the convergence of Al resistance and P efficiency *via* pleiotropic genes could have a significant impact in enhancing global food security. In the next section, we will briefly review the components comprising mechanisms that might jointly control Al resistance and P nutrition. We will then explore the emerging, underlying basis for such pleiotropy and will close with a brief discussion of the future directions to further explore Al resistance genes as tools to improve P acquisition and crop performance on acidic soils.

OVERVIEW OF POSSIBLE PLEIOTROPIC MECHANISMS CONTROLLING BOTH AL RESISTANCE AND ROOT TRAITS THAT MAY LEAD TO ENHANCED PHOSPHORUS ACQUISITION UNDER LOW P CONDITIONS

Physiological Basis

The ability of a plant to tolerate low P availability in the soil may be achieved both by internal mechanisms, acting to optimize the way plants internally utilize phosphorus, and by mechanisms to improve phosphorus acquisition from the soil. Mendes et al. (2014) genetically assessed the contribution of those mechanisms in maize grown on a tropical soil with low P availability and found that 80% of the QTLs mapped for P acquisition efficiency co-localized with those for P use efficiency (i.e., the ratio between grain yield and the amount of P supplied to the crop), indicating that the efficiency in acquiring P is the main determinant of P use efficiency in tropical maize. Since P acquisition efficiency achieved *via* changes in root morphology is the physiological basis of possible pleiotropy between Al resistance and better P nutrition, here we will briefly discuss this mechanism. For a broader view of mechanisms possibly contributing to enhanced crop performance under low P, which may involve modulation of P transporters, root system architecture modifications in response to low P, exudation of organic acids (OAs) and phosphatases, and mycorrhizal associations, in addition to internal mechanisms of P efficiency, readers are directed to recent reviews in this area (e.g., López-Arredondo et al., 2014).

Since P is in general highly unavailable on acidic soils, results such as those reported by Mendes et al. (2014) are expected, as enhanced capacity to acquire P is the logical first limiting step for P efficiency. However, other mechanisms have also been shown to exert beneficial effects on crop performance under low P in the field (López-Arredondo et al., 2014). The work by Gamuyao et al. (2012) provided a molecular foundation for the importance of root system architecture on the efficiency with which plants acquire P on soils with low P availability. The rice serine/threonine receptor-like kinase, OsPSTOL1, which is a member of the LRK10L-2 subfamily, was shown to enhance early root growth and grain yield on a P-deficient soil *via* increased P uptake, regulating crown root development (Gamuyao et al., 2012). Subsequently, a low but positive correlation between root surface area assessed in younger plants and grain yield under low P was instrumental in the identification of sorghum homologs of *OsPSTOL1*, designated *SbPSTOL1* genes, that also act to enhance root growth, thereby leading to enhanced P acquisition and grain yield in a sorghum association panel (Hufnagel et al., 2014). Mechanistically, plant P deficiency leads to inhibition of primary root growth due to a shift from an indeterminate to a determinate developmental program, which is caused by reduced cell elongation followed by the loss of meristematic cells in the root apical meristem (RAM) (Sánchez-Calderón et al., 2005). Hence, this release of apical dominance leads to enhanced proliferation of lateral

roots, and increased lateral root branching increasing P uptake as observed in maize (Zhu and Lynch, 2004; Postma et al., 2014).

From the physicochemical standpoint, the supply of a nutrient like P from the soil solution toward the root surface *via* a diffusive flow can be modeled by the Fick's law (Nobel, 1991), which depends on the P concentration gradient generated by the interplay between root P absorption and P in the soil solution. This concentration gradient can thus be thought as the "force" driving diffusion fluxes; as the root system grows into new soil regions still rich in P, the distance through which diffusion occurs is reduced, thus enhancing the diffusive flow (Novais and Smith, 1999), which is also maintained by the uptake process. Finally, we point out that changes in the three-dimensional configuration of the root system, such as proliferation of shallow roots, can also enhance P uptake [for more details on such mechanisms, please see Li et al. (2016) and Lynch (2011)].

Molecular Basis

Malate and Citrate Transporters

Organic acid transport and homeostasis is emerging as a central hub in a network of acidic soil stress responses. The first OA transporters involved in Al resistance were the wheat TaALMT1 and Arabidopsis AtALMT1, both shown to encode plasma membrane anion channel proteins that mediate root tip malate efflux (Sasaki et al., 2004; Hoekenga et al., 2006; Piñeros et al., 2008; Zhang et al., 2008). Although being the founding members of a novel class of plant anion transporters, it is now well established that, as a family, ALMT functions extend well beyond Al resistance, and participate in a variety of other physiological processes, including guard cell regulation, fruit quality, anion homeostasis, seed development, and plant-microbe interactions (Sharma et al., 2016). However, electrophysiological analysis of TaALMT1 and AtALMT1 (i.e., those transporters associated with Al-dependent responses) in heterologous systems has shown a distinct functional feature of these two transporters in that although they have transport activity in the absence of extracellular Al³⁺, this activity is enhanced by extracellular Al³⁺ (Hoekenga et al., 2006; Piñeros et al., 2008). This so-called "Al activation" is analogous to processes occurring in ligand-gated channels, with the agonistic binding of Al³⁺ to the ALMT protein triggering a conformational change that favors its open state, consequently increasing its transport activity and facilitating anion (i.e., malate) flux. Although the molecular determinants involved in the binding of Al³⁺ to the ALMT protein remain unknown, a combination of functional analysis of structurally modified TaALMT1 and AtALMT proteins and phylogenetic studies on ALMTs indicate that several different domains in these two proteins are likely to act together in the Al-mediated enhancement of transport activity (Sasaki et al., 2004; Furuichi et al., 2010; Ligaba et al., 2013). Overall, the Al-dependent enhancement of the transport activity of an anion channel mediating the selective efflux of malate represents an elegant regulatory component of root malate exudation associated with Al exclusion processes.

More recently, a second novel transport substrate and new regulatory mechanisms have been described for the TaALMT1 transporter (Ramesh et al., 2015, 2018). It has generally been assumed that malate efflux is the primary transport function associated with TaALMT1. Recently, it was shown that TaALMT1 also has a high permeability to the non-protein amino acid, gamma-aminobutyric acid (GABA), a zwitterion molecule associated with signaling cascades in plants. GABA is not only transported by TaALMT1 but also modulates the activity of the transporter protein. Similarly, the apoplastic pH and anion composition also appear to regulate TaALMT1 transport activity, such that increased anion concentrations and/or more alkaline apoplastic conditions stimulate transport activity (Ramesh et al., 2015). These functional characteristics provide additional regulatory layers to Al³⁺-mediated regulation of TaALMT1 activity. Consequently, in alkaline environments, enhancement of TaALMT1 activity resulting in both malate and GABA efflux has been suggested by Ramesh et al. (2015) to promote extracellular acidification *via* H⁺ efflux coupled to the efflux of the malate anion, thereby potentially ameliorating and providing tolerance to high pH soils. Verification of such a tolerance mechanism operating in response to alkaline environments, and validation of the tantalizing functional plasticity of TaALMT1 in tolerance to abiotic stresses, awaits further investigation. It should be noted that the initial studies on this topic have not found increased tolerance or malate efflux in plants grown on alkaline soils and hydroponic media simulating alkaline field conditions (Silva et al., 2018).

The second type of Al resistance OA transporters belong to a subgroup of plasma membrane-localized MATE transporters identified from the map-based cloning of the major Al resistance loci in sorghum (*SbMATE*) (Magalhaes et al., 2004, 2007) and barley (*HvAACT1*) (Furukawa et al., 2007; Wang et al., 2007). Functional characterization of *SbMATE*, *HvAACT1*, and subsequently identified homologs in *Arabidopsis* (*AtMATE1*) (Liu et al., 2009), maize (*ZmMATE1*) (Maron et al., 2009), wheat (Ryan et al., 2009; Tovkach et al., 2013), rice bean (*VuMATE1/2*) (Yang et al., 2011; Liu et al., 2018), and rice (*OsFRD2/4*) (Yokosho et al., 2011, 2016) indicates that this subgroup of MATE transporters mediate citrate transport, and therefore as with ALMTs, these transporters underlie Al-exclusion *via* root tip OA root release. However, it is worthwhile to comment about the common assumption that ALMTs and MATEs are functionally very similar, as this is not the case. The functional analysis of several of the MATE transporters involved in Al resistance has established that, when expressed in heterologous systems, this subgroup of MATE transporters mediates constitutive pH-dependent citrate transport that is not activated by Al³⁺ in *Xenopus oocytes* (Magalhaes et al., 2007; Maron et al., 2009; Yang et al., 2011; Melo et al., 2013; Doshi et al., 2017; Liu et al., 2018), although some exceptions have been also reported both in *X. oocytes* (Furukawa et al., 2007; Yokosho et al., 2011) and tobacco suspension cells (Yokosho et al., 2016). Electrophysiological analysis indicates that, in the absence of exogenous intracellular citrate, these MATE transporters mediate an electrogenic transport that appears to be due to a large cation influx (H⁺, Na⁺, and/or K⁺). Differences in the OA transport

mechanism between ALMTs and MATEs raises interesting questions. Because of the large inwardly directed voltage gradient or membrane potential across the root cell plasma membrane, the efflux of the malate and citrate anions is a thermodynamically passive process. This is consistent with the ALMT transporters functioning as anion channels mediating the passive movement of the malate anion out of the root cell.

On the other hand, the MATE transporters use a thermodynamically active (H⁺-driven) antiport mechanism associated with the passive efflux of citrate²⁻ anions down its outwardly directed electrochemical gradient. One interesting and quite speculative explanation for this is that an alternative substrate, rather than the free citrate²⁻ anion, is the substrate being transported out of the root cells. In the recent publication by Doshi et al. (2017), electrophysiological, radiolabeled, and fluorescence-based transport assays in two heterologous expression systems (*oocytes* and yeast) demonstrated that *SbMATE* has a fairly broad substrate recognition, mediating proton and/or sodium-driven efflux of the ¹⁴C-citrate anion, as well as efflux of the organic monovalent cation, ethidium, but not its divalent analog, propidium.

Consistent with those findings, MATE proteins were found to transport a wide range of organic substrates (Omote et al., 2006), both anionic and cationic (Tanihara et al., 2007), and including ethidium in the case of the first characterized MATE family protein, the bacterial MATE, *NorM* (Morita et al., 2000). Nevertheless, it was somewhat surprising to the field of MATE researchers when it was discovered that the plant MATEs involved in Al resistance mediate the efflux of the anion, citrate. Thus, the findings in the recent Doshi et al. publication showing that at least *SbMATE* has a more broad transport substrate recognition allows us to very speculatively propose that *SbMATE* (and its orthologs) mediate the efflux of a complexed rather than free anionic form of citrate. This alternative could help explain the antiporter nature of these MATE transporters, as Al-citrate complexes, for instance, could actively be removed from the symplasm in a process energized by passive H⁺ influx. Under this scenario, this group of MATE transporters would still mediate an Al resistance response by actively removing and detoxifying Al from the symplasm of root cells (i.e., mediating resistance), rather than mediating a process where Al is prevented from entering the root cell.

Malate and Citrate Transporters as Part of a Common Stress-Responsive Hub

Transcription factors including the Cys₂His₂-type zinc finger transcription factors *OsART1* in rice (Yamaji et al., 2009) and *AtSTOP1* and 2 (Sawaki et al., 2009), *AtWRKY46* (Ding et al., 2013) in *Arabidopsis*, and the rice *ASR* (abscisic acid, stress, and ripening) 1 and 5 (Arenhart et al., 2013, 2016; Lima et al., 2011), are involved with the regulation of membrane transporter genes. *OsART1*, an *AtSTOP1* ortholog, modulates the expression of a number of membrane transporters involved in rice Al resistance, *OsNrat1*, *OsMGT1*, and *OsFRDL4* (Xia et al., 2010; Yokosho et al., 2011; Chen et al., 2013). Similarly, *AtSTOP1* modulates the expression of membrane transporters

and *AtALS3* (Liu et al.,2009;Sawaki et al.,2009), in response to both Al and H⁺ rhizotoxicity. Recently, as discussed in the next sections, changes in *AtSTOP1* regulation of *AtALMT1* have been shown to constitute a major component of P sensing pathways (Balzergue et al.,2017;Mora-Macías et al.,2017). Likewise, expression of *AtALMT1* is also regulated by other signaling pathways involving reactive oxygen species (ROS) and phytohormones (Daspute et al.,2017). Biotic stresses, such as that caused by infection of shoots by pathogenic *Pseudomonas syringae*, also triggered upregulation of *AtALMT1* expression and increased root malate exudation, which attracts the beneficial rhizobacterium, *Bacillus subtilis*, into the root microbiome and stimulates Arabidopsis immune responses (Rudrappa et al., 2008). Overall, these more recent observations indicate that the regulatory role of *AtSTOP1* on *AtALMT1* expression and associated physiological stress responses extend well beyond the original signaling roles associated with Al and H⁺ stress.

Al Resistance Transporters That Do Not Transport Organic Acids: Aluminum-Sensitive 3 (ALS3)

Screening for Arabidopsis mutants with altered responses to Al toxicity led to the identification of mutants with increased sensitivity to Al, within which the recessive Al sensitive mutant, *als3*, showed 80% root growth inhibition by Al compared to 24–38% inhibition in the wild type (Larsen et al.,1996). This Al sensitive response was unrelated to enhanced Al uptake by *als3* plants (Larsen et al.,1997). Subsequently, map-based cloning identified ALS3 as an ABC transporter-like protein that is localized to leaf hydathodes and the phloem, in addition to the root cortex (Larsen et al.,2005). Based on its likely plasma membrane localization, it was suggested that ALS3 functions in an Al-specific manner to move Al away from sensitive tissues, thus providing Al resistance. ABC transporters contain both a nucleotide (ATP)-binding domain and a transmembrane (TM) domain (Rea,2007). Larsen and colleagues noted that both ALS3 and the homologous putative bacterial metal resistance protein, *ybbM*, do not possess the ATP binding domain, which is normally needed for ABC transporters to function.

The ABC transporter, *sensitive to Al rhizotoxicity* (*AtSTAR1*), which possesses only the ATP-binding domain and not the TM domain, was implicated in Al resistance in Arabidopsis (Huang et al.,2010). *AtSTAR1* is a homolog of rice *OsSTAR1*.Huang et al. (2009) showed that *OsSTAR1* (which contains the nucleotide-binding domain) forms an ABC complex with *OsSTAR2* (which contains the TM domain), which results in an active ABC transporter involved in Al resistance possibly by mediating UDP glucose efflux into the rice root cell wall. The actual mechanism whereby this activated form of glucose may provide Al tolerance still remains to be elucidated. However, Huang and collaborators hypothesize that UDP glucose may be transported by membrane-localized *STAR1*–*STAR2* from the cytosol into vesicles, from which either UDP-glucose or derived glycoside would be released into the apoplast *via* exocytosis across the plasma membrane, and used to mask the sites for Al binding in the cell wall, thus providing Al resistance. In Arabidopsis,Huang et al.(2010) presented findings suggesting that *AtSTAR1* may form a complex with ALS3, with ALS3 providing the TM domain enabling the

formation of a functional *AtSTAR1/ALS3* complex, which may mediate Al efflux from the outer cell layers of the root tip. These findings indicate that Arabidopsis Al resistance is complex, and also include *AtALMT1* (Hoekenga et al.,2006) and *AtMATE* (Liu et al.,2009) providing root Al exclusion *via* root malate and citrate efflux. In addition to ALS3, a number of other putative Al transporters have been identified that could mediate Al resistance. These include *OsNrat1*, a rice root plasma membrane uptake transporter that ultimately results in Al storage in the root vacuole (Xia et al.,2010), *AtNIP1*, a root tip plasma membrane aquaporin protein that mediates root Al uptake (as an Al–malate complex) and sequestration (Wang et al.,2017), and another Arabidopsis ABC transporter, *ALS1* (Larsen et al.,2007;Nezames et al.,2012).

Research based on suppressor screens have focused on the identification of molecular factors in the form of mutations that could complement the Al-sensitive phenotype of *als3* (Gabrielson et al.,2006). These studies implicated DNA damage as a biochemical target of Al (Rounds and Larsen,2008;Nezames et al.,2012;Sjogren et al.,2015;Sjogren and Larsen,2017), which is viewed as a possible venue to enhance crop Al resistance (Eekhout et al.,2017). One component is the cell cycle checkpoint factor, *ALUMINUM TOLERANT2* (*ALT2*), which may recruit members of the machinery involved with the detection and repair of DNA damage elicited by Al toxicity (Nezames et al., 2012). Accordingly, it was proposed that *ALT2*, and also ataxia telangiectasia-mutated and Rad3-related (*ATR*), impair the cell cycle and drive quiescent center differentiation in response to DNA damage caused by Al, leading to root growth arrest elicited by Al. It will be very interesting to assess the effect of the molecular factors involved with the biochemical targets of Al toxicity, such as DNA damage, in enhancing crop performance on acidic soils. Genetic manipulation of the underlying factors for Al toxicity is thought to hold potential for increasing global food security on acidic soils (Rounds and Larsen,2008). Within the realm of natural variation for Al resistance in crop plants, the allelic effects of such factors may prove to be milder compared to that of major Al resistance genes encoding plasma membrane transporters. Nevertheless, exploiting such distinct biochemical pathways in concert, in the context of plant breeding, may offer potential for identifying transgressive segregants that could enhance even further crop perform on acidic soils.

POSSIBLE PLEIOTROPIC EFFECTS UNDERLYING Al RESISTANCE AND P ACQUISITION EFFICIENCY

SbMATE and TaALMT1 Increase Grain Yield on Al-Toxic and P-Deficient Soils

Overexpression of the wheat Al resistance gene, *TaALMT1*, in transgenic barley under the control of the ubiquitin promoter has been shown to enhance both P uptake and grain production on an acidic, high P-fixing soil (Delhaize et al.,2009). This effect was attributed in large part to the role of *TaALMT1* in maintaining root growth under soil acidity, which likely results

from Al resistance. However, the observed greater P uptake per unit length in *TaALMT1*-expressing barley lines might also have resulted to some extent from P mobilization from the soil clays by the malate released into the rhizosphere, thus favoring P uptake (Delhaize et al.,2009). When the soil was limed, which substantially reduced Al saturation, grain yield of the transgenic and non-transgenic lines were similar, suggesting that enhanced P uptake under soil acidity was indeed largely achieved as an indirect effect of *TaALMT1* enhancing Al resistance. It should be noted that clay acidic soils generally have a strong buffering capacity and, although liming can be used to reduce Al^{3+} in the topsoil, neutralization of subsoil Al^{3+} is often difficult to achieve. In the absence of liming, Al resistance can have an important indirect effect on crop performance *via* both enhanced root proliferation in the topsoil, where P is primarily located on acidic soils (Lynch and Brown,2001), and improved water acquisition by better root development in the subsoil. With liming, Al tolerance may most strongly benefit crop yields by enhanced water acquisition from deeper, acidic soils layers.

Allelic variation at the sorghum chromosome 3 Al resistance locus, *Alt_{SB}* (Magalhaes et al.,2004), where the citrate transporter, *SbMATE*, resides (Magalhaes et al.,2007), explains a large portion of the sorghum Al resistance phenotype. Recently, a sorghum recombinant inbred line (RIL) population was assessed for Al resistance both in lab-based hydroponics (relative root growth) and in the field (grain yield) under \pm Al exposure, in a phenotyping site located at the Embrapa Maize and Sorghum station in Brazil (Carvalho et al.,2016). In that study, sorghum hybrids were also constructed that were either homozygous for the Al-sensitive or -resistant *SbMATE* allele, or heterozygous for *SbMATE*. These hybrids were isogenic, so that *Alt_{SB}* alleles from different donors could be compared within a homogeneous genetic background, thus isolating the effect of *SbMATE* from genetic background effects.

The resulting isogenic hybrids were assessed for grain yield in the field on control (absence of Al toxicity in the soil) or in an Al toxic soil with 56% Al saturation in the top soil (0–20 cm) and 70% Al saturation in the sub-soil (20–40 cm). A major QTL underlying both Al resistance assessed in hydroponics and grain yield under Al toxicity in the field was co-located with *SbMATE* on sorghum chromosome 3, and explained a large portion of the genetic variance in the Al toxic but not in the non Al-toxic soil. The allele associated with increased Al resistance was donated by the Al tolerant parent, SC283, and the Al resistance allele did not decrease grain yield in the absence of Al toxicity, indicating that no yield penalty arises from Al-induced citrate release elicited by *SbMATE*. This genetic approach allowed the authors to estimate a consistent effect of a single Al resistance allele of *SbMATE* as a grain yield increase of ~ 0.6 ton ha⁻¹, both in the RILs and in hybrid combinations. The rather additive gene action of *SbMATE* in grain yield production indicates that, when in homozygosity, *SbMATE* increases grain yield by more than 1.0–ha⁻¹, or more than 50% over the population mean. The Al saturation level in the Al toxic site, 56%, is well above the 20% critical level beyond which sorghum yields are reduced (Gourley,1987). Therefore, most of the yield advantage of *SbMATE* is likely caused by its effect on Al resistance itself. However, the typical acidic soil in

question also has high P fixation capacity and P diffusion is known to be highly depend on the soil water content (Novais and Smith,1999). Therefore, as Al stress and low P availability in general co-exist on acidic soils, a smaller portion of the yield advantage caused by *SbMATE* may have originated from citrate-based enhanced P mobilization (Drouillon and Merckx,2003) from the soil clays into the root surface, which is expected to favor P uptake.

A more compelling evidence for a pleiotropic effect of *SbMATE* on P acquisition comes from a genome-wide association mapping study conducted in West Africa (Leiser et al.,2014), which included gene-specific markers developed for *SbMATE* (Caniato et al.,2014). This study revealed that *SbMATE* SNPs were highly associated with grain yield and the associations were found especially under low P conditions for sorghum cultivated in soils at 29 different sites in West Africa, explaining up to 16% of the genotypic variance (Leiser et al., 2014). The average Al saturation was only 10% in the 16 field trials that were analyzed for Al saturation in the Leiser et al. (2014) study, and only one site had Al saturation reasonable above (27.5%) the critical level of Al saturation determined for sorghum (20%,Gourley,1987). This suggests a direct pleiotropic effect of Al-activated citrate release promoted by *SbMATE* in enhancing P uptake and sorghum yields under low P availability in West Africa. It should be noted, however, that Al toxicity varies according to the chemical and mineral nature of the soils, which ultimately controls free Al^{3+} activity in the soil solution. Therefore, in sandy soils, such as those commonly found in West Africa, we cannot rule out that higher Al^{3+} activity in some of the sites may have led *SbMATE* activity to improve sorghum grain yield *via* Al resistance.

Evidence for a Pleiotropic Role of the STOP1/ALMT1 Module and ALS3 on P Acquisition *via* Changes in Root Morphology in Response to P Deficiency

Recent research findings exposed a possible direct link between *AtALMT1* function and both Al resistance and changes in root growth triggered by response to low P (Balzergue et al.,2017; Mora-Macías et al.,2017). Previously, an antagonistic connection was established between phosphate and Fe availability, leading to adjustments in root growth (Müller et al.,2015). It was found that the *LPR1* (ferroxidase)/*PDR2* (P5-type ATPase) module enhances cell-specific Fe and callose deposition in the meristem and elongation zones under low P conditions. Under low Pi, accumulated ROS, possibly resulting from Fe toxicity triggered by Fe^{3+} accumulation in the apoplast *via* *LPR1*-dependent Fe oxidation, may lead to callose deposition. In turn, according to the proposed model, callose deposition in the RAM under low P impairs cell-to-cell movement of the *SHORT-ROOT* (*SHR*) transcription factor, which is important for stem cell maintenance, hence providing a checkpoint for primary root growth control in response to low P.

A mutation screen in *Arabidopsis* indicated that both *ALMT1* and its transcriptional regulator, *STOP1*, repress primary root growth under $-P$ conditions (Mora-Macías et al.,2017).

Furthermore, P deficiency was also shown to upregulate *ALMT1* expression in Arabidopsis, and experiments where exogenous malate was applied to the RAM restored the short root phenotype in *almt1* and *stop1* mutants in a concentration-dependent manner. Fe accumulation in the RAM was found to be required to activate the inhibition of primary root growth under -P conditions (Müller et al., 2015). Hence, the primary root growth inhibition by malate was suggested to occur *via* malate chelating and solubilizing Fe in the rhizosphere, which would promote Fe accumulation in the RAM apoplast (Mora-Macías et al., 2017). Accordingly, the resulting RAM exhaustion process leading to inhibition of the primary root growth under low P (Sánchez-Calderón et al., 2005) happens in the presence of Fe in the growth medium. Callose deposition, which is stimulated by ROS, may be involved in the root elongation inhibition following the model proposed by Müller et al. (2015). Hence, impaired cell-to-cell movement of the SHR transcription factor, which is important for stem cell maintenance, was suggested to lead to meristem exhaustion, inhibiting primary root growth (Müller et al., 2015; Mora-Macías et al., 2017). Because the enhanced proliferation of lateral roots coincides with the inhibition of the primary root (release of root apical dominance) under low P conditions (Sánchez-Calderón et al., 2005), *ALMT1* may ultimately increase P uptake on acidic soils *via* increases in total root surface area, thereby favoring P diffusion toward the root surface.

A strikingly similar mechanism for an Al resistance gene leading to changes in root growth as a response to P deficiency has been proposed for *ALS3* (Larsen et al., 1996, 2005) and *AtSTAR1* (Huang et al., 2010; Belal et al., 2015; Dong et al., 2017). Together, *STAR1* and *STAR2* (a rice homolog of *als3*) form an ABC transporter implicated in Al resistance likely *via* the transport of UDP glucose into the root apoplast, which is believed to modify the cell wall leading to Al resistance (Huang et al., 2009) as previously discussed in Section “Al Resistance Transporters That do not Transport Organic Acids: Aluminum-Sensitive 3 (*ALS3*).” The commonality between the putative pleiotropic pathways mediated by *ALMT1* and *ALS3/AtSTAR1* is striking, particularly taking into consideration that those genes underlie distinctly different Al resistance mechanisms. Both pathways involve cross-talk between low P responses and Fe homeostasis, with involvement of LOW PHOSPHATE ROOT (*LPR*) oxidases; mutations in *LPR* leads to reduced Fe³⁺ accumulation in roots and thereby root growth insensitivity to low Pi (Müller et al., 2015; Dong et al., 2017; Mora-Macías et al., 2017). However, the *ALS3* pathway involves UDP glucose, which reverses Fe³⁺ overaccumulation and rescues the short root phenotype in *als3* subjected to - P conditions (Dong et al., 2017). However, unlike the T-DNA mutants for *AtALMT1* and *STOP1*, *als3* shows enhanced inhibition of primary root growth under P deficiency (Dong et al., 2017), suggesting possible antagonism between Al resistance conferred by *ALS3* and P acquisition.

These studies offer a radically different stance on root OA release enhancing resistance to low P solely *via* increased P availability in the rhizosphere, as root developmental changes caused by *ALMT1/STOP1* and *ALS3* appear to be a low P-specific response that is focused on root development. A common

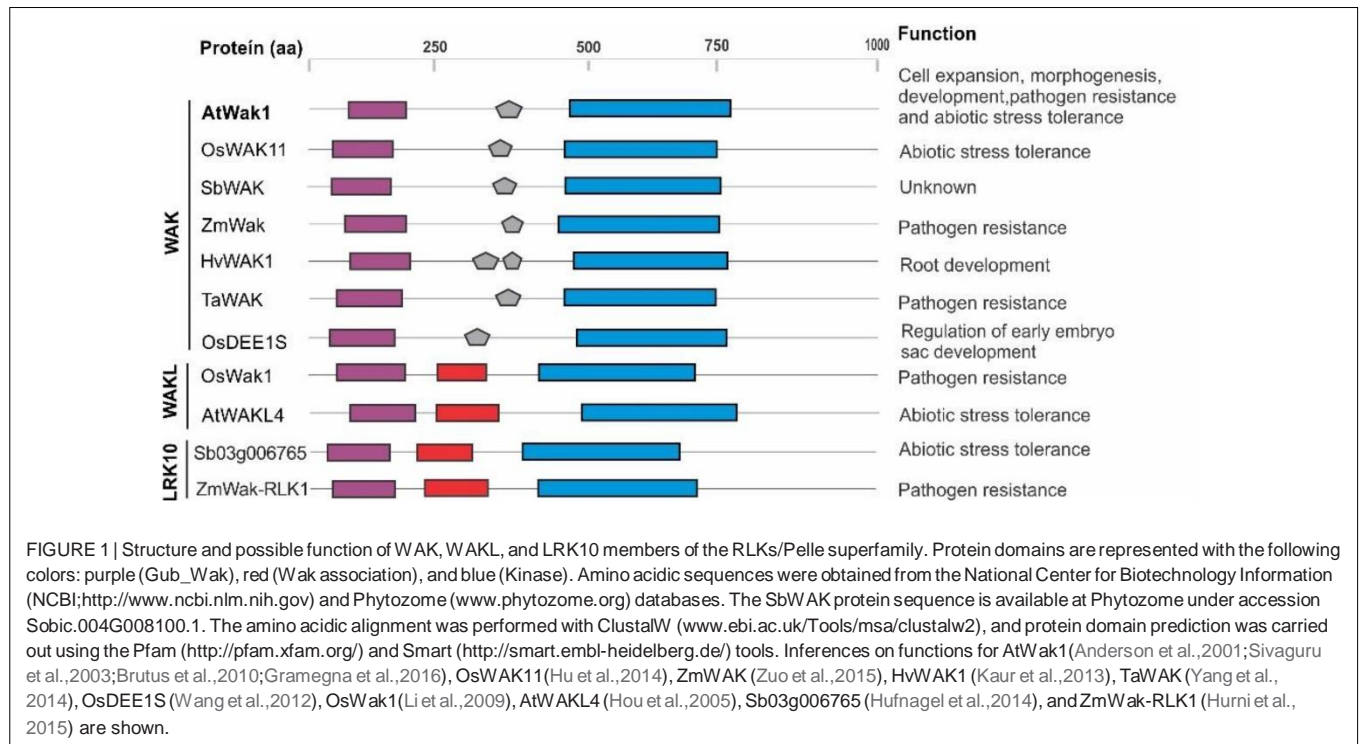
physiological basis centered on Fe homeostasis underlying the effect of distinctly different Al resistance pathways encoded by *ALMT1/STOP1* and *ALS3* on root remodeling under low P seems likely. Should those responses prove to persist for crops cultivated on acidic soils, it will be tempting to speculate that the close soil chemistry associations between Al toxicity and low P availability, which is centered on the presence of Fe and Al oxides, may have resulted in co-selective pressure for pleiotropic mechanisms enabling plants both to tolerate Al³⁺ and to acquire P more efficiently. Nevertheless, there is a strong need for strategies to validate whether the direction of this hypothetical pleiotropic effect is consistent with a positive net benefit on acidic soil performance.

Are Wall-Associated Kinases Associated With a Joint Effect on Al Resistance and P Acquisition?

Wall-associated kinases (WAKs), which are receptor-like kinase proteins (Kohorn and Kohorn, 2012) that span the plasma membrane and extend out into the cell wall (He et al., 1999), have been shown to play roles in cell expansion, development, morphogenesis, and defense responses to environmental stimuli (Sivaguru et al., 2003; Brutus et al., 2010; Kohorn and Kohorn, 2012; Gramegna et al., 2016; Mangeon et al., 2016). Sivaguru et al. (2003) reported that *AtWAK1* expression was rapidly induced by Al and disappeared after 9 h of Al exposure and that transgenic plants overexpressing *AtWAK1* showed enhanced Al resistance. Recently, a T-DNA knockout of the glycine-rich protein, *AtGRP3*, which interacts with *AtWAK1* (Park et al., 2001), has also been shown to enhance Al resistance in Arabidopsis, similar to *AtWAK1* (Mangeon et al., 2016). However, *AtGRP3* expression was not modulated by Al and *grp3* had a long root phenotype in the absence of Al exposure. Therefore, it remains to be verified whether the lower root growth inhibition in *grp3* exposed to Al compared to the wt is in fact due to a mechanism enhancing Al resistance or is influenced to some extent by a leaky *grp* mutation, based on the role for *AtGRP3* in repressing root growth.

Wall-associated kinases form a subfamily within the receptor kinase (RLKs)/Pelle superfamily, which includes other subfamilies such as WAK-like kinase (WAKL) and Leaf rust 10 disease-resistance locus receptor-like protein kinase (LRK10), that share similar protein architectures with the WAK proteins (Shiu and Bleecker, 2003; Hou et al., 2005; Lim et al., 2014). The general WAK protein architecture features an extracellular moiety containing a cysteine-rich (Cys-rich) galacturonan-binding domain (Gub_Wak), epidermal growth factor (EGF) repeats, and a TM domain, in addition to a cytoplasmic serine/threonine kinase domain (Anderson et al., 2001; Decreux and Messiaen, 2005; Decreux et al., 2006).

Using association mapping, Hufnagel et al. (2014) showed that sorghum homologs of the rice serine/threonine receptor kinase, OsPSTOL1 (Gamuyao et al., 2012), are involved in increases in root surface area leading to enhanced P acquisition



and grain yield under low P availability in the soil. In sorghum, these SbPSTOL1 proteins are predicted to have a signal peptide consistent with the targeting to a secretory pathway, as well as a TM domain and cell wall association domains. For example, the Sb03g006765 protein associated with P efficiency and increased root surface area is predicted to have a Cys-rich GUB_Wak domain and a wall-associated receptor kinase domain (WAK_association) located C-terminal to the GUB_Wak domain. Similarities between SbPSTOL1 and WAK proteins such as AtWAK1, which appears to be involved in Al resistance (Sivaguru et al., 2003), arise primarily from the presence of the GUB_Wak and TM domains, similar intron-exon organization, and a genomic localization in tight physical clusters (Hufnagel et al., 2014). Recent studies have suggested that amino acids in the Gub_Wak domain bind covalently to native pectins and oligogalacturonides in the cell wall (Verica and He, 2002; Decreux and Messiaen, 2005; Decreux et al., 2006; Kohorn and Kohorn, 2012; Kohorn et al., 2016). This leads us to speculate that SbPSTOL1 proteins may function as WAKs, functioning as receptors for the activation of signaling cascades in response to extracellular stimuli (in this case, P deficiency). However, in place of the EGF repeats, which is a hallmark of WAK proteins (Kanneganti and Gupta, 2008), WAKL and LRK10 members, including Sb03g006765, possess a WAK_association domain.

The GUB_Wak domain is present in certain plant proteins suggested to be involved in responses to abiotic and biotic stresses that belong to three subfamilies in the RLK superfamily, the WAKL, WAK, and LRK10 subfamilies (with Sb03g006765 within the LRK10 subfamily). These proteins are depicted in **Figure 1**. Sequence alignment of the GUB_Wak amino acidic

sequences in these proteins does not show a high degree of conservation. However, this domain has conserved clusters of hydrophobicity that are essential for the association of these proteins *via* the extracellular residues, including a Cys-rich region and a conserved YPF motif. Therefore, it remains to be seen whether the SbPSTOL1 proteins functionally work as WAKs such as AtWAK1. If so, given the predicted role for SbPSTOL1 in enhancing root growth and P uptake in sorghum, this class of proteins could jointly control Al resistance and P uptake.

CONCLUSION

We are at a stage in research on crop plant adaptation to acidic soils where a number of different Al resistance genes have been identified. These genes have been discovered using a variety of both forward and reverse genetic strategies, ranging from candidate genes validated primarily *via* ectopic overexpression in transgenic plants or identified *via* mutant screens to map-based cloning of Al resistance genes underlying loci previously known to play a role in the genetic variation of Al resistance. In most cases, very little work has been done to translate the findings from the basic research used to identify and characterize the genes to practical applications to generate crop varieties in breeding programs. The research that connects with genetic variation present within crop species to identify Al resistance genes is certainly the most amenable to providing molecular tools for the breeding of crops with improved production on acidic soils. In the cases where genetic determinants of Al resistance have been found by other

approaches, efforts to assess whether those determinants are also active in crop plants in field conditions are sorely needed if the ultimate goal is indeed to generate crops more adapted to cultivation on acidic soils. While the effect of Al resistance on crop performance on acidic soils is known, pleiotropic effects of such genes on P uptake efficiency needs to be explored in crop species grown in the field. In both cases, detailed quantification is needed to gauge the true potential of Al resistance genes in coping with agriculture in stress-prone areas. Particularly in a scenario where global climate change is resulting in greater drought stress, the potential of those genes to ensure food security worldwide may be far greater than initially believed.

REFERENCES

- Anderson, C. M., Wagner, T. A., Perret, M., He, Z. H., He, D., and Kohorn, B. D. (2001). WAKs: cell wall-associated kinases linking the cytoplasm to the extracellular matrix. *Plant Mol. Biol.* 47, 197–206. doi: 10.1023/A:1010691701578
- Arenhart, R. A., De Lima, J. C., Pedron, M., Carvalho, F. E. L., Da Silveira, J. A. G., Rosa, S. B., et al. (2013). Involvement of ASR genes in aluminium tolerance mechanisms in rice. *Plant Cell Environ.* 36, 52–67. doi: 10.1111/j.1365-3040.2012.02553.x
- Arenhart, R. A., Schunemann, M., Neto, L. B., Margis, R., Wang, Z. Y., and Margis-Pinheiro, M. (2016). Rice ASR1 and ASR5 are complementary transcription factors regulating aluminium responsive genes. *Plant Cell Environ.* 39, 645–651. doi: 10.1111/pce.12655
- Bahia Filho, A. F. C., Magnavaca, R., Schaffert, R. E., and Alves, V. M. C. (1997). "Identification, utilization, and economic impact of maize germplasm tolerant to low levels of phosphorus and toxic levels of exchangeable aluminum in Brazilian soils," in *Plant-Soil Interactions at Low pH: Sustainable Agriculture and Forestry Production*, eds A. C. Moniz, A. M. C. Furlani, R. E. Schaffert, N. K. Fageria, C. A. Rosolem, and H. Cantarella (Campinas/Viçosa: Brazilian Soil Science Society), 59–70.
- Balzergue, C., Darteville, T., Godon, C., Laugier, E., Meisrimler, C., Teulon, J. M., et al. (2017). Low phosphate activates STOP1-ALMT1 to rapidly inhibit root cell elongation. *Nat. Commun.* 8:15300. doi: 10.1038/ncomms15300
- Belal, R., Tang, R., Li, Y., Mabrouk, Y., Badr, E., and Luan, S. (2015). An ABC transporter complex encoded by aluminum sensitive 3 and NAP3 is required for phosphate deficiency responses in *Arabidopsis*. *Biochem. Biophys. Res. Commun.* 463, 18–23. doi: 10.1016/j.bbrc.2015.05.009
- Brutus, A., Sicilia, F., Macone, A., Cervone, F., and De Lorenzo, G. (2010). A domain swap approach reveals a role of the plant wall-associated kinase 1 (WAK1) as a receptor of oligogalacturonides. *Proc. Natl. Acad. Sci. U.S.A.* 107, 9452–9457. doi: 10.1073/pnas.1000675107
- Caniato, F. F., Hamblin, M. T., Guimaraes, C. T., Zhang, Z., Schaffert, R. E., Kochian, L. V., et al. (2014). Association mapping provides insights into the origin and the fine structure of the sorghum aluminum tolerance locus, AltSB. *PLoS One* 9:e87438. doi: 10.1371/journal.pone.0087438
- Carvalho, G Jr, Schaffert, R. E., Malosetti, M., Viana, J. H., Menezes, C. B., Silva, L. A., et al. (2016). Back to acid soil fields: the citrate transporter SbMATE is a major asset for sustainable grain yield for sorghum cultivated on acid soils. *G3* 6, 475–484. doi: 10.1534/g3.115.025791
- Chen, Z. C., Yokosho, K., Kashino, M., Zhao, F. J., Yamaji, N., and Ma, J. F. (2013). Adaptation to acidic soil is achieved by increased numbers of cis-acting elements regulating ALMT1 expression in *Holcus lanatus*. *Plant J.* 76, 10–23. doi: 10.1111/tpj.12266
- Daspute, A. A., Sadhukhan, A., Tokizawa, M., Kobayashi, Y., Panda, S. K., and Koyama, H. (2017). Transcriptional regulation of aluminum-tolerance genes in higher plants: clarifying the underlying molecular mechanisms. *Front. Plant Sci.* 8:1358. doi: 10.3389/fpls.2017.01358
- Decreux, A., and Messiaen, J. (2005). Wall-associated kinase WAK1 interacts with cell wall pectins in a calcium-induced conformation. *Plant Cell Physiol.* 46, 268–278. doi: 10.1093/pcp/pci026
- Decreux, A., Thomas, A., Spies, B., Brasseur, R., Cutsem, P., Van, et al. (2006). In vitro characterization of the homogalacturonan-binding domain of the wall-associated kinase WAK1 using site-directed mutagenesis. *Phytochemistry* 67, 1068–1079. doi: 10.1016/j.phytochem.2006.03.009
- Delhaize, E., Gruber, B. D., and Ryan, P. R. (2007). The roles of organic anion permeases in aluminium resistance and mineral nutrition. *FEBS Lett.* 581, 2255–2262. doi: 10.1016/j.febslet.2007.03.057
- Delhaize, E., Ma, J. F., and Ryan, P. R. (2012). Transcriptional regulation of aluminium tolerance genes. *Trends Plant Sci.* 17, 341–348. doi: 10.1016/j.tplants.2012.02.008
- Delhaize, E., and Ryan, P. R. (1995). Aluminum toxicity and tolerance in plants. *Plant Physiol.* 107, 315–321. doi: 10.1104/pp.107.2.315
- Delhaize, E., Taylor, P., Hocking, P. J., Simpson, R. J., Ryan, P. R., and Richardson, A. E. (2009). Transgenic barley (*Hordeum vulgare* L.) expressing the wheat aluminium resistance gene (TaALMT1) shows enhanced phosphorus nutrition and grain production when grown on an acid soil. *Plant Biotechnol. J.* 7, 391–400. doi: 10.1111/j.1467-7652.2009.00403.x
- Ding, Z. J., Yan, J. Y., Xu, X. Y., Li, G. X., and Zheng, S. J. (2013). WRKY46 functions as a transcriptional repressor of ALMT1, regulating aluminum-induced malate secretion in *Arabidopsis*. *Plant J.* 76, 825–835. doi: 10.1111/tpj.12337
- Dong, J., Piñeros, M. A., Li, X., Yang, H., Liu, Y., Murphy, A. S., et al. (2017). An *Arabidopsis* ABC transporter mediates phosphate deficiency-induced remodeling of root architecture by modulating iron homeostasis in roots. *Mol. Plant* 10, 244–259. doi: 10.1016/j.molp.2016.11.001
- Doshi, R., McGrath, A. P., Piñeros, M., Szcwyczyk, P., Garza, D. M., Kochian, L. V., et al. (2017). Functional characterization and discovery of modulators of SbMATE, the agronomically important aluminium tolerance transporter from *Sorghum bicolor*. *Sci. Rep.* 7:17996. doi: 10.1038/s41598-017-18146-8
- Doumbia, M. D., Hossner, L. R., and Onken, A. B. (1993). Variable sorghum growth in acid soils of subhumid West Africa. *Arid Soil Res. Rehabil.* 7, 335–346. doi: 10.1080/15324989309381366
- Doumbia, M. D., Hossner, L. R., and Onken, A. B. (1998). Sorghum growth in acid soils of West Africa: variations in soil chemical properties. *Arid Land Res. Manage.* 12, 179–190. doi: 10.1080/15324989809381507
- Drouillon, M., and Merckx, R. (2003). The role of citric acid as a phosphorus mobilization mechanism in highly P-fixing soils. *Gayana. Bot.* 60, 55–62. doi: 10.4067/S0717-66432003000100009
- Eekhout, T., Larsen, P., and De Veylder, L. (2017). Modification of DNA checkpoints to confer aluminum tolerance. *Trends Plant Sci.* 22, 102–105. doi: 10.1016/j.tplants.2016.12.003
- FAO and ITPS (2015). *Status of the World's Soil Resources (Main Report)*. Rome: FAO.
- Foy, C. D., Duncan, R. R., Waskom, R. M., and Miller, D. R. (1993). Tolerance of sorghum genotypes to an acid, aluminum toxic *Tatum subsoil*. *J. Plant Nutr.* 16, 97–127. doi: 10.1080/01904169309364517
- Furuichi, T., Sasaki, T., Tsuchiya, Y., Ryan, P. R., Delhaize, E., and Yamamoto, Y. (2010). An extracellular hydrophilic carboxy-terminal domain regulates the activity of TaALMT1, the aluminum-activated malate transport protein of wheat. *Plant J.* 64, 47–55. doi: 10.1111/j.1365-313X.2010.04309.x
- Furukawa, J., Yamaji, N., Wang, H., Mitani, N., Murata, Y., Sato, K., et al. (2007). An aluminum-activated citrate transporter in barley. *Plant Cell Physiol.* 48, 1081–1091. doi: 10.1093/pcp/pcm091

AUTHOR CONTRIBUTIONS

JM and MP delineated and wrote this review. LM and LK wrote this review. LK also edited the manuscript.

FUNDING

JM and LM acknowledge support from the Fundação de Amparo a Pesquisa do Estado de Minas Gerais (FAPEMIG) and the National Council for Scientific and Technological Development (CNPq).

- Gabrielson, K. M., Cancel, J. D., Morua, L. F., and Larsen, P. B. (2006). Identification of dominant mutations that confer increased aluminum tolerance through mutagenesis of the Al-sensitive *Arabidopsis* mutant, als3-1. *J. Exp. Bot.* 57, 943–951. doi: 10.1093/jxb/erj080
- Gamuyao, R., Chin, J. H., Pariasca-tanaka, J., Pesaresi, P., Catausan, S., Dalid, C., et al. (2012). The protein kinase Pstol1 from traditional rice confers tolerance of phosphorus deficiency. *Nature* 488, 535–539. doi: 10.1038/nature11346
- Godfray, H. C. J., Beddington, J. R., Crute, I. R., Haddad, L., Lawrence, D., Muir, J. F., et al. (2010). Food security: the challenge of feeding 9 billion people. *Science* 327, 812–818. doi: 10.1126/science.1185383
- Gourley, J. M. (1987). “Finding and utilizing exotic Al-tolerant sorghum germplasm,” in *Sorghum for Acid Soils: Proceedings of a Workshop on Evaluating Sorghum for Tolerance to Al-toxic Tropical Soils in Latin America*, eds L. M. Gourley and J. G. Salinas (Palmira: CIAT), 293–309.
- Gramegna, G., Modesti, V., Savatin, D. V., Sicilia, F., Cervone, F., and De Lorenzo, G. (2016). GRP-3 and KAPP, encoding interactors of WAK1, negatively affect defense responses induced by oligogalacturonides and local response to wounding. *J. Exp. Bot.* 67, 1715–1729. doi: 10.1093/jxb/erv563
- He, Z. H., Cheeseman, I., He, D., and Kohorn, B. D. (1999). A cluster of five cell wall-associated receptor kinase genes, wak1-5, are expressed in specific organs of *Arabidopsis*. *Plant Mol. Biol.* 39, 1189–1196. doi: 10.1023/A:1006197318246
- Hoekenga, O. A., Maron, L. G., Piñeros, M. A., Cançado, G. M. A., Shaff, J., Kobayashi, Y., et al. (2006). AtALMT1, which encodes a malate transporter, is identified as one of several genes critical for aluminum tolerance in *Arabidopsis*. *Proc. Natl. Acad. Sci. U.S.A.* 103, 9738–9743. doi: 10.1073/pnas.0602868103
- Hou, X., Tong, H., Selby, J., Dewitt, J., Peng, X., and He, Z. H. (2005). Involvement of a cell wall-associated kinase, WAKL4, in *Arabidopsis* mineral responses. *Plant Physiol.* 139, 1704–1716. doi: 10.1104/pp.105.066910
- Hu, W., Lv, Y., Lei, W., Li, X., Chen, Y., Zheng, L., et al. (2014). Cloning and characterization of the *Oryza sativa* wall-associated kinase gene OsWAK11 and its transcriptional response to abiotic stresses. *Plant Soil* 384, 335–346. doi: 10.1007/s11104-014-2204-8
- Huang, C.-F., Yamaji, N., and Ma, J. F. (2010). Knockout of a bacterial-type ATP-binding cassette transporter gene, AtSTAR1, results in increased aluminum sensitivity in *Arabidopsis*. *Plant Physiol.* 153, 1669–1677. doi: 10.1104/pp.110.155028
- Huang, C. F., Yamaji, N., Mitani, N., Yano, M., Nagamura, Y., and Ma, J. F. (2009). A bacterial-type ABC transporter is involved in aluminum tolerance in rice. *Plant Cell* 21, 655–667. doi: 10.1105/tpc.108.064543
- Hufnagel, B., de Sousa, S. M., Assis, L., Guimaraes, C. T., Leiser, W., Azevedo, G. C., et al. (2014). Duplicate and conquer: multiple homologs of PHOSPHORUS-STARVATION TOLERANCE1 enhance phosphorus acquisition and sorghum performance on low-phosphorus soils. *Plant Physiol.* 166, 659–677. doi: 10.1104/pp.114.243949
- Hufnagel, B., Guimaraes, C. T., Craft, E. J., Shaff, J. E., Schaffert, R. E., Kochian, L. V., et al. (2018). Exploiting sorghum genetic diversity for enhanced aluminum tolerance: allele mining based on the *Al5B* locus. *Sci. Rep.* 8:10094. doi: 10.1038/s41598-018-27817-z
- Hurni, S., Scheuermann, D., Krattinger, S. G., Kessel, B., Wicker, T., Herren, G., et al. (2015). The maize disease resistance gene Htn1 against northern corn leaf blight encodes a wall-associated receptor-like kinase. *Proc. Natl. Acad. Sci. U.S.A.* 112, 8780–8785. doi: 10.1073/pnas.1502522112
- Kanneganti, V., and Gupta, A. K. (2008). Wall associated kinases from plants – An overview. *Physiol. Mol. Biol. Plants* 14, 109–118. doi: 10.1007/s12298-008-0010-6
- Kaur, R., Singh, K., and Singh, J. (2013). A root-specific wall-associated kinase gene, HvWAK1, regulates root growth and is highly divergent in barley and other cereals. *Funct. Integr. Genomics* 13, 167–177. doi: 10.1007/s10142-013-0310-y
- Kochian, L. V. (1995). Cellular mechanisms of aluminum toxicity and resistance in plants. *Annu. Rev. Plant Physiol. Plant Mol. Biol.* 46, 237–260. doi: 10.1146/annurev.pp.46.060195.001321
- Kochian, L. V., Hoekenga, O. A., and Piñeros, M. A. (2004). How do crop plants tolerate acid soils? Mechanisms of aluminum tolerance and phosphorus efficiency. *Annu. Rev. Plant Biol.* 55, 459–493. doi: 10.1146/annurev.arplant.55.031903.141655
- Kochian, L. V., Piñeros, M. A., Liu, J., and Magalhaes, J. V. (2015). Plant adaptation to acid soils: the molecular basis for crop aluminum resistance. *Annu. Rev. Plant Biol.* 66, 571–598. doi: 10.1146/annurev-arplant-043014-114822
- Kohorn, B. D., Hoon, D., Minkoff, B. B., Sussman, M. R., and Kohorn, S. L. (2016). Rapid oligo-galacturonide induced changes in protein phosphorylation in *Arabidopsis*. *Mol. Cell. Proteom.* 15, 1351–1359. doi: 10.1074/mcp.M115.055368
- Kohorn, B. D., and Kohorn, S. L. (2012). The cell wall-associated kinases, WAKs, as pectin receptors. *Front. Plant Sci.* 3:88. doi: 10.3389/fpls.2012.00088
- Larsen, P. B., Cancel, J., Rounds, M., and Ochoa, V. (2007). *Arabidopsis* ALS1 encodes a root tip and stele localized half type ABC transporter required for root growth in an aluminum toxic environment. *Planta* 225, 1447–1458. doi: 10.1007/s00425-006-0452-4
- Larsen, P. B., Geisler, M. J. B., Jones, C. A., Williams, K. M., and Cancel, J. D. (2005). ALS3 encodes a phloem-localized ABC transporter-like protein that is required for aluminum tolerance. *Plant J.* 41, 353–363. doi: 10.1111/j.1365-313X.2004.02306.x
- Larsen, P. B., Kochian, L. V., and Howell, S. H. (1997). Al inhibits both shoot development and root growth in als3, an Al-sensitive *Arabidopsis* mutant. *Plant Physiol.* 114, 1207–1214. doi: 10.1104/pp.114.4.1207
- Larsen, P. B., Tai, C. Y., Kochian, L. V., and Howell, S. H. (1996). *Arabidopsis* mutants with increased sensitivity to aluminum. *Plant Physiol.* 110, 743–751. doi: 10.1104/pp.110.3.743
- Leiser, W. L., Rattunde, H. F. W., Weltzien, E., Cisse, N., Abdou, M., Diallo, A., et al. (2014). Two in one sweep: aluminum tolerance and grain yield in P-limited soils are associated to the same genomic region in West African Sorghum. *BMC Plant Biol.* 14:206. doi: 10.1186/s12870-014-0206-6
- Li, H., Zhou, S. Y., Zhao, W. S., Su, S. C., and Peng, Y. L. (2009). A novel wall-associated receptor-like protein kinase gene, OsWAK1, plays important roles in rice blast disease resistance. *Plant Mol. Biol.* 69, 337–346. doi: 10.1007/s11103-008-9430-5
- Li, X., Zeng, R., and Liao, H. (2016). Improving crop nutrient efficiency through root architecture modifications. *J. Integr. Plant Biol.* 58, 193–202. doi: 10.1111/jipb.12434
- Ligaba, A., Dreyer, I., Margaryan, A., Schneider, D. J., Kochian, L., and Piñeros, M. (2013). Functional, structural and phylogenetic analysis of domains underlying the Al sensitivity of the aluminum-activated malate/anion transporter, TaALMT1. *Plant J.* 76, 766–780. doi: 10.1111/tjp.12332
- Lim, C. W., Yang, S. H., Shin, K. H., Lee, S. C., and Kim, S. H. (2014). The AtLRK10L1.2, *Arabidopsis* ortholog of wheat LRK10, is involved in ABA-mediated signaling and drought resistance. *Plant Cell Rep.* 34, 447–455. doi: 10.1007/s00299-014-1724-2
- Lima, J. C., Arenhart, R. A., Margis-Pinheiro, M., and Margis, R. (2011). Aluminum triggers broad changes in microRNA expression in rice roots. *Genet. Mol. Res.* 10, 2817–2832. doi: 10.4238/2011.November.10.4
- Liu, J., Magalhaes, J. V., Shaff, J., and Kochian, L. V. (2009). Aluminum-activated citrate and malate transporters from the MATE and ALMT families function independently to confer *Arabidopsis aluminum* tolerance. *Plant J.* 57, 389–399. doi: 10.1111/j.1365-313X.2008.03696.x
- Liu, M. Y., Lou, H. Q., Chen, W. W., Piñeros, M. A., Xu, J. M., Fan, W., et al. (2018). Two citrate transporters coordinately regulate citrate secretion from rice bean root tip under aluminum stress. *Plant. Cell Environ.* 41, 809–822. doi: 10.1111/pce.13150
- López-Arredondo, D. L., Leyva-González, M. A., González-Morales, S. I., López-Bucio, J., and Herrera-Estrella, L. (2014). Phosphate nutrition: improving low-phosphate tolerance in crops. *Annu. Rev. Plant Biol.* 65, 95–123. doi: 10.1146/annurev-arplant-050213-035949
- Lynch, J. P. (2011). Root phenes for enhanced soil exploration and phosphorus acquisition: tools for future crops. *Plant Physiol.* 156, 1041–1049. doi: 10.1104/pp.111.175414
- Lynch, J. P., and Brown, K. M. (2001). Topsoil foraging – An architectural adaptation of plants to low phosphorus availability. *Plant Soil* 237, 225–237. doi: 10.1023/A:1013324727040
- Ma, J. F., Ryan, P. R., and Delhaize, E. (2001). Aluminium tolerance in plants and the complexing role of organic acids. *Trends Plant Sci.* 6, 273–278. doi: 10.1016/S1360-1385(01)01961-6
- Magalhaes, J. V., Garvin, D. F., Wang, Y., Sorrells, M. E., Klein, P. E., Schaffert, R. E., et al. (2004). Comparative mapping of a major aluminum tolerance gene in sorghum and other species in the Poaceae. *Genetics* 167, 1905–1914. doi: 10.1534/genetics.103.023580

- Magalhaes, J. V., Liu, J., Guimarães, C. T., Lana, U. G. P., Alves, V. M. C., Wang, Y.-H., et al. (2007). A gene in the multidrug and toxic compound extrusion (MATE) family confers aluminum tolerance in sorghum. *Nat. Genet.* 39, 1156–1161. doi: 10.1038/ng2074
- Mangeon, A., Pardal, R., Menezes-Salgueiro, A. D., Duarte, G. L., de Seixas, R., Cruz, F. P., et al. (2016). AtGRP3 is implicated in root size and aluminum response pathways in *Arabidopsis*. *PLoS One* 11:e0150583. doi: 10.1371/journal.pone.0150583
- Maron, L. G., Piñeros, M. A., Guimarães, C. T., Magalhaes, J. V., Pleiman, J. K., Mao, C., et al. (2009). Two functionally distinct members of the MATE (multi-drug and toxic compound extrusion) family of transporters potentially underlie two major aluminum tolerance QTLs in maize. *Plant J.* 61, 728–740. doi: 10.1111/j.1365-3113X.2009.04103.x
- Marschner, H. (ed.). (1995). “Adaptation of plants to adverse chemical soil conditions,” in *Mineral Nutrition of Higher Plants* (London: Academic Press), 596–657. doi: 10.1016/B978-012473542-2/50018-3
- Melo, J. O., Lana, U. G. P., Piñeros, M. A., Alves, V. M. C., Guimarães, C. T., Liu, J., et al. (2013). Incomplete transfer of accessory loci influencing SbMATE expression underlies genetic background effects for aluminum tolerance in sorghum. *Plant J.* 73, 276–288. doi: 10.1111/tj.12029
- Mendes, F. F., Guimarães, L. J. M., Souza, J. C., Guimarães, P. E. O., Magalhaes, J. V., Garcia, A. A. F., et al. (2014). Genetic architecture of phosphorus use efficiency in tropical maize cultivated in a low-P soil. *Crop Sci.* 54, 1530–1538. doi: 10.2135/cropsci2013.11.0755
- Mora-Macías, J., Ojeda-Rivera, J. O., Gutiérrez-Alanís, D., Yong-Villalobos, L., Oropeza-Aburto, A., Raya-González, J., et al. (2017). Malate-dependent Fe accumulation is a critical checkpoint in the root developmental response to low phosphate. *Proc. Natl. Acad. Sci. U.S.A.* 114, E3563–E3572. doi: 10.1073/pnas.1701128114
- Morita, Y., Kataoka, A., Shiota, S., Mizushima, T., and Tsuchiya, T. (2000). NorM of *Vibrio parahaemolyticus* is an Na⁺-driven multidrug efflux pump. *J. Bacteriol.* 182, 6694–6697. doi: 10.1128/JB.182.23.6694-6697.2000
- Müller, J., Toev, T., Heisters, M., Teller, J., Moore, K. L., Hause, G., et al. (2015). Iron-dependent callose deposition adjusts root meristem maintenance to phosphate availability. *Dev. Cell* 33, 216–230. doi: 10.1016/j.devcel.2015.02.007
- Nezames, C. D., Sjogren, C. A., Barajas, J. F., and Larsen, P. B. (2012). The *Arabidopsis* cell cycle checkpoint regulators TANMEI/ALT2 and ATR mediate the active process of aluminum-dependent root growth inhibition. *Plant Cell Online* 24, 608–621. doi: 10.1105/tpc.112.095596
- Nobel, P. S. (1991). *Physicochemical and Environmental Plant Physiology*. London: Academic Press.
- Novais, R. F., and Smith, T. F. (1999). “Difusão,” in *Fósforo em Solo e Planta em Condições Tropicais*, eds R. F. Novais and T. F. Smith (San Francisco, CA: Scribd), 213–234.
- Omote, H., Hiasa, M., Matsumoto, T., Otsuka, M., and Moriyama, Y. (2006). The MATE proteins as fundamental transporters of metabolic and xenobiotic organic cations. *Trends Pharmacol. Sci.* 27, 587–593. doi: 10.1016/j.tips.2006.09.001
- Park, A. R., Cho, S. K., Yun, U. J., Jin, M. Y., Lee, S. H., Sachetto-Martins, G., et al. (2001). Interaction of the *Arabidopsis* receptor protein kinase Wak1 with a glycine-rich protein, AtGRP-3. *J. Biol. Chem.* 276, 26688–26693. doi: 10.1074/jbc.M101283200
- Piñeros, M. A., Cancado, G. M. A., and Kochian, L. V. (2008). Novel properties of the wheat aluminum tolerance organic acid transporter (TaALMT1) revealed by electrophysiological characterization in *Xenopus oocytes*: functional and structural implications. *Plant Physiol.* 147, 2131–2146. doi: 10.1104/pp.108.119636
- Postma, J. A., Dathe, A., and Lynch, J. P. (2014). The optimal lateral root branching density for maize depends on nitrogen and phosphorus availability. *Plant Physiol.* 166, 590–602. doi: 10.1104/pp.113.233916
- Ramesh, S. A., Kamran, M., Sullivan, W., Chirkova, L., Okamoto, M., Degryse, F., et al. (2018). Aluminum-activated malate transporters can facilitate GABA transport. *Plant Cell* 30, 1147–1164. doi: 10.1105/tpc.17.00864
- Ramesh, S. A., Tyerman, S. D., Xu, B., Bose, J., Kaur, S., Conn, V., et al. (2015). GABA signalling modulates plant growth by directly regulating the activity of plant-specific anion transporters. *Nat. Commun.* 6:7879. doi: 10.1038/ncomms8879
- Rea, P. A. (2007). Plant ATP-binding Cassette transporters. *Annu. Rev. Plant Biol.* 58, 347–375. doi: 10.1146/annurev.arplant.57.032905.105406
- Rounds, M. A., and Larsen, P. B. (2008). Aluminum-dependent root-growth inhibition in *Arabidopsis* results from AtATR-regulated cell-cycle arrest. *Curr. Biol.* 18, 1495–1500. doi: 10.1016/j.cub.2008.08.050
- Rudrappa, T., Czymbek, K. J., Paré, P. W., and Bais, H. P. (2008). Root-secreted malic acid recruits beneficial soil bacteria. *Plant Physiol.* 148, 1547–1556. doi: 10.1104/pp.108.127613
- Ryan, P. R., Raman, H., Gupta, S., Horst, W. J., and Delhaize, E. (2009). A second mechanism for aluminum resistance in wheat relies on the constitutive efflux of citrate from roots. *Plant Physiol.* 149, 340–351. doi: 10.1104/pp.108.129155
- Sanches, P. A., and Salinas, J. G. (1981). Low input technology for managing oxisol and utisols in tropical America. *Adv. Agron.* 34, 229–406.
- Sánchez-Calderón, L., López-Bucio, J., Chacón-López, A., Cruz-Ramírez, A., Nieto-Jacobo, F., Dubrovsky, J. G., et al. (2005). Phosphate starvation induces a determinate developmental program in the roots of *Arabidopsis thaliana*. *Plant Cell Physiol.* 46, 174–184. doi: 10.1093/pcp/pci011
- Sasaki, T., Yamamoto, Y., Ezaki, B., Katsuhara, M., Ahn, S. J., Ryan, P. R., et al. (2004). A wheat gene encoding an aluminum-activated malate transporter. *Plant J.* 37, 645–653. doi: 10.1111/j.1365-3113X.2003.01991.x
- Sawaki, Y., Iuchi, S., Kobayashi, Y. Y., Kobayashi, Y. Y., Ikka, T., Sakurai, N., et al. (2009). STOP1 regulates multiple genes that protect *Arabidopsis* from proton and aluminum toxicities. *Plant Physiol.* 150, 281–294. doi: 10.1104/pp.108.134700
- Sharma, T., Dreyer, I., Kochian, L., and Piñeros, M. A. (2016). The ALMT family of organic acid transporters in plants and their involvement in detoxification and nutrient security. *Front. Plant Sci.* 7:1488. doi: 10.3389/fpls.2016.01488
- Shaw, J. N. (2001). Iron and aluminum oxide characterization for highly-weathered Alabama ultisols. *Commun. Soil Sci. Plant Anal.* 32, 49–64. doi: 10.1081/CSS-100102992
- Shiu, S., and Bleecker, A. B. (2003). Expansion of the receptor-like kinase/Pelle gene family and receptor-like proteins in *Arabidopsis*. *Plant Physiol.* 132, 530–543. doi: 10.1104/pp.103.021964.tochaud
- Silva, C. M. S., Zhang, C., Habermann, G., Delhaize, E., and Ryan, P. R. (2018). Does the major aluminium-resistance gene in wheat, TaALMT1, also confer tolerance to alkaline soils? *Plant Soil* 424, 451–462. doi: 10.1007/s11104-017-3549-6
- Sivaguru, M., Ezaki, B., He, Z. H., Tong, H., Osawa, H., Baluska, F., et al. (2003). Aluminum-induced gene expression and protein localization of a cell wall-associated receptor kinase in *Arabidopsis*. *Plant Physiol.* 132, 2256–2266. doi: 10.1104/pp.103.022129.plasma
- Sjogren, C. A., Bolaris, S. C., and Larsen, P. B. (2015). Aluminum-dependent terminal differentiation of the *Arabidopsis* root tip is mediated through an ATR-, ALT2-, and SOG1-regulated transcriptional response. *Plant Cell* 27, 2501–2515. doi: 10.1105/tpc.15.00172
- Sjogren, C. A., and Larsen, P. B. (2017). SUV2, which encodes an ATR-related cell cycle checkpoint and putative plant ATRIP, is required for aluminium-dependent root growth inhibition in *Arabidopsis*. *Plant Cell Environ.* 40, 1849–1860. doi: 10.1111/pce.12992
- Tanihara, Y., Masuda, S., Sato, T., Katsura, T., Ogawa, O., and Inui, K. (2007). Substrate specificity of MATE1 and MATE2-K, human multidrug and toxin extrusions/H⁺-organic cation antiporters. *Biochem. Pharmacol.* 74, 359–371. doi: 10.1016/j.bcp.2007.04.010
- Tanksley, S. D., and McCouch, S. R. (1997). Seed banks and molecular maps: unlocking genetic potential from the wild. *Science* 277, 1063–1066. doi: 10.1126/science.277.5329.1063
- Tovkach, A., Ryan, P. R., Richardson, A. E., Lewis, D. C., Rathjen, T. M., Ramesh, S., et al. (2013). Transposon-mediated alteration of TaMATE1B expression in wheat confers constitutive citrate efflux from root apices. *Plant Physiol.* 161, 880–892. doi: 10.1104/pp.112.207142
- Tully, K., Sullivan, C., Weil, R., and Sanchez, P. (2015). The state of soil degradation in sub-Saharan Africa: baselines, trajectories, and solutions. *Sustain* 7, 6523–6552. doi: 10.3390/su7066523
- Verica, J., and He, Z. (2002). The cell wall-associated kinase (WAK) and WAK-like kinase gene family. *Plant Physiol.* 129, 455–459. doi: 10.1104/pp.011028.1
- von Uexküll, H. R., and Mutert, E. (1995). Global extent, development and economic impact of acid soils. *Plant Soil* 171, 1–15. doi: 10.1007/BF00009558
- Wang, J., Raman, H., Zhou, M., Ryan, P. R., Delhaize, E., Hebb, D. M., et al. (2007). High-resolution mapping of the Alp locus and identification of a candidate

- gene HvMATE controlling aluminium tolerance in barley (*Hordeum vulgare* L.). *Theor. Appl. Genet.* 115, 265–276. doi: 10.1007/s00122-007-0562-9
- Wang, N., Huang, H.-J., Ren, S.-T., Li, J.-J., Sun, Y., Sun, D.-Y., et al. (2012). The rice wall-associated receptor-like kinase gene OsDEES1 plays a role in female gametophyte development. *Plant Physiol.* 160, 696–707. doi: 10.1104/pp.112.203943
- Wang, Y., Li, R., Li, D., Jia, X., Zhou, D., Li, J., et al. (2017). NIP1;2 is a plasma membrane-localized transporter mediating aluminum uptake, translocation, and tolerance in *Arabidopsis*. *Proc. Natl. Acad. Sci. U.S.A.* 114, 5047–5052. doi: 10.1073/pnas.1618557114
- Xia, J., Yamaji, N., Kasai, T., and Ma, J. F. (2010). Plasma membrane-localized transporter for aluminum in rice. *Proc. Natl. Acad. Sci. U.S.A.* 107, 18381–18385. doi: 10.1073/pnas.1004949107
- Yamaji, N., Huang, C. F., Nagao, S., Yano, M., Sato, Y., Nagamura, Y., et al. (2009). A zinc finger transcription factor ART1 regulates multiple genes implicated in aluminum tolerance in rice. *Plant Cell* 21, 3339–3349. doi: 10.1105/tpc.109.070771
- Yang, K., Qi, L., and Zhang, Z. (2014). Isolation and characterization of a novel wall-associated kinase gene TaWAK5 in wheat (*Triticum aestivum*). *Crop J.* 2, 255–266. doi: 10.1016/j.cj.2014.04.010
- Yang, X. Y., Yang, J. L., Zhou, Y., Piñeros, M. A., Kochian, L. V., Li, G. X., et al. (2011). A de novo synthesis citrate transporter, *Vigna umbellata* multidrug and toxic compound extrusion, implicates in Al-activated citrate efflux in rice bean (*Vigna umbellata*) root apex. *Plant Cell Environ.* 34, 2138–2148. doi: 10.1111/j.1365-3040.2011.02410.x
- Yokosho, K., Yamaji, N., Fujii-Kashino, M., and Ma, J. F. (2016). Functional analysis of a MATE gene OsFRDL2 revealed its involvement in Al-induced secretion of citrate, but a lower contribution to Al tolerance in rice. *Plant Cell Physiol.* 57, 976–985. doi: 10.1093/pcp/pcw026
- Yokosho, K., Yamaji, N., and Ma, J. F. (2011). An Al-inducible MATE gene is involved in external detoxification of Al in rice. *Plant J.* 68, 1061–1069. doi: 10.1111/j.1365-313X.2011.04757.x
- Zhang, W.-H., Ryan, P. R., Sasaki, T., Yamamoto, Y., Sullivan, W., and Tyerman, S. D. (2008). Characterization of the TaALMT1 protein as an Al³⁺-activated anion channel in transformed tobacco (*Nicotiana tabacum* L.) cells. *Plant Cell Physiol.* 49, 1316–1330. doi: 10.1093/pcp/pcn107
- Zhu, J., and Lynch, J. P. (2004). The contribution of lateral rooting to phosphorus acquisition efficiency in maize (*Zea mays*) seedlings. *Funct. Plant Biol.* 31:949. doi: 10.1071/FP04046
- Zuo, W., Chao, Q., Zhang, N., Ye, J., Tan, G., Li, B., et al. (2015). A maize wall-associated kinase confers quantitative resistance to head smut. *Nat. Genet.* 47, 151–157. doi: 10.1038/ng.3170

Conflict of Interest Statement: The authors declare that the research was conducted in the absence of any commercial or financial relationships that could be construed as a potential conflict of interest.

The reviewer MD and handling Editor declared their shared affiliation.

Copyright © 2018 Magalhaes, Piñeros, Maciel and Kochian. This is an open-access article distributed under the terms of the Creative Commons Attribution License (CC BY). The use, distribution or reproduction in other forums is permitted, provided the original author(s) and the copyright owner(s) are credited and that the original publication in this journal is cited, in accordance with accepted academic practice. No use, distribution or reproduction is permitted which does not comply with these terms.

OBJETIVOS

Objetivo Geral

Validar a função dos genes *PSTOL1* na modulação do sistema radicular de milho e sorgo.

Objetivos Específicos

Capítulo 2

Avaliar as modificações morfológicas do sistema radicular, o acúmulo de biomassa e o conteúdo de fósforo de plantas de milho transgênico com superexpressão dos genes *OsPSTOL1*, *SbPSTOL1* e *ZmPSTOL1*, cultivados em solo com baixa disponibilidade de P.

Capítulo 3

Classificar filogeneticamente as proteínas S**p**PSTOL1

Confirmar os modelos gênicos dos genes *SbPSTOL1*

Investigar os mecanismos regulatórios envolvidos no controle transcricional dos genes *SbPSTOL1*

Definir a localização subcelular das proteínas S**p**PSTOL1

CAPÍTULO 2

Overexpression of *PSTOL1-like* genes increases root surface area and biomass accumulation for maize cultivated under low P availability

Overexpression of *PSTOLI*-like genes increases root surface area and biomass accumulation for maize cultivated under low P availability

Laiane S. Maciel^{a,c,1}, Bárbara F. Negri^{a,b,1}, Antônio Marcos Coelho^a, Beatriz A. Barros^a, Claudia T Guimarães^{a,b,c*}, Sylvania M. de Sousa^{a,b*}, Jurandir V. Magalhães^{a,b,c*}.

^aEmbrapa Milho e Sorgo, 35701-970 Sete Lagoas, MG, Brazil

^bUniversidade Federal de São João Del Rei, 36301-160 São Joao Del Rei, MG, Brazil

^cUniversidade Federal de Minas Gerais, 31270-901 Belo Horizonte, MG, Brazil

¹L.S.M and B.F.N contributed equally to this work.

*Corresponding author

ABSTRACT

Low phosphorus (P) availability in the soil is one of the major constraints for crop development and grain yield, mainly in tropical regions. In tropical soils, the bioavailability of P is low due to its fixation in the soil clay fraction with iron (Fe) and aluminum (Al) oxides. In order to adapt to this limitation, plants have developed different mechanisms to maximize P acquisition efficiency. These changes include alterations in root morphology and architecture in order to increase the area of the soil explored by the roots. In rice (*Oryza sativa*), the protein kinase *Phosphorus-Starvation Tolerance1* (*OsPSTOLI*) enhances total root length and total root surface area, increasing P acquisition and grain yield under P deficiency. *OsPSTOLI* homologs in sorghum (*Sorghum bicolor*, *SbPSTOLI*) and maize (*Zea mays*, *ZmPSTOLI*) were characterized via QTL and association mapping, and were found to affect root morphology and architecture under P deficiency. In addition, *SbPSTOLI* genes were associated with increased P acquisition and grain yield under low P availability in the soil. We overexpressed *OsPSTOLI*, *SbPSTOLI* (*Sb07g002840*, *Sb03g031690* and *Sb03g006765*) and *ZmPSTOLI* (*ZmPSTOLI_8.05*, *ZmPSTOLI_3.06* and *ZmPSTOLI_8.02*) in maize B104 in order to functionally characterize the role of these genes. Our data showed a strong negative correlation between root diameter and root length, and moreover, a strong positive correlation between root length with shoot dry weight. These results suggest that *OsPSTOLI* and *SbPSTOLI* genes in maize modulate the root system by increasing proliferation of very fine roots enhancing P uptake and biomass accumulation under low and high P conditions. No significant differences were detected between the *ZmPSTOLI* events and the non-transgenic line, possibly because B104 express high endogenous levels of the *ZmPSTOLI* genes. All evidence so far, indicate that *PSTOLI* genes have a more general role in the root system, which resulted in the enhanced P acquisition, which could benefit cereal production worldwide.

INTRODUCTION

One of the greatest challenges in modern agriculture is to increase food production without expanding agriculture into new areas to preserve the environment and biodiversity. Thus, although food production needs to be increased at a global scale to cope with a continuously growing population (Godfray *et al.*, 2010; Rojas *et al.*, 2016), efficient production systems are equally essential for sustainability. Most of the crop production areas in the world are located on tropical and subtropical regions, where the soils are often acidic (von Uexküll and Mutert, 1995; Lynch, 2011).

The clay fraction of the tropical soils is enriched in Al and Fe oxides, which bind stably to soil P, restricting bioavailability (Marschner, 1996; Heuer *et al.*, 2009). In addition, P shows low mobility in the soil and is more available in the soil superficial layer [0-20 cm (Raghothama, 1999; Rausch and Bucher, 2002; Vance *et al.*, 2003)]. Soil amendment with P fertilizers is the most common strategy to increase yield on soils with low-P availability. However, phosphate fertilizers are extracted from rock phosphate reserves, a natural non-renewable resource that can be depleted over the next 50 years; in addition, intensive use of P-fertilizers increases production costs (Cordell *et al.*, 2009; Sattari *et al.*, 2012). Therefore, the development of cultivars that use P more efficiently becomes an important strategy to improve food security worldwide.

Phosphorus is an essential macronutrient for plant growth and development (Abel *et al.*, 2002; Vance *et al.*, 2003; Niu *et al.*, 2013). Plants acquire P from the soil solution in the orthophosphate forms, H_2PO_4^- and HPO_4^{2-} . Throughout evolution, plants have developed mechanisms to overcome low-P availability in the soil, which act to optimize P internal utilization or to enhance P acquisition from the soil (Vance *et al.*, 2003). The mechanisms of internal translocation and acquisition of P are orchestrated by modulation of phosphate transporters, exudation of organic acids, secretion of phosphatases, association with mycorrhizae, chemical modifications of the rhizosphere, root morphology and architecture remodeling (Reviewed by Lopez-Arredondo *et al.*, 2014). Previous studies indicated that P use efficiency in maize and sorghum cultivated on a tropical low-P soils is largely determined by mechanisms that act to enhance P acquisition rather than internal efficiency mechanisms (Parentoni and Souza, 2008; Mendes *et al.*, 2014; Bernardino *et al.*, 2019).

Changes in root morphology and architecture, such as adventitious root proliferation and changes in crown root angle, lead to a broader dispersion of lateral branching that may enhance P uptake (Lynch, 2011; Lambers *et al.*, 2011, 2013). Increase of shallow roots increase topsoil foraging where most of P is available. In maize, increased adventitious root length has been considered as an adaptive response that enable plants to explore more efficiently soil patches enriched in P (Richardson *et al.*, 2011). The density, length and longevity of root hairs are also relevant for P efficiency. In common bean (*Phaseolus vulgaris*), genotypes with both long root

hairs and shallow roots had 298% greater biomass accumulation than short-haired, deep-rooted phenotypes under low P-conditions when grown in a low-P soil (Miguel *et al.*, 2015).

Identification of genes that control root morphology and architecture provide important leads to enhance crop yield under low-P availability (Gamuyao *et al.*, 2012; Ma *et al.*, 2013; Li *et al.*, 2016; Lee *et al.*, 2016; Wang *et al.*, 2017; Chen *et al.*, 2018; Zhang *et al.*, 2018). In rice, *Phosphorus-Starvation Tolerance 1* (*OsPSTOL1*) enhances root surface area, P acquisition and grain yield in rice cultivated under low-P conditions. *OsPSTOL1* is a serine/threonine receptor-like kinase of the LRK10L-2 subfamily, involved in the development control of early root growth (Gamuyao *et al.*, 2012). Proteins that share more than 55% identity with *OsPSTOL1* were identified in sorghum (*SbPSTOL1*) and maize (*ZmPSTOL1*) (Hufnagel *et al.*, 2014; Azevedo *et al.*, 2015). QTL mapping indicated that *SbPSTOL1* genes co-localize with QTLs related to root morphology and increased performance in soils with low P availability (Hufnagel *et al.*, 2014; Bernardino *et al.*, 2019). In addition, single-nucleotide polymorphisms (SNPs) within *SbPSTOL1* genes were associated with grain yield, root morphology, and root system architecture under low P conditions (Hufnagel *et al.*, 2014). In maize, *ZmPSTOL1* genes also co-localized with QTLs related to root morphology and P acquisition efficiency (Azevedo *et al.*, 2015).

OsPSTOL1 as well as maize and sorghum *PSTOL1*-like proteins share a conserved serine/threonine kinase C-terminal domain. The sorghum *SbPSTOL1* proteins differed from the rice and maize *PSTOL1* proteins by the presence of an extracellular N-terminal portion, composed of a cysteine-rich wall-associated receptor kinase galacturonan-binding (Gub), and an also cysteine-rich wall-associated receptor kinase C-terminal (Wak) domain (Hufnagel *et al.*, 2014). Here, we overexpressed the genes *OsPSTOL1*, *Sb07g002840*, *Sb03g006765*, *Sb03g031690*, *ZmPSTOL1_8.05*, *ZmPSTOL1_3.06*, *ZmPSTOL1_8.03* driven by the ubiquitin promoter in maize to characterize their function in root morphology and biomass accumulation in a low-P soil. Our data demonstrated that the overexpression of *OsPSTOL1* and *SbPSTOL1*, but not of the *ZmPSTOL1* homologs, enhanced total root length and shoot biomass for maize cultivated in low and high-P soils. These results suggest *OsPSTOL1* and *SbPSTOL1* may have a more global effect than simply increasing P uptake, leading to enhanced uptake of other mineral nutrients and possibly water.

MATERIALS AND METHODS

Maize transformation via *Agrobacterium tumefaciens* with rice, maize and sorghum *PSTOL1*

The coding sequence of *Sb07g002840*, *Sb03g006765*, *Sb03g031690* were obtained from the sorghum BR007 line (Hufnagel *et al.*, 2014). *ZmPSTOL1_8.05* and *ZmPSTOL1_8.03*

sequences were obtained from the maize line L22, whereas *ZmPSTOL1_3.06* sequence was obtained from L3 (Azevedo *et al.*, 2015). These coding sequences in addition to *OsPSTOL1* (BAK26566) were synthesized by Genscript (Piscataway, NJ). The *PSTOL1* genes were introduced into the pMCG1005 binary vector (McGinnis *et al.*, 2005), where gene expression is driven by the maize ubiquitin promoter (Ubi), and contained the *octopine synthase* gene terminator from *Agrobacterium tumefaciens* (OCs3'). This plasmid contains the *phosphinothricin acetyltransferase* gene (*Bar*) as the plant selection marker, whose expression is driven by the CaMV35S promoter, and contained the *Nopaline synthase* gene terminator from *A. tumefaciens* [NOS (Fig. 2A)].

Maize transformation of the inbred line B104 was mediated by *A. tumefaciens* and carried out at Iowa State University Plant Transformation Center (Iowa State University, Ames, IA), according to Frame *et al.* (2011). The events were named according to the gene used in the transformation (*OsPSTOL1*, *Sb07g002840*, *Sb03g031690*, *Sb03g006765*, *ZmPSTOL1_8.05*, *ZmPSTOL1_3.06* and *ZmPSTOL1_8.02*) followed by the underline character () and the event number (1 to 21).

The maize transgenic progeny T1 was obtained backcrossing the regenerated events T0 with wild -type B104. First, the 204 independent transgenic events for all constructs were grown in a paper pouch system for 14 days in hydroponics with low P (2.5 μ M) and sprayed with 0.5% Finale® herbicide [glufosinate ammonium (Bayer CropScience)], to eliminate the non-transgenic plants. A bulk of nine plants was used to evaluate *PSTOL1* expression by quantitative real-time PCR (qRT-PCR), and together with total root length trait was used to select the events for the next generations.

Forty-six independent transgenic events were grown in greenhouse and self-pollinated to obtain T2 progeny. Sixteen seeds from each T2 event, were soaked with 0.2% Finale and incubated at 20 °C for 6 hours, before being planted in soil. DNA from each individual plant was extracted and a semi-quantitative PCR was performed to screen for homozygous plants. T2 events with one copy were self-pollinated to multiply homozygous plants (T3 and T4), that were used for phenotypic characterization under hydroponics and greenhouse conditions. Mendelian segregation based on herbicide resistance was tested for maize transgenic generations T1 and T4 using the chi-square test (χ^2).

Phenotypic assessment of root morphology in hydroponics

Root morphology traits were assessed in nutrient solution as described by de Sousa *et al.* (2012), using a randomized block design with three replicates. Maize seeds were surface-sterilized using 0.5% (w/v) sodium hypochlorite, washed with distilled water and placed in moistened paper rolls. After 4 days, uniform seedlings were transferred to moistened blotting

papers and placed into paper pouches (24 × 33 × 0.02 cm) after removing the endosperm (de Sousa *et al.*, 2012).

Each experimental unit consisted of one pouch with three seedlings per pouch, whose bottom 3 cm was immersed in containers filled with 5 L of modified Magnavaca's nutrient solution (Magnavaca *et al.*, 1987) at pH 5.65 and 2.5 μM P, which was changed every three days. The containers were kept in a growth chamber at 27/20° C day/night temperatures and a 12-h photoperiod under continuous aeration.

After 13 days, root images were acquired using a digital camera Nikon D300S SLR. Images were analyzed using the RootReader2D (<http://www.plantmineralnutrition.net/software/rootreader2d/>) and WinRhizo (<http://www.regent.qc.ca/>) softwares. We assessed total root length (cm), average root diameter (mm), total root surface area (cm²), surface area of very fine roots with diameter between 0 and 1 mm (cm²), surface area of fine roots with diameter between 1 and 2 mm (cm²), shoot dry weight (mg) and shoot P content (g).

Root tissues were frozen in liquid nitrogen and stored at -80° C until RNA extraction and shoot tissues were dried at 65°C in a forced-air oven until constant weight to obtain shoot dry weight. For P concentration analysis, shoot tissues were subjected to a nitric perchloric acid digestion followed by P quantification with an inductively-coupled argon plasma (ICP) emission spectrometry (Silva, 2009). Phosphorus content was calculated by multiplying dry weight and P concentration.

Expression analysis of *PSTOLI* genes under low-P

Total RNA was isolated from a bulk of nine roots grown in nutrient solution with low P, using the SV Total RNA Isolation System kit (Promega, Madison, WI), according to the manufacturer's instructions. Total RNA (1 μg) was used for cDNA synthesis using the High Capacity cDNA Reverse Transcription kit (Applied Biosystems, Foster City, CA). Transcript expression levels were assessed by quantitative real-time PCR (qPCR-RT) using SYBR Green I (for *OsPSTOLI* and *SbPSTOLI* genes) and TaqMan (for *ZmPSTOLI* genes) assays in ABI Prism 7500 Fast System (Applied Biosystems, Foster City, CA), using *18s rRNA* as an endogenous constitutive control and gene-specific primers (Table S1). Calculation of relative gene expression with three technical replicates was performed using the 2^{-ΔΔC_t} method (Schmittgen and Livak, 2008).

Phenotypic assessment of maize biomass accumulation and plant height under low and high P concentrations in the soil

The experiment was conducted in a greenhouse using a randomized complete block design with four replicates. Each experimental unit consisted of a pot with three plants. The soil was a red-latosol with very clayey texture, pH 6.0 and low P (2.8 mg/dm³), supplemented with 2 g/kg of the dolomite lime and 0.5 g/kg of gypsum. For the high P treatment, 0.225 g of super triple phosphate per kg of soil was added.

Seeds of transgenics events were surface-sterilized using sodium hypochlorite 0.5% for 5 min, washed with distilled water and placed in moistened paper rolls. After seven days, three uniform seedlings of each transgenic event were transferred to pots containing 30 kg of soil. One gram of urea was added to each pot, 15 and 30 days after transplanting. Irrigation was performed daily based on the field capacity.

After 45 days of transplanting, plant height was determined by measuring the distance from the base of the stem to the last fully expanded leaf. Then, the shoots were harvested and dried at 65°C in a forced-air oven until constant weight. Shoot was ground in a Wiley mill prior determining P content. Chemical analyses were conducted in the Plant Chemical Analysis Laboratory at Embrapa Maize and Sorghum using inductively-coupled argon plasma (ICP-OES) (Nogueira and Souza 2005).

Statistical analyses

Analysis of variance (ANOVA) was performed using the package *Agricole* (Mendiburu, 2019) in R (RCore Team, 2018). Differences between means were assessed by the t-test considering a 5% significance level (α). Scott-Knott clustering analyses were performed considering 5%, 10% and 15% significance level for root morphology, shoot dry weight and plant height, respectively [α (Jelihovschi, 2014)]. Pearson's correlation coefficients were estimated based on trait means for root morphology, shoot dry weight, shoot P content, and *PSTOL1* gene expression [measured by delta Ct (Zhang et al., 2015)] with the R package *Psych* (Revelle, 2018).

RESULTS

Root morphology of non-transgenic lines

In order to phenotypically characterize the non-transgenic background, the root system of B104 was initially compared with L3 and L22, which were previously classified as P-efficient and P-inefficient lines, respectively based on grain yield assessed in low-P soil (Parentoni et al., 2010; de Sousa *et al.*, 2012). In addition, L3 and L22 were used as parents of the RIL population that previously indicated that the *PSTOL1-like* genes in maize co-localize with QTLs for root

morphology, biomass accumulation and P content (Azevedo *et al.*, 2015).

The P-efficient line, L3, showed higher total root length, total root surface area, surface area of very fine roots and fine roots compared to L22 (Fig. 1A-B). Shoot dry weight and shoot P content in a low-P nutrient solution were also higher in L3 compared to L22. These results confirm previous findings indicating that L3 is more efficient than L22, to some extent due to root morphology changes that enhances P acquisition efficiency (de Sousa *et al.*, 2012). Total root length and surface area of fine roots in B104 was higher compared to L3.

B104 showed higher expression of the *ZmPSTOL1* genes, *ZmPSTOL1_8.05*, *ZmPSTOL1_3.06* and *ZmPSTOL1_8.02* (Fig. 1C) than L3. B104 genome was recently sequenced (www.maizegdb.org) and harbors one copy of each *ZmPSTOL1*.

Selection of transgenics events

The maize line B104 was transformed with the constructs shown in Fig. 2A. Twenty-one independent T3 transgenic maize events were selected from a total of forty-six independent T1 transgenic maize events. The selection was based on the increase in total root length under low P availability compared to B104. (Table S2). At least one T3 event for each transgenic maize construct (*OsPSTOL1_1*, *Sb07g002840_5*, *Sb03g031690_8*, *Sb03g06765_10*, *Sb03g06765_11*, *ZmPSTOL1_8.05_14*, *ZmPSTOL1_3.06_18* and *ZmPSTOL1_8.02_19*) increased total root length under low availability P (Table S2). Segregation analysis in the T4 generation indicated that the maize events for *OsPSTOL1_1*, *Sb07g002840_5*, *ZmPSTOL1_8.05_14* and *ZmPSTOL1_8.02_19* were still segregating (Table S2).

Phenotypic characterization of maize events overexpressing *PSTOL1* for root morphology in nutrient solution with low-P

We performed a correlation analysis with root morphology traits, shoot dry weight, shoot P content and transgene expression (Fig.3). Total root length was highly and positively correlated with root surface area of very fine ($r = 0.96$, $p < 0.01$) and fine roots ($r = 0.68$, $p = 0.064$), whereas increased root length was strongly associated with reduced root diameter ($r = -0.80$, $p = 0.016$). Shoot dry matter accumulation, which reflects maize performance in hydroponics, was highly associated with increased root length, surface area of very fine and fine roots ($r > 0.7$) and negatively correlated with root diameter ($r = -0.84$, $p < 0.01$), which is consistent with the significant negative association between fine root proliferation and root diameter. Shoot P content was neither associated with root length nor root surface area but tended to be negatively correlated with root diameter, which was positively correlated with shoot dry weight. Increased *PSTOL1* expression resulted in higher root surface area via enhanced proliferation of finer roots, which

lead to increased shoot dry weight and P content of maize transgenic events cultivated under low-P (Fig. 3).

Events expressing rice (*OsPSTOLI_1*) and sorghum (*Sb07g002840_5*, *Sb03g031690_8*, *Sb03g006765_10* and *Sb03g006765_11*) *PSTOLI* genes showed enhanced total root length and surface area when compared to the non-transgenic B104 [$p < 0.05$ (Fig. 4A-B)]. Root length, root surface area of very fine and fine roots of *Sb07g002840_5* were increased by 35%, 46% and 20% respectively, compared to B104 ($p < 0.05$). Root length and root surface of very fine roots were also increased by 10% and 19% in *OsPSTOLI_1*, 16% and 25% in *Sb03g3g31690_8* and 24%-12% and 18%-20% for the maize events overexpressing *Sb03g006765* (*Sb03g006765_10* and *Sb03g006765_11*) ($p > 0.05$). Transgenic *OsPSTOLI* and *SbPSTOLI* events showed a reduction in root diameter from 5.4% (*Sb03g006765_10*) to 8.3% (*Sb03g031690_8*) in comparison with the wild type B104 ($p < 0.1$). However, the events for *ZmPSTOLI* presented no significant differences for root traits compared to wild-type B104.

A linear regression model fitted to B104 and the *PSTOLI* transgenic events suggested that, in general, overexpression of *PSTOLI* genes led to an increase in root length specifically of finer roots (Fig. 4C). These root traits were negatively correlated ($r = -0.8$ and $p < 0.05$), suggesting that the increased total root length tended to reduce its diameter.

Overexpression of *PSTOLI* genes increases shoot dry matter accumulation in a low P soil

We assessed dry matter accumulation of selected transgenic and wild type B104 lines in pots containing soil supplemented with 0 or 200 kg P ha⁻¹. B104 line flowers late, the kernels do not always mature before the end of the growing season, hampering routine seed yield evaluations of biotech traits introduced in B104 at many geographical locations (Feys *et al.*, 2018), thus we evaluated the plant performance before flowering. The ANOVA analysis for shoot dry weight and plant height showed significant effects of P and genotype but non-significant P x genotype (Table 1).

Shoot biomass for *OsPSTOLI_1*, *Sb03g031690_8*, *Sb03g006765_10*, and *Sb03g006765_11* was significantly increased by 22% (*OsPSTOLI_1*) and 11% (*Sb03g006765_10*) compared to B104 [$p < 0.10$ (Fig. 5A)]. There was no significant difference for root dry weight (Fig. 5C). Plant height of transgenic maize was also enhanced compared with B104 (Fig. 5B). The differences found were ~10% for *OsPSTOLI_1*, ~13% for *Sb03g006765_10*, ~6% for *Sb03g006765_11*, and ~9% for *ZmPSTOLI_3.06_18* ($p < 0.15$). No significant difference was detected on shoot biomass accumulation between transgenic maize lines expressing maize *PSTOLI* genes and B104.

A correlation analysis among total root length assessed in hydroponics and shoot dry matter accumulation in a low P soil revealed a significant and positive correlation [$r = 0.6$, $p >$

0.01 (Fig. 5C)]. Differences in the development of transgenic maize grown with low P availability were also visually detected (Fig. 5D).

DISCUSSION

The knowledge of the molecular mechanisms involved in the regulation of phenotypic plasticity in roots can assist plant breeders to develop strategies to select cultivars more adapted to abiotic stresses (Villordon *et al.*, 2014; Topp, 2016). Studies conducted with important crops, such as maize and rice, confirmed the association between genes and root system modulation, which increased grain yield in soils with nutrient or water deprivation (Saengwilai *et al.*, 2014; Lee *et al.*, 2016; Wang *et al.*, 2017). Unravelling adaptive mechanisms associated to root morphology and architecture is crucial for crops cultivated in regions with marginal soil fertility and in low-input agricultural systems, where low P availability is a major constraint can significantly improve food security worldwide.

We showed that the overexpression in maize of rice *PSTOL1* (*OsPSTOL1*) and its sorghum homologs (*Sb07g002840*, *Sb03g006765* and *Sb03g031690*) increased total root length and surface area of very fine and fine roots in maize seedlings grown in nutrient solution with low-P. In addition, these transgenic lines improved shoot dry weight in high and low-P soil in greenhouse low P soil. In rice, overexpression of *OsPSTOL1* increased total root length and surface area of transgenic seedlings and led to an enhancement of more than 60% of grain yield (Gamuyao *et al.*, 2012). In maize, the presence of *OsPSTOL1* increased the biomass accumulation by 22%, suggesting that this gene has potential to be used in different species to improve P acquisition efficiency and yield.

Total root length in nutrient solution was positively correlated with shoot biomass accumulation in low P soil, being the highest for transgenic maize overexpressing *OsPSTOL1*, *Sb03g031690* and *Sb03g006765* (Fig. 5B). Although, *Sb07g002840* presented higher root surface area of fine roots in nutrient solution (Fig. 4), its shoot biomass accumulation and height on soil were similar to the wild type B104 (Fig. 5). These results suggested that overexpression of the *Sb07g002840* gene could interfere with plant development, as lethality was observed in some events overexpressing *Sb07g002840*. The lethal phenotype has been described for other genes that were overexpressed, such as the more root transcription factor (TaMOR-D) in wheat (Li *et al.*, 2016), and auxin-responsive genes in petunia and rice (Tobeña-Santamaria *et al.*, 2002; Yamamoto *et al.*, 2007).

Although, *ZmPSTOL1* genes co-localize with QTLs for root and P-acquisition traits in hydroponics (Azevedo *et al.*, 2015) and were coincident with QTLs for grain yield (Mendes *et al.*, 2014), the transgenic events for *ZmPSTOL1_8.05*, *ZmPSTOL1_3.06* and *ZmPSTOL1_8.03* presented the same performance as the wild type B104. Unlike the *Pup1* QTL that explains 80%

of the phenotypic variance for P-efficiency in rice (Wissuwa *et al.*, 2002), maize QTLs explain from 6.87% to 15.17% (Azevedo *et al.*, 2015), having a much minor effect than *OsPSTOL1*. *ZmPSTOL1* genes co-localized with QTLs for root morphology, biomass accumulation and/or P content are preferentially expressed in roots of the parental lines that contributed the alleles enhancing the respective phenotypes (Azevedo *et al.*, 2015). One possible explanation for the absence of phenotypic differences of the expression of *ZmPSTOL1* genes could be the high expression of such genes in the B104 inbred line, which was higher than in L3 and L22, the parental lines of our QTL mapping study (Azevedo *et al.*, 2015). The high endogenous expression levels of such transcripts could mask their phenotypic effect of the *ZmPSTOL1* transgenes and could explain the superior root development under low P compared to the tropical maize line L3.

Increased root surface area, especially of finer roots in transgenic maize overexpressing *SbPSTOL1* genes is consistent with the results obtained in an association mapping undertaken in two sorghum panels and in a biparental QTL mapping phenotyped for P uptake, root system morphology in hydroponics (Hufnagel *et al.*, 2014; Bernardino *et al.*, 2019). *SbPSTOL1* alleles reducing root diameter enhanced P uptake under low P in hydroponics, whereas *Sb03g006765* and *Sb03g0031680* alleles increase root surface area and grain yield in a low-P soil. Tightly linked or pleiotropic QTL underlying the surface area of fine roots and grain yield co-located with *Sb03g006765* and *Sb03g031690*. *Sb07g02840* appears to enhance grain yield via small increases in root diameter. In sorghum, root surface area was positively associated with grain yield (Hufnagel *et al.*, 2014; Bernardino *et al.*, 2019) and maize overexpressing *SbPSTOL1* genes presented a significant correlation between root length and shoot biomass. There was no interaction between the transgenic events and P treatment in a greenhouse. However, *PSTOL1*-like genes were under the control of the constitutive promoter *Ubiquitin* and most *PSTOL1* genes do not respond strongly to low P (Gamuyao *et al.*, 2012; Azevedo *et al.*, 2015). Sorghum homologs of *OsPSTOL1* seemed to be linked with enhanced early root growth and grain yield under low-P availability.

The significant negative correlation of root diameter and surface area of very fine roots and total root length indicate that overexpression of *OsPSTOL1* and *SbPSTOL1* increased root surface area via enhanced proliferation of very fine roots, but not root dry weight, leading to an increasing of absorption surface with a minimal metabolic cost (Wu *et al.*, 2016). Proliferation of fine roots allows greater soils exploration and nutrient uptake, especially for nutrients with low mobility such as P. For cylindrical roots, root diameter determines the ratio of root length to root volume, which can be directly compared to the root length/root dry mass ratio (i.e. specific root length, SRL, [Eissenstat, 1991]). Zhu and Lynch (2004) found a negative correlation between SRL and average root diameter of both lateral and non-lateral roots in maize RILs. These authors implicated the elongation ability of lateral roots to their smaller diameter and greater SRL than non-lateral roots in most maize genotypes, which is related to the P investment for lateral root

growth. All evidences so far, indicate that *PSTOL1* genes have a more general role in the root system, which results in the enhancement of P acquisition, benefiting cereal production worldwide.

SUPPLEMENTARY DATA

Supplemental Table S1: Primers used for PCR and RT-qPCR assays

Supplemental Table S2: Description of maize transgenic events overexpressing *OsPSTOL1*, *SbPSTOL1* and *ZmPSTOL1* genes

ACKNOWLEDGEMENTS

The authors would like to acknowledge funding from Embrapa Macroprogram grant (02.14.10.003.00.01) and Generation Challenge Programme. PhD fellowship for BFN was granted by Coordenação de Aperfeiçoamento de Pessoal de Nível Superior (CAPES) and for LSM was granted by Conselho Nacional de Desenvolvimento Científico e Tecnológico (CNPq). We thank all staff and trainees of Embrapa and Sorghum that indirectly collaborated in the execution of this work.

REFERENCE

- Abel S, Ticconi CA, Delatorre CA.** 2002. Minireview Phosphdaate sensing in higher plants. *Physiologia Plantarum* **115**, 1–8.
- Azevedo GC, Cheavegatti-Gianotto A, Negri BF, Hufnagel B, e Silva L da C, Magalhaes J V, Garcia AAF, Lana UGP, de Sousa SM, Guimaraes CT.** 2015. Multiple interval QTL mapping and searching for PSTOL1 homologs associated with root morphology, biomass accumulation and phosphorus content in maize seedlings under low-P. *BMC Plant Biology* **15**, 172.
- Bernardino KC, Pastina MM, Menezes CB, et al.** 2019. The genetic architecture of phosphorus efficiency in sorghum involves pleiotropic QTL for root morphology and grain yield under low phosphorus availability in the soil. *BMC Plant Biology* **19**, 87.
- Chen Y, Wu P, Zhao Q, Tang Y, Chen Y, Li M, Jiang H, Wu G.** 2018. Overexpression of a Phosphate Starvation Response AP2/ERF Gene From Physic Nut in Arabidopsis Alters Root Morphological Traits and Phosphate Starvation-Induced Anthocyanin Accumulation. *Frontiers in Plant Science* **9**, 1186.
- Cordell D, Drangert J.- O, White S.** 2009. The story of phosphorus. Global food security and food for thought. *Global Environmental Change* **19**, 292–305.
- de Sousa SM, Clark RT, Mendes FF, Carlos de Oliveira A, Vilaça de Vasconcelos MJ, Parentoni SN, Kochian L V, Guimarães CT, Magalhães JV.** 2012. A role for root morphology and related candidate genes in P acquisition efficiency in maize. *Functional Plant Biology* **39**, 925–935.
- Eissenstat DM.** 1991. On the relationship between specific root length and the rate of root proliferation: a field study using citrus rootstocks. *New Phytologist* **118**, 63–68.
- Feys K, Demuynck K, De Block J, Bisht A, De Vliegheer A, Inzé D, Nelissen H.** 2018. Growth rate rather than growth duration drives growth heterosis in maize B104 hybrids. *Plant, Cell & Environment* **41**, 374–382.
- Frame B, Main M, Schick R, Wang K.** 2011. Genetic Transformation Using Maize Immature Zygotic Embryos BT - Plant Embryo Culture: Methods and Protocols. In: Thorpe TA, In: Yeung EC, eds. Totowa, NJ: Humana Press, 327–341.
- Gamuyao R, Chin JH, Pariasca-Tanaka J, Pesaresi P, Catausan S, Dalid C, Slamet-Loedin I, Tecson-Mendoza EM, Wissuwa M, Heuer S.** 2012. The protein kinase Pstol1 from traditional rice confers tolerance of phosphorus deficiency. *Nature* **488**, 535–539.
- Godfray HCJ, Beddington JR, Crute IR, Haddad L, Lawrence D, Muir JF, Pretty J, Robinson S, Thomas SM, Toulmin C.** 2010. Food Security: The Challenge of Feeding 9 Billion People. *Science* **327**, 812–818.
- Hallauer AR, Lamkey KR, White PR.** 1997. Registration of Five Inbred Lines of Maize: B102, B103, B104, B105, and B106. *Crop Science* **37**, 1405–1406.
- Heuer S, Lu X, Chin JH, et al.** 2009. Comparative sequence analyses of the major quantitative trait locus phosphorus uptake 1 (Pup1) reveal a complex genetic structure. *Plant Biotechnology Journal* **7**, 456–471.
- Hufnagel B, de Sousa SM, Assis L, et al.** 2014. Duplicate and conquer: multiple homologs of

PHOSPHORUS-STARVATION TOLERANCE1 enhance phosphorus acquisition and sorghum performance on low-phosphorus soils. *Plant Physiology* **166**, 659–77.

Hund A, Trachsel S, Stamp P. 2009. Growth of axile and lateral roots of maize. I. Development of a phenotyping platform. *Plant Soil* **325**, 335–349.

Jelihovschi EG, FJC and AIB. 2014. ScottKnott: A Package for Performing the Scott-Knott Clustering Algorithm in R. *Trends in Applied and Computational Mathematics* **15**, 3–17.

Lambers H, Clements JC, Nelson MN. 2013. How a phosphorus-acquisition strategy based on carboxylate exudation powers the success and agronomic potential of lupines (*Lupinus*, Fabaceae). *American Journal of Botany* **100**, 263–288.

Lambers H, Finnegan PM, Laliberté E, Pearse SJ, Ryan MH, Shane MW, Veneklaas EJ. 2011. Phosphorus Nutrition of Proteaceae in Severely Phosphorus-Impoverished Soils: Are There Lessons To Be Learned for Future Crops? *Plant Physiology* **156**, 1058 LP-1066.

Lee D-K, Jung H, Jang G, Jeong JS, Kim YS, Ha S-H, Do Choi Y, Kim J-K. 2016. Overexpression of the OsERF71 Transcription Factor Alters Rice Root Structure and Drought Resistance. *Plant physiology* **172**, 575–588.

Li B, Liu D, Wang J, Li Q, Chang X, Mao X, Jing R. 2016. Overexpression of wheat gene TaMOR improves root system architecture and grain yield in *Oryza sativa*. *Journal of Experimental Botany* **67**, 4155–4167.

Lopez-Arredondo LD, Leyva-González MA, González-Morales SI, Opez-Bucio J, Herrera-Estrella L. 2014. Phosphate Nutrition: Improving Low-Phosphate Tolerance in Crops. *Annual Review of Plant Biology* **65**, 95–123.

Lynch JP. 2011. Root phenes for enhanced soil exploration and phosphorus acquisition: tools for future crops. *Plant Physiology* **156**, 1041–1049.

Ma N, Wang Y, Qiu S, Kang Z, Che S, Wang G, Huang J. 2013. Overexpression of OsEXPA8, a Root-Specific Gene, Improves Rice Growth and Root System Architecture by Facilitating Cell Extension. *PLOS ONE* **8**, e75997.

Magnavaca R, Gardner CO, Clark RB. 1987. Evaluation of inbred maize lines for aluminium tolerance in nutrient solution. *Genetic aspects of Plant mineral nutrition*, 255–265.

Marschner H. 1996. *Mineral nutrition of higher plants*. Academic Press, London.

McGinnis K, Chandler V, Cone K, et al. 2005. Transgene-Induced RNA Interference as a Tool for Plant Functional Genomics. *RNA Interference*. Academic Press, 1–24.

Mendes FF, Guimarães LJM, Souza JC, Guimarães PEO, Magalhaes J V, Garcia AAF. 2014. Genetic architecture of phosphorus use efficiency in tropical maize cultivated in a low-P soil. *Crop Science* **54**, 1–9.

Mendiburu FD. 2019. agricolae: Statistical Procedures for Agricultural Research. R Package Version 1.2-3.

Miguel MA, Postma JA, Lynch JP. 2015. Phene synergism between root hair length and basal root growth angle for phosphorus acquisition. *Plant physiology* **167**, 1430–9.

Niu YF, Chai RS, Jin GL, Wang H, Tang CX, Zhang YS. 2013. Responses of root architecture

- development to low phosphorus availability: A review. *Annals of Botany* **112**, 391–408.
- Parentoni SN, Souza CL.** 2008. Phosphorus acquisition and internal utilization efficiency in tropical maize genotypes. *Pesquisa Agropecuaria Brasileira* **43**, 893–901.
- Parentoni SN, Souza Jr CL, Carvalho Alves VMC, Gama EEG, Coelho AM, Oliveira AC.** 2010. Inheritance and breeding strategies for phosphorus efficiency in tropical maize (*Zea mays* L.). *Maydica* **55**, 1–15.
- Raghothama KG.** 1999. Phosphate acquisition. *Annual Review of Plant Physiology and Plant Molecular Biology* **50**, 665–693.
- Rausch C, Bucher M.** 2002. Molecular mechanisms of phosphate transport in plants. *Planta* **216**, 23–37.
- Revelle W.** 2018. *psych: Procedures for Psychological, Psychometric, and Personality Research.*
- Richardson AE, Lynch JP, Ryan PR, et al.** 2011. Plant and microbial strategies to improve the phosphorus efficiency of agriculture. *Plant and Soil* **349**, 121–156.
- Rojas RV, Achouri M, Maroulis J, Caon L.** 2016. Healthy soils: a prerequisite for sustainable food security. *Environmental Earth Sciences* **75**, 180.
- Saengwilai P, Tian X, Lynch JP.** 2014. Low Crown Root Number Enhances Nitrogen Acquisition from Low-Nitrogen Soils in Maize. *Plant Physiology* **166**, 581 LP-589.
- Saghai-Marooif MA, Soliman KM, Jorgensen RA, Allard RW.** 1984. Ribosomal DNA spacer length polymorphisms in barley: Mendelian inheritance, chromosomal location, and population dynamics. *Proceedings of the National Academy of Sciences of the USA* **81**, 8014–8018.
- Sattari SZ, Bouwman AF, Giller KE, van Ittersum MK.** 2012. Residual soil phosphorus as the missing piece in the global phosphorus crisis puzzle. *Proceedings of the National Academy of Sciences of the USA* **109**, 6348–6353.
- Schmittgen TD, Livak KJ.** 2008. Analyzing real-time PCR data by the comparative CT method. *Nature protocols* **3**, 1101–1108.
- Silva FC da.** 2009. *Manual de análises químicas de solos, plantas e fertilizantes.* Brasília.
- Team RC al C.** 2018. *R: A Language and Environment for Statistical Computing.*
- Tobeña-Santamaria R, Bliet M, Ljung K, Sandberg G, Mol JNM, Souer E, Koes R.** 2002. FLOOZY of petunia is a flavin mono-oxygenase-like protein required for the specification of leaf and flower architecture. *Genes & Development* **16**, 753–763.
- Topp CN.** 2016. Hope in Change: The Role of Root Plasticity in Crop Yield Stability. *Plant Physiology* **172**, 5 LP-6.
- Vance CP, Uhde-Stone C, Allan DL.** 2003. Phosphorus acquisition and use: critical adaptations by plants for securing a nonrenewable resource. *New Phytologist* **157**, 423–447.
- Villordon AQ, Ginzberg I, Firon N.** 2014. Root architecture and root and tuber crop productivity. *Trends in Plant Science* **19**, 419–425.

- von Uexküll HR, Mutert E.** 1995. Global extent, development and economic impact of acid soils. *Plant and Soil* **171**, 1–15.
- Wang J, Pei L, Jin Z, Zhang K, Zhang J.** 2017. Overexpression of the protein phosphatase 2A regulatory subunit a gene *ZmPP2AA1* improves low phosphate tolerance by remodeling the root system architecture of maize. *PLOS ONE* **12**, e0176538.
- Wissuwa M, Wegner J, Ae N, Yano M.** 2002. Substitution mapping of *Pup1*: a major QTL increasing phosphorus uptake of rice from a phosphorus-deficient soil. *Theoretical and Applied Genetics* **105**, 890–897.
- Wu Q, Pagès L, Wu J.** 2016. Relationships between root diameter, root length and root branching along lateral roots in adult, field-grown maize. *Annals of Botany* **117**, 379–390.
- Yamamoto Y, Kamiya N, Morinaka Y, Matsuoka M, Sazuka T.** 2007. Auxin Biosynthesis by the *YUCCA* Genes in Rice. *Plant Physiology* **143**, 1362 LP-1371.
- Zhang C, Simpson RJ, Kim CM, Warthmann N, Delhaize E, Dolan L, Byrne ME, Wu Y, Ryan PR.** 2018. Do longer root hairs improve phosphorus uptake? Testing the hypothesis with transgenic *Brachypodium distachyon* lines overexpressing endogenous RSL genes. *New Phytologist* **217**, 1654–1666.
- Zhu J, Lynch JP.** 2004. The contribution of lateral rooting to phosphorus acquisition efficiency in maize (*Zea mays*) seedlings. *Functional Plant Biology* **31**, 949–958.

TABLE**Table 1:** Analysis of variance for three quantitative traits of transgenic maize grown in greenhouse conditions with low and high P.

	Df	Mean Square		
		Shoot dry weight	Plant height	Root dry weight
Block	3	239.1*	546.4***	14.55
Genotype	8	118.6	114.9	7.67
Phosphorus	1	31224.6***	28751.4***	1175.24***
Phosphorus X Genotype	8	66.2	49.2	2.08
Residuals	51	79.2	68.9	10.51

Df: degree of freedom (n-1). Values are significant at p-value <0.05 (*), <0.01 (**), and <0.01 (***).

Supplemental Table S1: Primers used for PCR and RT-qPCR assays

Gene ID	Assays	Primer sequence 5' - 3'	Product length (bp)
<i>Bar</i>	PCR	Bar F: AGAAACCCACGTCATGC Bar R: GTGGTTGACGATGGTGCA	427
<i>OsPSTOL1</i>	PCR	Ubi_F: GTGTTTAGCAAGGGCGAAAA sp_R: TCAGATGGCACAGTTTGCTC	707
	RT-qPCR SYBR Green	F: GTTTGTGGTGCATACAACCTCGT R: GGTTCCCTCAAAAACAGAAGATG	165
<i>Sb07g002840</i>	PCR	Ubi_F: GTGTTTAGCAAGGGCGAAAA sp_R CAGCGGGTAGGTAAGCAAGA	667
	RT-qPCR SYBR Green	F: CACCAGCCTCGATTTTCATACAA R: AGCCGCACCGGAAGTAGAC	59
<i>Sb03g03190</i>	PCR	Ubi_F: GTGTTTAGCAAGGGCGAAAA sp_R TTGGTAGGGCACCTCTGAAG	721
	RT-qPCR SYBR Green	F: CGCTCCTCCTTGCTGTCTTG R: TGTAATCGTCGTCGGAAGGAT	60
<i>Sb03g006765</i>	PCR	Ubi_F: GTGTTTAGCAAGGGCGAAAA sp_R CACTCCACGAGAAACCCATT	738
	RT-qPCR SYBR Green	F: CGCCGACGATGAACATCTC R: TGGCTCTGCTGAAGACGAA	57
<i>18 S rRNA</i>	RT-qPCR SYBR Green	F: CGTCCTAGTCTCAACCATAAACG R: CCCCAGAACCCAAAGACT	82
<i>ZmPSTOL1_8.05</i>	PCR	Ubi_F: GTGTTTAGCAAGGGCGAAAA sp_R: TAGGTATTCGAGCCCTCTGG	733
	RT-qPCR Taqman	F: ATCAAAAAGAAAAGAAGCAGCA R: AAGGATGTGAGAATGACTAGACAC Probe: AACGGCAACAGCACCAACAATAGG	78
<i>ZmPSTOL1_3.06</i>	PCR	Ubi_F: GTGTTTAGCAAGGGCGAAAA sp_R: GGCCAATCCAAAGTCAGAGA	670
	RT-qPCR Taqman	F: AGTATCAGCAGGACTTGTCATG R: CGCCCTCTTGGATCCTTG Probe: CAAGCAGAACCCCGTCAGTGTC	97
<i>ZmPSTOL1_8.02</i>	PCR	Ubi_F: GTGTTTAGCAAGGGCGAAAA sp_R: CCATCCTAAAACCTGCCTTCG	736
	qRT-PCR Taqman	F: TGGTTTTCAAGGGAAGGCTAG R: CCGTCACCTTTGGAGTCATG Probe: CAGGAATTTCACTGCAACTAGACGACCA	73

Ubi= Ubiquitin gene. sp = specific gene. F= forward. R =reverse. Taqman assay: 18S rRNA is a primer pair re-designed from the TaqMan® Eukaryotic 18S rRNA (Applied Biosystems, Foster City, CA) and used as endogenous control.

Supplemental Table S2: Description of maize transgenic events overexpressing *OsPSTOL1*, *SbPSTOL1* and *ZmPSTOL1* genes

Event	Selection of transgenics events maize				
	T1		T3		T4
	χ^2 value	Relative expression	Total Root Length (cm)	Relative expression	χ^2 value
OsPSTOL1_1+	0.529*	937	467	1.15	0.01**
OsPSTOL1_2	0.250*	593	319	2.47	
OsPSTOL1_3	0.067*	393	355	2.3	
Sb07g002840_4	0.429*	1	325	2.24	
Sb07g002840_5+	0.800*	6	575	1.89	0.05**
Sb07g002840_6	1.190*	12	264	3.86	
Sb03g031690_7	6	1	400	1.08	
Sb03g031690_8+	0.200*	4308	493	414.1	-
Sb03g031690_9	0.200*	1764	331	70.2	
Sb03g006765_10+	0.474*	709	525	1.65	-
Sb03g006765_11+	0.474*	1124	474	7.79	-
Sb03g006765_12	0.182*	1253	402	6.69	
ZmPSTOL1_8.05_13	0.154*	25	295	58.44	
ZmPSTOL1_8.05_14+	5	4180	418	1649.51	2.97**
ZmPSTOL1_8.05_15	2.33*	2828	375	2935.19	
ZmPSTOL1_3.06_16	3.20*	6	254	19.46	
ZmPSTOL1_3.06_17	0.200*	20	295	51.76	
ZmPSTOL1_3.06_18+	6	19	375	9.43	-
ZmPSTOL1_8.02_19+	0.474*	38	387	49.29	4.76
ZmPSTOL1_8.02_20	0.250*	64	340	11.03	
ZmPSTOL1_8.02_21	0.474*	3	395	3.29	
B104			424		

+ selected maize transgenic events. χ^2 =chi-square test. * $\chi^2 < 3.841$, follows the 1:1 segregation (p <0.05). ** $\chi^2 < 3.841$, follows the 3:1 segregation (p <0.05).

FIGURE LEGENDS

Figure 1: Phenotypic characterization of non-transgenic maize lines in low P conditions. (A) Images of the B104, L3 and L22 root systems. (B) Phenotypic means for total root length (cm); root diameter (mm); total root surface area (cm²); root surface area 1 (very fine roots, diameter between 0 and 1 mm) (cm²); root surface area 2 (fine roots, diameter between 1 and 2 mm) (cm²); shoot dry weight (mg) and shoot P content (g). (C) Expression profile of *ZmPSTOL1* genes in B104, L3 and L22. Root image, root morphology traits and expression profile were assessed after 13 days in nutrient solution with low-P. Error bars are shown. Different letters indicated statistical differences by the t-test (p-values ≤ 0.5).

Figure 2: Schematic structure of pMCG1005-*PSTOL1* cassette. (A) LB: left border T-DNA. RB: right border T-DNA. *Ubi*: ubiquitin promoter. *Adn1-intron*: enhancer of the ubiquitin promoter. *OCs3'* terminator (*octopine synthase* gene *A. tumefaciens*). *4x35S*: *Cauliflower mosaic virus* (CaMV) 35S promoter tetramer. *Bar*: *phosphinothricin acetyltransferase* gene. *NOS*: terminator (*nopaline synthase* gene in *A. tumefaciens*). (B) Protein domain prediction of *OsPSTOL1*, *Sb07g002840*, *Sb03g006765*, *Sb03g031690*, *ZmPSTOL1_8.05*, *ZmPSTOL1_3.06*, *ZmPSTOL1_8.02*. Predicted domains are in color. Wall-associated receptor kinase galacturonan-binding (GUB_WAK). Wall-associated receptor kinase C-terminal (Wak). Serine/threonine kinase C-terminal (Kinase).

Figure 3: Correlation analysis of root morphology traits, shoot dry weight and shoot P content traits and *PSTOL1* expression (ΔCt). All traits were assessed after 13 days of treatment in nutrient solution with low-P. The root morphology traits assessed were root length (cm), root diameter (mm), root surface area 1 (very fine roots, diameter between 0 and 1 mm) (cm²) root surface area 2 (fine roots, diameter between 1 and 2 mm) (cm²). Pearson correlation coefficients (r) and p values (p).

Figure 4: Phenotypic characterization of wild type B104 and transgenic lines *PSTOL1* (*OsPSTOL1*, *SbPSTOL1* and *ZmPSTOL1*) in nutrient solution with low-P. (A) Images of the B104, *OsPSTOL1* (*OsPSTOL1_1*), *SbPSTOL1* (*Sb07g002840_5*, *Sb03g031690_8*, *Sb03g006765_10* and *Sb03g006765_11*) and *ZmPSTOL1* (*ZmPSTOL1_8.05_14*, *ZmPSTOL1_3.06_18*, *ZmPSTOL1_8.02_19*) events root systems. (B) Phenotypic means for total root length (cm); root diameter (mm); root surface area 1 (very fine roots, diameter between 0 and 1 mm) (cm²) and root surface area 2 (fine roots, diameter between 1 and 2 mm) (cm²). Significance level of Scott-Knott test, p-value ≤ 0.05 for total root length, root surface area 1 and root surface area 2; p-value ≤ 0.10

for root diameter. (C) Linear regression between total root length and root diameter. Pearson correlation coefficients (r) and p-values (p) are shown. B104, *ZmPSTOLI*-*OsPSTOLI*-*SbPSTOLI*-expressing lines are depicted by black, red and blue circles, respectively.

Figure 5: Phenotypic characterization of wild type B104 and transgenic lines *PSTOL1* (*OsPSTOLI*, *SbPSTOLI* and *ZmPSTOLI*) grown in a low P soil. (A) Shoot dry weight (g). (B) Plant height (cm). (C) Root dry weight (g) were assessed after 45 days in soil with low and high-P. Error bars are shown. Different letters indicated statistical differences by the Scott-Knott test (p-values \leq 0.15). (D) Linear regression between total root length (cm) of plants grown in nutrient solution under low-P and shoot dry weigh (g) of the plants grown in soil with low-P in the greenhouse. Pearson correlation coefficients (r) and p-values (p) are shown. B104, *ZmPSTOLI*, *OsPSTOLI*, *SbPSTOLI* expressing lines are depicted by black, red and blue circles, respectively. (E) Images comparing the wild type B104, *OsPSTOLI_1*, *Sb03g006765_10* and *Sb03g006765_11* events after 45 days in low soil.

FIGURES

Figure 1

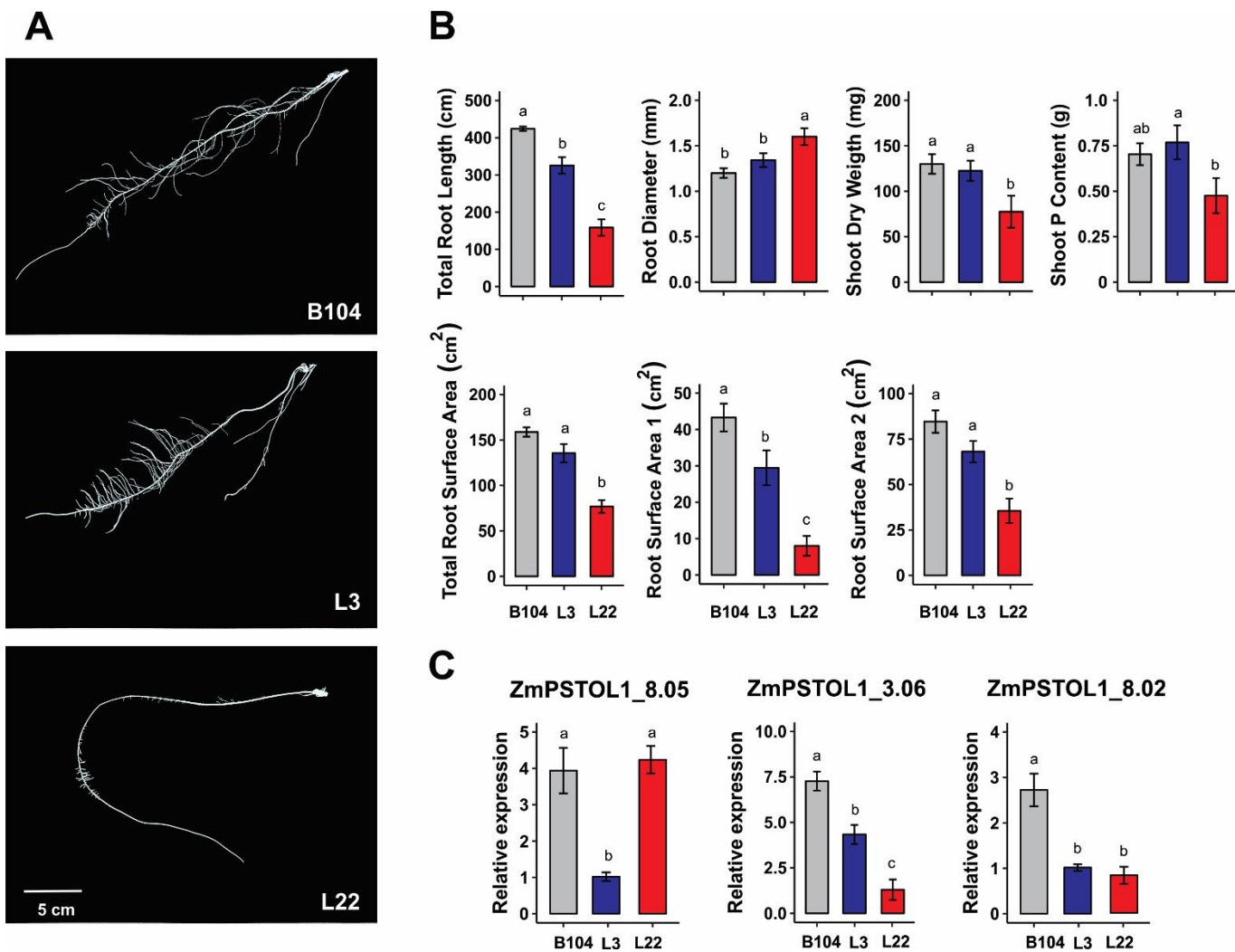


Figure 2

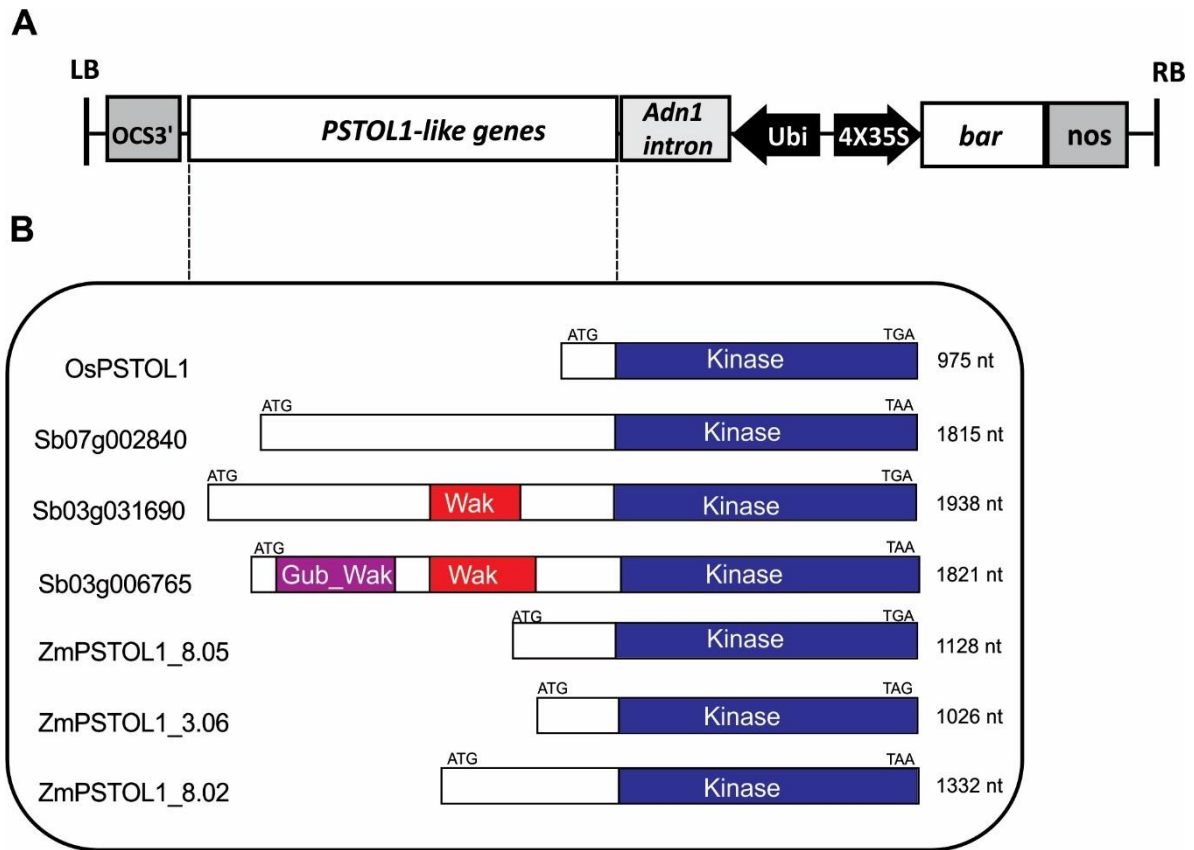


Figure 3

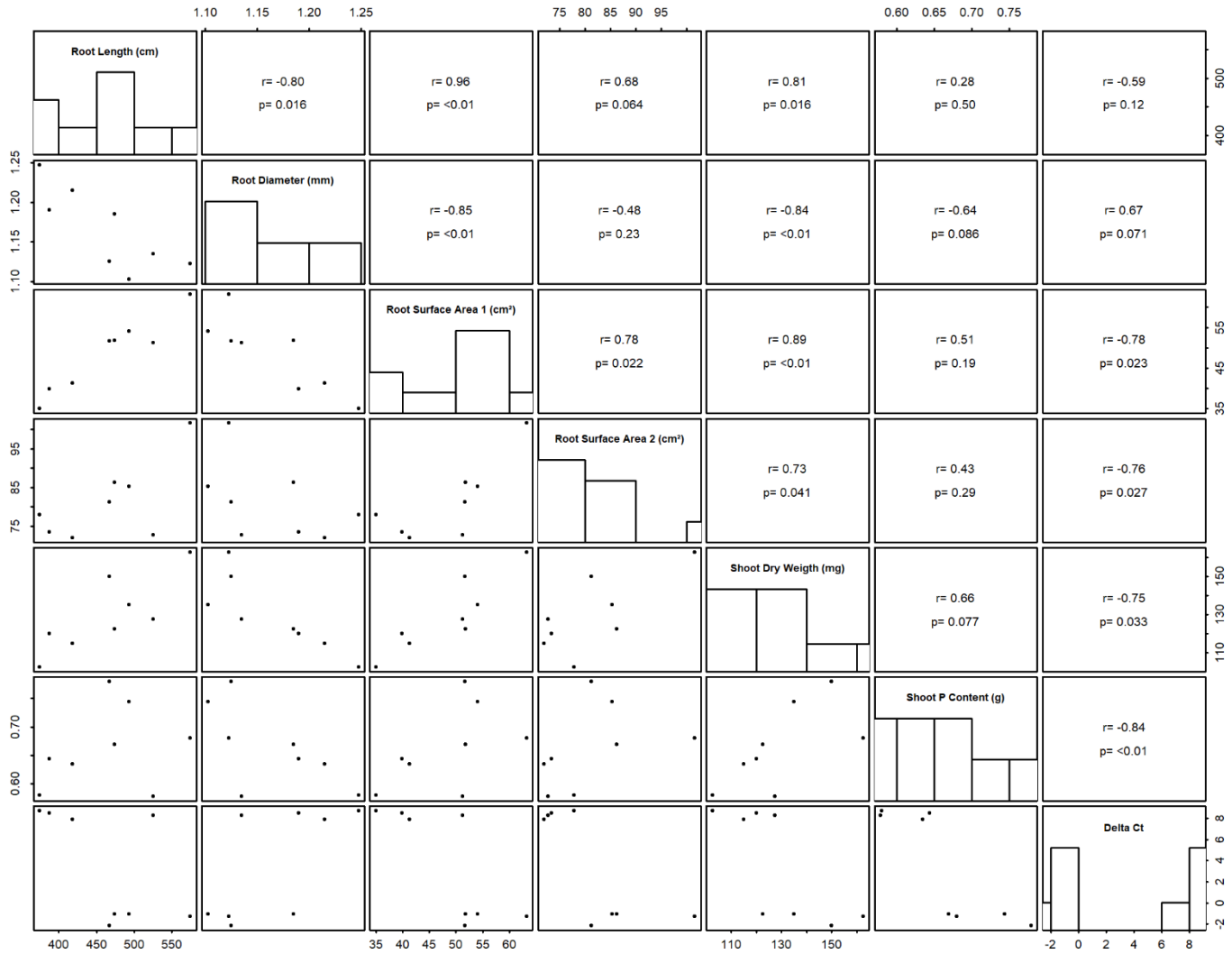
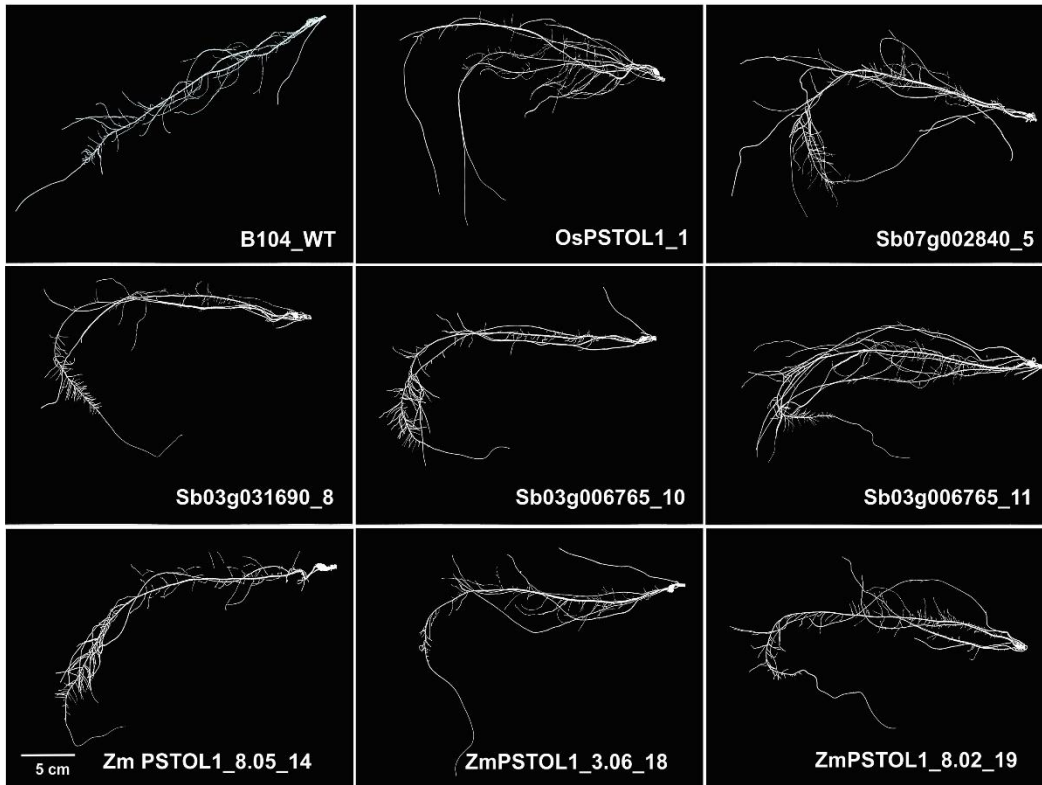
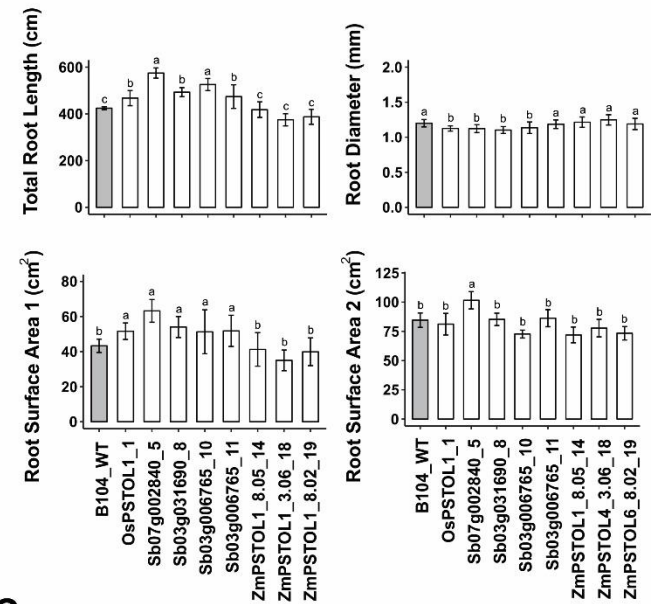


Figure 4

A



B



C

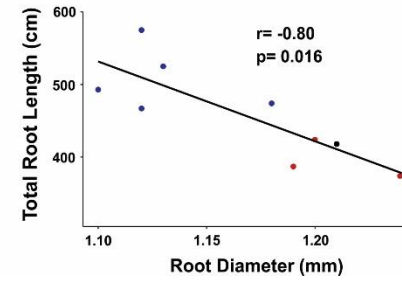
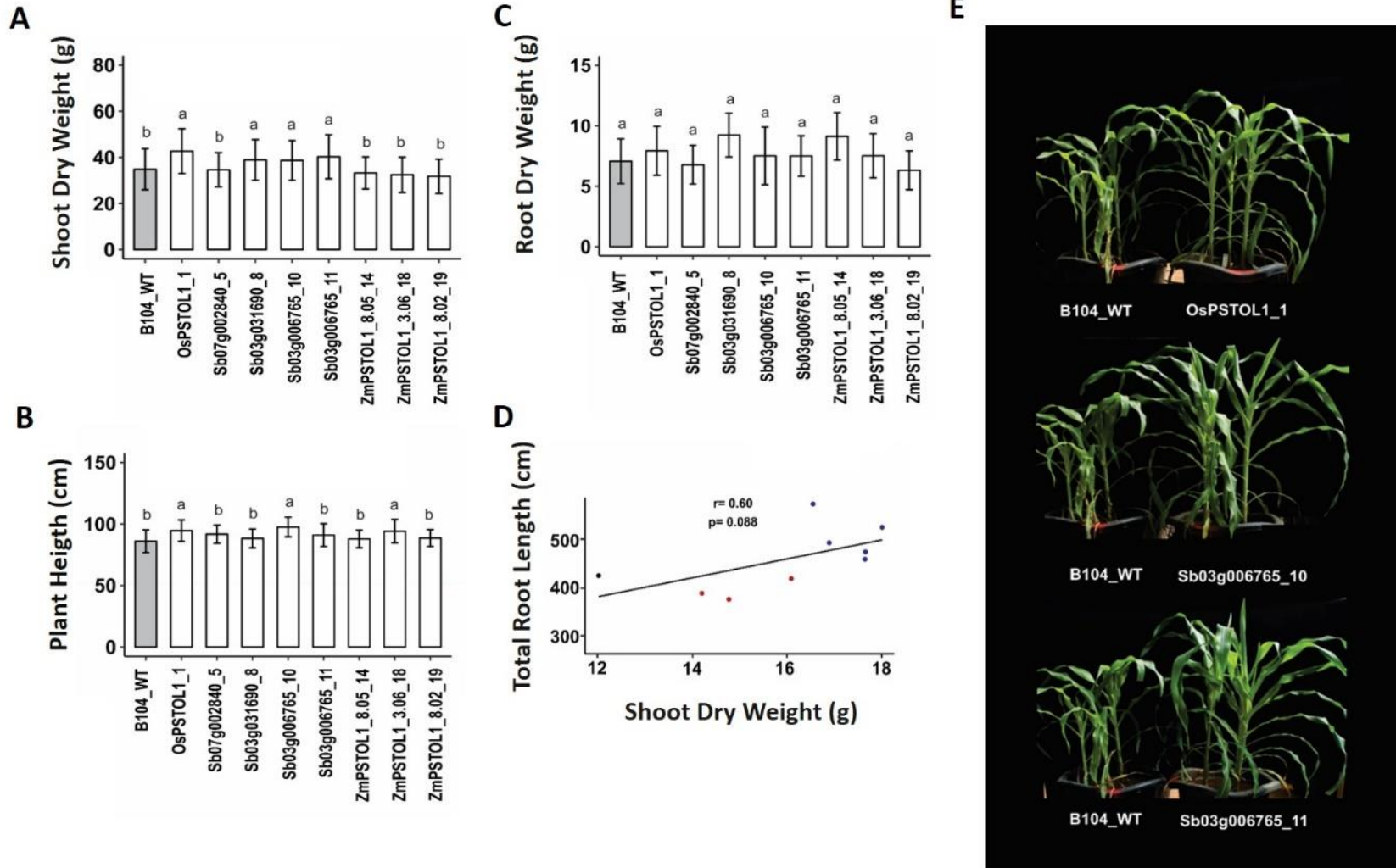


Figure 5



CAPÍTULO 3

O envolvimento de *Phosphorus Starvation Tolerance 1* sobre a morfologia do sistema radicular em sorgo

INTRODUÇÃO

A deficiência de fósforo (P) é considerada uma das maiores limitações para a produção agrícola, visto que uma porção considerável da agricultura mundial está sobre solos com baixa disponibilidade de P (Lynch, 2011). Em regiões tropicais, como no Cerrado brasileiro, a biodisponibilidade de P é baixa. Isso acontece devido ao fenômeno de fixação do P, principalmente via formação de complexos com óxidos de alumínio e de ferro na fração argila do solo (Heuer *et al.*, 2009). A difusão do P é lenta (10^{-12} a 10^{-15} m²s⁻¹) e altamente dependente do teor de umidade do solo, o que torna ainda mais limitante a difusão do P entre o solo e a superfície radicular (Rausch and Bucher, 2002).

As raízes são primordiais para o desenvolvimento das plantas, estabelecendo interações que possibilitam a absorção de água e de nutrientes, ancoramento da planta no solo, e relações biológicas com organismos patogênicos e simbioses presente na rizosfera (Paez-Garcia *et al.*, 2015). A alteração espacial da morfologia e arquitetura radicular configuram um mecanismo adaptativo à deficiência de P nas plantas vasculares (Zhu *et al.*, 2005). Essas modificações possibilitam maior exploração das camadas superficiais do solo, onde o P tende a ser mais disponível, com baixo custo metabólico (Marschner, 1995; Zhu *et al.*, 2010, Lynch & Ho, 2005). Dentre as respostas adaptativas à deficiência de P, destacam-se a redução do crescimento da raiz primária, a melhor exploração do solo com raízes mais ramificadas e finas, e a formação de pelos radiculares mais longos e densos, (Nacry *et al.*, 2005; Perez-Torres *et al.*, 2008, Miguel *et al.*, 2015 Lynch, 2011; Wu *et al.*, 2016). Diversos componentes como fitohormônios, reguladores transcricionais, miRNAs e açúcares estão envolvidos nas vias de sinalização que controlam a plasticidade da morfologia e arquitetura radicular (Lopez-Arredondo *et al.*, 2014, Niu *et al.*, 2013).

Os genes induzidos pela deficiência de P podem ser regulados por diferentes fatores de transcrição (Baek *et al.*, 2017). O fator de transcrição *Phosphate Starvation Response 1 (PHR1)* atua como um regulador chave na expressão de genes induzidos pela privação de P, e no desenvolvimento do sistema radicular (Rubio *et al.*, 2001; Nilsson *et al.*, 2007; Zhou *et al.*, 2008; Bustos *et al.*, 2010; Wang *et al.*, 2013). Em *Arabidopsis*, foi relatado que *PHR1* é regulado positivamente na raiz pelos fatores de transcrição *Auxin Response Factor 7 (ARF7)* e *Auxin Response Factor 19 (ARF19)* (Huang *et al.*, 2018). ARF7 e ARF19 funcionam como mediadores para o aumento da sensibilidade das células da raiz a auxina, um fitohormônio essencial para modulação do sistema radicular (Perez-Torres *et al.*, 2008; López-Bucio *et al.*, 2002; Al-Ghazi *et al.*, 2003; Nacry *et al.*, 2005; Jain *et al.*, 2007).

A família dos receptores quinases (*Receptores-like kinases, RLKs/Pelle*) apresenta uma ampla diversidade de domínios e é considerada como uma das maiores representantes de proteínas quinases em plantas (Shiu and Bleeker, 2003). Estima-se que essas proteínas originaram antes

da divergência entre algas e plantas terrestres (Lehti-Shiu *et al.*, 2009). Os membros da família RLKs/*Pelle* podem ser divididos em dois grupos, as proteínas quinases citoplasmáticas (RLCKs), que não apresentam domínio extracelular, e as proteínas receptoras quinases (RLKs), que são caracterizadas pela presença de domínio extracelular, domínio transmembrana e domínio quinase citoplasmático (Shiu & Bleeker, 2001). As proteínas RLCKs e RLKs são classificadas em subfamílias, com base na similaridade entre as seqüências de aminoácidos, sendo que a alta diversidade de domínios é responsável pela multifuncionalidade desta família proteica (Shiu and Bleeker, 2001, 2003; Lehti-Shiu *et al.*, 2009). As vias de sinalização ativadas pelas proteínas RLKs/*Pelle* podem estar associadas ao crescimento e regulação celular (Wang *et al.*, 2012), simbiose (Parniske, 2008), resistência a doenças (Afzal *et al.*, 2008; Zuo *et al.*, 2015; Hurni *et al.*, 2015), tolerância a estresses abióticos (Sivaguru *et al.*, 2003; Hou, 2005, Hufnagel *et al.*, 2014, Azevedo *et al.*, 2015) e sinalização por brassinoesteróides (Kim & Wang, 2010).

Em arroz (*Oryza sativa*), uma proteína da superfamília das RLKs/*Pelle*, membro da subfamília LRK10L-2, denominada *Phosphorus Starvation Tolerance 1* (OsPSTOL1), atua como um regulador positivo do crescimento e desenvolvimento inicial das raízes da coroa. A proteína OsPSTOL1 apresenta domínio serina/ treonina quinase citoplasmático que possibilita o aumento da área de superfície radicular, associado com o aumento da aquisição de P, e maior produtividade de grãos em solos com baixa disponibilidade de P (Gamuyao *et al.*, 2012). Seis proteínas homologas a proteína OsPSTOL1 foram caracterizadas em sorgo [*Sorghum bicolor* (L) Moench], e nomeadas como Sb07g002840, Sb03g031700, Sb03g031690, Sb03g031680, Sb03g031670 e Sb03g006765. A arquitetura dos domínios das proteínas PSTOL1 em sorgo é similar a OsPSTOL1 pela presença do domínio citoplasmático serina/treonina quinase, no entanto, diferem pela presença do domínio transmembrana, e dos domínios extracelulares *Wall-associated receptor kinase domain* (Wak_assos) e *Cysteine-rich galacturonan_binding domain* (Gub Wak) na porção N-terminal (Hufnagel *et al.*, 2014). Diante da presença dos domínios extracelulares, as proteínas SbPSTOL1 são classificadas como proteínas RLKs.

Os genes que codificam para as proteínas PSTOL1 em sorgo foram validados via mapeamento associativo e mapeamento de QTLs (Hufnagel *et al.*, 2014; Bernardino *et al.*, 2019). As análises de mapeamento associativo indicam associação entre os genes *Sb07g002840*, *Sb03g031700*, *Sb03g031690*, *Sb03g031680*, *Sb03g031670*, *Sb03g006765* e características de morfologia radicular, aquisição de P e produtividade de grãos em solos tropicais com baixa disponibilidade de P (Hufnagel *et al.*, 2014). O mapeamento de QTLs para características múltiplas indicou a co-localização dos genes *Sb03g031700*, *Sb03g031690*, *Sb03g031680*, *Sb03g031670* e *Sb03g006765* com QTLs relacionados ao aumento da área de superfície do sistema radicular e produtividade de grãos. Já o gene *Sb07g002840* co-localizou com QTLs para diâmetro da raiz e produtividade de grãos (Bernardino *et al.*, 2019). Em milho, quatro genes *PSTOL1* (*ZmPSTOL3.06*, *ZmPSTOL4.05*, *ZmPSTOL8.05_1* e *ZmPSTOL8.05_2*) co-localizaram

com QTLs para acúmulo de biomassa, diâmetro médio da raiz e comprimento radicular total (Azevedo *et al.*, 2015). Assim como relatado para população RILs de milho cultivado em solos com baixa disponibilidade de P, o mapeamento de QTLs para população RILs de sorgo indicou que a eficiência do uso de P está mais relacionada a mecanismos que atuam na aquisição de P, do que a mecanismos relacionados à utilização interna do P (Mendes *et al.*, 2014; Bernardino *et al.*, 2019). Nesse contexto, os genes *PSTOL1*, se destacam como um potencial para o melhoramento de cultivares de milho e sorgo em regiões com baixa disponibilidade de P.

No capítulo anterior, caracterizamos fenotipicamente eventos independentes de milho transgênico superexpressando os genes *OsPSTOL1*, *Sb07g002840*, *Sb03g031690*, *Sb03g006765*, *ZmPSTOL18.02*, *ZmPSTOL13.06*, e *ZmPSTOL18.05*. A função dos genes *OsPSTOL1* e *SbPSTOL1* na modulação do sistema radicular foi relacionada a maior proliferação de raízes finas em solução nutritiva sob baixo P, bem como o maior acúmulo de biomassa em solo com baixa disponibilidade P. Neste capítulo discutimos as relações filogenéticas das proteínas *SbPSTOL1* na superfamília das *RLKs-Pelle*, os possíveis elementos *cis* envolvidos nos mecanismos regulatórios que controlam a expressão dos genes *SbPSTOL1*, e o perfil de expressão dos genes *SbPSTOL1* em genótipos contrastantes para morfologia radicular submetidos a condições de baixo e alto P. Finalmente, apresentamos e discutimos os resultados referentes à localização subcelular das proteínas *OsPSTOL1* e *SbPSTOL1*. Até o momento, os resultados sugerem que as proteínas quinases *PSTOL1* atuam em cascatas de sinalização envolvidas em mecanismos relacionados a expansão celular.

MATERIAIS E MÉTODOS

Análise Filogenética

A reconstrução filogenética de proteínas da superfamília das RLKs-*Pelle* foi realizada com as seqüências de aminoácidos do domínio citoplasmático quinase. A seleção das proteínas foi suportada por revisão bibliográfica sobre a nomenclatura e a classificação dos membros representativos das subfamílias das RLKs/*Pelle* em diferentes espécies vegetais. Para suportar os agrupamentos na reconstrução filogenética, três superfamílias de proteínas quinases distantemente relacionadas às RLKs/*Pelle* foram incluídas como *outgroup*. As superfamílias utilizadas como *outgroup* foram Raf (AtCTR1), MAPKKK (AtMAPKKK13) e CK2 (GmCK2, AICKA2 e AtCKA1).

As seqüências de aminoácidos foram alinhadas utilizando a ferramenta ClustalW2 (<http://www.ebi.ac.uk/clustalw/index.html>). A árvore filogenética foi construída com o método *Maximum likelihood* (modelo JTT, bootstrap = 1000) com auxílio do *software* MEGA 7 (Kumar *et al.*, 2016). A predição dos domínios extracelulares, juntamente com o domínio intracelular quinase, foram acessadas nos bancos de dados *Pfam* (<https://pfam.xfam.org/search/sequence>) e *ScanProsite* (<https://prosite.expasy.org/scanprosite>).

Estabelecimento da estrutura gênica dos genes *SbPSTOL1*

Os transcritos *Sb07g002840*, *Sb03g031690*, *Sb03g031670* e *Sb03g006765* foram amplificados para confirmação dos modelos gênicos preditos na versão 1.4 do genoma do sorgo (<https://phytozome.jgi.doe.gov>). O RNA total foi extraído a partir de raízes de plântulas com 13 dias de idade do genótipo de sorgo BR007. A extração do RNA total foi realizada com o Kit *RNeasy Plant Mini* (Qiagen, Valencia, CA), seguindo as recomendações do fabricante. A síntese de cDNA foi conduzida com 1 µg de RNA total tratado com *DNase I*, e o Kit *High Capacity cDNA Reverse Transcription* (Applied Bio-systems, Foster City, CA) foi utilizado conforme as instruções do fabricante. Os oligonucleotídeos para amplificação dos genes estão descritos na tabela 1. Reação em cadeia da polimerase (PCR) foi conduzida com a enzima *Platinum™ Taq DNA Polymerase High Fidelity* (Invitrogen, CA) seguindo as orientações do fabricante. Os produtos da amplificação foram confirmados por sequenciamento.

Amplificação da região 5'UTR

O experimento para amplificação da região 5'UTR dos genes *SbPSTOL1* foi conduzido com o Kit *FirstChoice® RLM-RACE* (Ambion, CA). O RNA total foi extraído conforme descrito no item “Estabelecimento da estrutura gênica dos genes *SbPSTOL1*”. A amplificação da região

5'UTR foi conduzida com 1 µg de RNA total, seguindo as orientações do fabricante do Kit *FirstChoice® RLM-RACE* (Ambion, CA) para procedimentos em pequena escala. O cDNA foi amplificado por *Nested PCR* com a enzima *Platinum™ Taq DNA Polymerase High Fidelity* (Invitrogen, CA) seguindo as orientações do fabricante. As sequências dos oligonucleotídeos estão descritas na tabela 1. Os produtos das amplificações por *Nested PCR* foram sequenciados e comparados com as sequências dos transcritos *SbPSTOLI* disponibilizadas no *Phytozome* (<https://phytozome.jgi.doe.gov>).

Análise *in silico* dos elementos *cis* regulatórios

A análise *in silico* dos elementos *cis* regulatórios possivelmente envolvidos no controle transcricional dos genes *PSTOLI* foi realizada com sequências de 2 kb à montante ao códon de início da tradução. As sequências foram obtidas no banco de dados *Phytozome* (<https://phytozome.jgi.doe.gov>). O software *MaTInspector* (Cartharius *et al.*, 2005) foi utilizado para busca dos possíveis elementos *cis* regulatórios, com ênfase nos elementos envolvidos com modificações na morfologia da raiz e na homeostase de P.

Isolamento e clonagem da região promotora

A sequência de nucleotídeos da região promotora dos genes *Sb03g031690* e *Sb03g006765* foi amplificada a partir de DNA genômico de raiz de sorgo BR007 e inseridas no vetor binário pTF102. O DNA genômico foi extraído conforme descrito por Saghai-Marouf *et al.* (1984). Os oligonucleotídeos utilizados nesse experimento estão descritos na tabela 1. Sítios para as enzimas de restrição *EcoRI* e *BamHI* foram adicionados aos oligonucleotídeos. As reações de amplificação das regiões promotoras foram conduzidas com a enzima *Platinum™ Taq DNA Polymerase High Fidelity* (Invitrogen, CA) seguindo as orientações do fabricante. Os produtos das reações de PCR foram digeridos com as enzimas *EcoRI* e *BamHI* e ligados ao vetor pTF102 também digerido com as mesmas enzimas. A reação de ligação foi conduzida com a enzima *T4 ligase* (Invitrogen, CA) conforme as orientações do fabricante.

As construções gênicas pSb03g031690::GUS e pSb03g006765::GUS foram transformadas em *E. coli* DH5α via choque térmico (Sambrook, *et al.*, 1989), e as colônias bacterianas transformadas foram selecionadas em meio de cultura *Circle Grow* (CG) suplementado com o antibiótico espectinomicina (100 mg/L). O DNA plasmidial dos transformantes foi extraído com o *Kit Wizard® Plus SV Minipreps DNA Purification System* de acordo com as instruções do fabricante, e os clones foram confirmados por sequenciamento. As construções gênicas pSb03g031690::GUS e pSb03g006765::GUS confirmadas por sequenciamento foram clonadas em *Agrobacterium tumefaciens* EH101 por eletroporação

(Sambrook, et al., 1989). As colônias bacterianas transformadas foram selecionadas em meio de cultura *Yeast Extract Peptone* (YEP) suplementado com os antibióticos espectinomicina (100 mg/L) e rifampicina (10 mg/L).

Transformação de milho

A construção gênica pSb03g031690::GUS foi transformada em milho via *A. tumefaciens*. O procedimento de transformação foi conduzido em embriões imaturos de milho HiII conforme descrito por Frame *et al.* (2011). O gene *Phosphinothricin Acetyltransferase* (*Bar*) de resistência ao herbicida foi utilizado como agente de seleção dos transformantes (1,5 mg/L biolaphos). As plântulas regeneradas, designadas como T0, foram transplantadas em casa de vegetação para obtenção posterior de eventos homozigóticos para os transgenes.

Teste histoquímico do GUS

O teste histoquímico foi conduzido em raízes de plântulas de milho transgênico T0 expressando o gene *GUS* sob controle do promotor nativo pSb03g031690. A localização da atividade histoquímica do *GUS* foi feita conforme descrito por Jefferson (1987). O tecido radicular das plântulas transgênicas foi coletado e imerso em tampão fosfato de sódio 50 mM (pH 7.0) e 5-bromo-4chloro-3indolyl- β -D-glucuronic acid 1 mM (Clontech, Palo Alto, CA) por 24 horas a 37°C. As imagens foram obtidas em estereoscópio Axio Zoom V16 (Zeiss).

Análise da morfologia de raiz, acúmulo de biomassa e conteúdo de P em sistema de hidroponia em condições de baixo e alto P

As linhagens de sorgo SC103, BTx399, BTx635 e BTx623 do banco de germoplasma da Embrapa Milho e Sorgo (Sete Lagoas-MG, Brasil) foram caracterizadas quanto a morfologia radicular, o acúmulo de biomassa e o conteúdo de P. As características de morfologia da raiz foram avaliadas conforme descrito por de Sousa *et al.* (2012) e Hufnagel *et al.* (2014). O delineamento utilizado no experimento foi em blocos casualizados com cinco repetições biológicas, compostas por três plântulas para cada repetição, e dois tratamentos baixo (2,5 μ M) e alto (250 μ M) P.

Inicialmente, as sementes foram desinfestadas com hipoclorito de sódio 0,5% (w/v) por 5 minutos e em seguida lavadas com água destilada. Após a desinfestação, as sementes foram colocadas para germinar em papel umedecido com água por quatro dias. Três plântulas com crescimento uniforme de cada genótipo foram selecionadas para cada uma das cinco repetições biológicas. As plântulas foram conduzidas em sistema de hidroponia com a utilização de pastas

de papel em solução nutritiva Magnavaca modificada (Magnavaca *et al.*, 1987) com duas concentrações de P: baixo P (2,5 μM) e alto P (250 μM). A solução nutritiva foi trocada a cada três dias, e o pH da solução mantido a 5.6. As condições da câmara de crescimento foram ajustadas para 12 horas de fotoperíodo, 330 $\mu\text{mol m}^{-2} \text{s}^{-1}$ de intensidade de luz, sob contínua aeração, com temperatura diurna de 27 ± 3 °C e temperatura noturna de 20 ± 3 °C.

O sistema radicular das plântulas foi avaliado 13 dias após a montagem do experimento. As imagens com a morfologia das raízes foram adquiridas usando uma câmera digital Nikon D300S SLR e os resultados foram processados com os softwares RootReader2D (<http://www.plantmineralnutrition.net/software/rootreader2d/>) e WinRhizo (<http://www.regent.qc.ca/>). As características de morfologia da raiz avaliadas foram comprimento total (cm^2), diâmetro médio (mm), área de superfície de raízes muito finas com diâmetro entre 0 e 1 mm (área de superfície 1- cm^2), área de superfície de raízes finas com diâmetro entre 1 e 2 mm (área de superfície de raízes 2 - cm^2) e volume total das raízes (cm^3).

Após a avaliação das características de morfologia radicular, os tecidos de raiz e parte aérea foram secos separadamente em estufa a 65 °C e pesados para obtenção do peso seco total de cada plântula. A concentração total de P foi determinada usando espectrofotômetro de emissão atômica por plasma indutivamente acoplado (Silva, 2009).

Perfil de expressão dos genes *SbPSTOL1*

O perfil de expressão dos genes *Sb07g002840*, *Sb03g031690* e *Sb03g006765* foi avaliado na raiz e na parte aérea dos genótipos de sorgo SC103, BTx399, BTx635 e BTx623 cultivados em solução nutritiva Magnavaca modificada contendo baixo (2,5 μM) e alto P (250 μM). A extração de RNA e a síntese de cDNA foram conduzidas conforme descrito no item “Estabelecimento da estrutura gênica dos genes *SbPSTOL1*”. A expressão dos genes *Sb07g002840*, *Sb03g031690* e *Sb03g006765* foi determinada por PCR quantitativa em tempo real (qRT-PCR) utilizando *SYBR Green I* no equipamento ABI Prism 7500 Fast System (Applied Biosystems, Foster City, CA). A quantificação relativa dos transcritos foi realizada com 20 ng de cDNA para os genes específicos e 0,02 ng para o controle endógeno constitutivo (*18S rRNA*). Os oligonucleotídeos foram desenhados usando a ferramenta *Primer Quest* (<https://www.idtdna.com/PrimerQuest/>) (Tabela 1). Os cálculos para a expressão relativa dos genes foram realizados de acordo com o método $2^{-\Delta\Delta\text{Ct}}$ (Schmittgen and Livak, 2008), com três réplicas técnicas.

Localização subcelular

A localização subcelular das proteínas OsPSTOL1, *Sb07g002840*, *Sb03g031690*, e *Sb03g006765* fusionadas a GFP foi realizada em *Nicotiana benthamiana*. As construções gênicas

foram sintetizadas com o kit *Gateway LR ClonaseTM II enzyme mix* (Invitrogen, CA) de acordo com o protocolo do fabricante. Inicialmente, a região codificadora dos genes foi amplificada conforme descrito no item “Estabelecimento da estrutura gênica dos genes *SbPSTOLI*”, e clonadas no vetor de entrada pENTR11 (Invitrogen, CA). Os oligonucleotídeos (Tabela 1) foram desenhados conforme as orientações do fabricante do vetor pENTR11. As construções inseridas no vetor de entrada pENTR11 foram transformados em *E. coli* DH5 α via choque térmico (Sambrook et al., 1989), selecionadas em meio de cultura CG acrescido com o antibiótico canamicina (100 mg/L), e confirmadas por sequenciamento. A subclonagem das construções gênicas no vetor pK7FWG2 foi realizada por recombinação homóloga usando o kit *GatewayTM LR ClonaseTM Enzyme mix* (Invitrogen, CA) de acordo com as recomendações do fabricante.

As quatro construções gênicas OsPSTOL1::eGFP Sb07g002840::eGFP, Sb03g031690::eGFP, Sb03g006765::eGFP, e o vetor vazio pK7FWG2 foram transformadas em *A. tumefaciens* GV3101 via eletroporação (Sambrook et al., 1989). O meio de cultura YEP suplementado com os antibióticos espectinomicina (100 mg/L) e rifampicina (10 mg/L) foi utilizado para seleção dos transformantes. As colônias transformadas foram cultivadas sob agitação de 150 rpm, a 28 °C por 12 horas. Após o crescimento as culturas bacterianas foram centrifugadas a 5000 g por 5 minutos, e ressuspendidas em 1 mL de meio de infiltração (10 mM MgCl₂, 10 mM de MES pH 5.6, e 100 μ M acetosseringona). A lavagem com o tampão de infiltração foi repetida 3 vezes. Após a última lavagem a solução bacteriana foi deixada em repouso por duas horas, e em seguida a OD foi ajustada em espectrofotômetro para OD₆₀₀ =0,3. As plantas de *N. benthamiana* foram crescidas em câmara de crescimento a 22 °C, e fotoperíodo de 12 horas, com 330 μ mol m⁻² s⁻¹ de intensidade de luz. A infiltração da solução de *A. tumefaciens* foi realizada em folhas de *N. benthamiana* com aproximadamente 3 semanas de idade. Após a infiltração as plantas foram mantidas por 48 horas em câmara de crescimento a 22 °C. A visualização da fluorescência foi observada em microscópio de fluorescência (Zeiss).

Análises estatísticas

As análises de variância (ANOVA) para as características relacionadas à morfologia radicular e ao perfil de expressão dos genes *SbPSTOLI* foram realizadas com o auxílio do pacote *Agricolae* (Mendiburu, 2019) do *software* R (RCore Team, 2018). Análises de agrupamento foram realizadas de acordo com o teste Scott-Knott (Jelihovschi, 2014), considerando o nível de significância (α) de 5%.

RESULTADOS E DISCUSSÃO

As proteínas SbPSTOL1 são RLKs/*Pelle* membros da subfamília LRK10L-2

A superfamília das RLKs/*Pelle* tem origem monofilética, e é considerada uma das maiores famílias de proteínas em plantas (Lehti-Shin & Shiu., 2012). Os membros das RLKs/*Pelle* são divididos em múltiplas subfamílias, que apresentam arquitetura dos domínios proteicos diversificada. Essa característica é responsável pela versatilidade da superfamília RLK/*Pelle* em plantas, e permite o reconhecimento de diferentes efetores no ambiente extracelular (De Smet *et al.*, 2009). No presente trabalho, investigamos a relação filogenética entre proteínas RLK/*Pelle* de diferentes subfamílias e proteínas PSTOL1 com base na sequência aminoacídica dos domínios quinase. Uma análise combinada entre a relação filogenética do domínio quinase e a estrutura dos domínios proteicos foi estabelecida para investigar se proteínas com domínios quinases similares apresentam os mesmos domínios extracelulares (Fig. 1).

A topologia da árvore filogenética comprova que as RLKs/*Pelle* formam clados distintos de acordo com a divisão conhecida em subfamílias (Fig. 1). Esses resultados estão de acordo com os relatos da literatura de que proteínas com domínios quinases similares apresentam os mesmos tipos de domínios extracelulares (Shiu & Bleeker, 2003). As análises *in silico* dos domínios proteicos presentes nas proteínas OsPSTOL1e SbPSTOL1 (Sb07g002840, Sb03g031700, Sb03g031690, Sb03g031680, Sb03g031670 e Sb03g006765) indicam que OsPSTOL1 possivelmente é uma proteína citoplasmática do tipo RLCK. Enquanto as proteínas SbPSTOL1 apresentam domínios extracelulares adicionais ao domínio citoplasmático e possivelmente são do tipo RLCKs. A topologia da árvore indica que ambas as proteínas PSTOL1 derivam de um ancestral comum e estão classificadas na subfamília das LRK10L-2 (Fig. 1). Em Arabidopsis, proteínas RLK e RLCK também já foram classificadas em uma mesma subfamília. A proteína quinase citoplasmática ARCK1 (*ABA- and Osmotic-Stress-Inducible Receptor-Like Cytosolic Kinase1*) e a proteína receptora citoplasmática CRK36 (Cysteine-rich receptor-like protein kinase 36) são membros da subfamília DUF26 (*Domain of Unknown Function 26*). Estudos de interação proteína-proteína revelam a interação entre ARCK1 e CRK36. A formação do complexo está associado à regulação negativa na sinalização do ácido abscísico e do estresse osmótico durante o crescimento pós germinativo da planta (Tanaka *et al.*, 2012).

As funções moleculares e fisiológicas das quinases LRK10L-2 (*Leaf rust 10 disease-resistance locus receptor-like kinase*), à qual pertence as proteínas PSTOL1 de arroz, milho e sorgo, são ainda pouco compreendidas. Inicialmente, o gene que codifica LRK10L-2 foi descrito em trigo (*TaLRK10*) como um gene de resistência à ferrugem do trigo [*Puccinia recondita* f. sp. *tritici* (Feuillet *et al.*, 1997)]. Os genes ortólogos a *TaLRK10* foram mapeados em Arabidopsis, sendo o gene *AtLRK10L1.2* caracterizado como um regulador positivo da tolerância à seca via

sinalização mediada por ácido abscísico, além de estar envolvido na modulação da abertura estomática (Lim *et al.*, 2014).

O domínio extracelular das proteínas LRK10L-2 é caracterizado pela presença de domínios de associação à parede celular, denominados de *Cysteine-rich galacturonan-binding domain* (Gub_Wak) e *Wall-associated receptor kinase domain* (Wak_assos). O domínio Gub_Wak foi caracterizado em proteínas da subfamília das WAKs pela ligação com pectinas nativas da matriz extracelular e pela ligação com oligogalacturonídeos liberados a partir da ação de DAMPs [do inglês, *Damage-Associated Molecular Patterns* (Kohorn, 2016)]. Em milho, a proteína ZmWak1RLK1 foi caracterizada como uma nova classe de receptor da imunidade inata, conferindo resistência ao fungo *Exserohilum turcicum* (Hurni *et al.*, 2015). A análise filogenética desse trabalho classifica a proteína ZmWak1RLK1 como uma LRK10L-2. Esses resultados, em conjunto, indicam que as proteínas LRK10L-2, assim como as proteínas WAKs (Zuo *et al.*, 2015; Hurni *et al.*, 2015; Hou *et al.*, 2005), podem estar relacionadas a mecanismos de expansão celular pela ligação com pectinas nativas e pela ativação do sistema imune inato por meio da ligação com oligogalacturonídeos.

Confirmação dos modelos gênicos dos genes *SbPSTOL1*

O banco de dados do *Phytozome* disponibiliza a anotação do genoma de diferentes espécies de plantas, dentre elas, o *Sorghum bicolor* (Goodstein *et al.*, 2012). Com o advento das tecnologias de sequenciamento de nova geração (NGS) tornam-se comuns as atualizações da anotação dos genomas. As sequências de nucleotídeos que codificam as proteínas SbPSTOL1 (Fig. 1) foram provenientes da versão 1.4 do genoma do sorgo (Hufnagel *et al.*, 2014). Como a anotação do genoma do sorgo foi atualizada para a versão 3.1.1, buscou-se a confirmação dos modelos gênicos Sb07g002840, Sb03g031690, Sb03g031670 e Sb03g006765.

A estrutura dos genes *Sb07g002840* e *Sb03g031690* manteve-se a mesma nas versões 1.4 e 3.1.1 (Fig. 2A-B). Para o gene *Sb07g002840* foi possível confirmar a região 5'UTR (295 pb) e a região codificadora, enquanto que para *Sb03g031690* foi possível confirmar apenas a região codificadora.

As anotações dos genes *Sb03g031670* e *Sb03g006765* apresentaram algumas modificações na versão 3.1.1 (Fig. 2C-D). O gene *Sb03g031670* foi predito na versão 1.4 com quatro exons, já na versão 3.1.1 o primeiro exon passou a ser anotado como um gene independente, e os outros três exons passaram a ser anotados como um segundo gene. Nossos resultados confirmam a estrutura gênica anotada na versão 1.4, onde foi possível definir a região 5'UTR (219 pb) e a região codificadora do gene *Sb03g031670*.

O gene *Sb03g006765* foi anotado com três exons em ambas as versões 1.4 e 3.1.1. A diferença entre as versões é que o primeiro exon da versão 1.4 está dentro do primeiro intron da

versão 3.1.1. Além disso, na versão 1.4, a região codificadora inicia com o códon CAG, que não se trata de um códon alternativo para a tradução, caracterizando-se como anotação incompleta. Diante disso, buscou-se no banco de dados o primeiro ATG à montante ao CAG, e que estava na mesma janela de leitura que a região codificadora definida no modelo gênico da versão 1.4. Após a amplificação da região codificadora, conseguimos confirmar o modelo gênico da versão 1.4 e definir exatamente o ponto de início da tradução (ATG). O transcrito predito na versão 3.1.1 pode ser um transcrito alternativo, no entanto não obtivemos sucesso para sua amplificação.

Após a confirmação dos transcritos anotados na versão 1.4 decidimos seguir os experimentos com os genes *Sb07g002840*, *Sb03g031690* e *Sb03g006765*. A escolha se justifica pelo fato dos genes *Sb03g031670* e *Sb03g031690* codificarem para proteínas com a mesma arquitetura de domínios (Fig.1).

Caracterização da região promotora

As sequências promotoras *pOsPSTOL1*, *pSb07g002840*, *pSb03g031690* e *pSb03g006765* (onde p denota a região promotora) foram analisadas para identificação *in silico* dos elementos *cis* regulatórios que podem atuar na regulação transcricional de cada um dos genes *PSTOL1*. A distribuição dos elementos *cis* regulatórios no *pOSPSTOL1* e *pSb07g002840* apresenta alta similaridade nos primeiros 800 pb à montante do gene. Nessa região, foram preditos sítios para ligação dos fatores de transcrição NACF e RAV5', relacionados a modificações na raiz lateral (Tabela 2 e Figura 3). Além disso, foram detectados sítios para ligação do fator de transcrição MIG, que está associado a homeostase de P, e sítios para os fatores de transcrição ZFAT e PHR1, ambos relacionados a modificação do sistema radicular e a homeostase de P (Tabela 2 e Figura 3).

As regiões promotoras dos genes *Sb03g031690* e *Sb03g006765* não se assemelham quanto à distribuição espacial dos elementos *cis* regulatórios observada para *pOsPSTOL1* e *pSb07g002840* (Figura 3). Uma característica interessante é que, enquanto a região promotora *pSb03g031690* é enriquecida com sítios para ligação do fator de transcrição MIG relacionado a homeostase de P (seis repetições), a região promotora *pSb03g006765* é enriquecida com elementos relacionados à formação de raízes laterais, especialmente o sítio para ligação do fator de transcrição LOB (seis repetições) (Tabela 2). Esses resultados indicam para a possibilidade dos genes *PSTOL1* em arroz e sorgo serem regulados por fatores de transcrição relacionados a plasticidade fenotípica do sistema radicular, e a indução pela privação de P.

O perfil espacial da expressão do gene *Sb03g031690* foi investigado a partir de plantas transgênicas de milho expressando o gene repórter *GUS* sob o controle do promotor nativo *pSb03g031690*. Os resultados preliminares conduzidos em plantas transgênicas T0 (regeneradas a partir de cultura de tecido) indicam que o promotor *pSb03g031690* direciona a expressão do

gene GUS para as raízes laterais (Fig. 4B-D), não sendo detectada a expressão na raiz primária (Fig. 4B) e nos pelos radiculares (Fig. 4D). Nas raízes laterais, a expressão do GUS parece ser direcionada para o cilindro vascular, desde a endoderme até os vasos do xilema e floema, incluindo o periciclo. Há uma nítida separação da região denominada sifonostelo, onde a atividade do GUS não foi detectada (Fig. 4E).

A detecção da atividade GUS nas raízes laterais dirigida pelo promotor *pSb03g031690* sugere que os sítios identificados *in silico* para fatores de transcrição RAV5', NACF, MYB96, ZFAT e/ou PHR1 podem ser funcionais (Tabela 2, Fig. 3). O padrão de expressão espacial do gene *PSTOL1* em arroz foi direcionado para os primórdios das raízes coronais, estando associado ao crescimento e ao desenvolvimento das raízes iniciais (Gamuyao *et al.*, 2012). A comparação entre os elementos *cis* regulatórios identificados em *pOsPSTOL1* e *pSb03g031690* indica a conservação dos sítios para ligação dos fatores de transcrição RAV5', ZFAT e PHR1 (Tabela 2, Fig. 3). Em *Arabidopsis*, o fator de transcrição ZFAT atua como um repressor do crescimento da raiz primária e está relacionado a modificações na morfologia e arquitetura radicular, que possibilitam a homeostase de P (Devaiah *et al.*, 2007). A região promotora do gene *AtPHR1* direciona a expressão gênica para as raízes laterais jovens, sendo fracamente detectado nas raízes laterais lignificadas e quase imperceptíveis nas raízes primárias (Huang *et al.*, 2018).

A construção gênica do promotor *pSb03g006765* fusionado ao gene *GUS* já foi clonada e transformada em *A. tumefaciens*. O próximo passo será a obtenção das plantas de milho transgênico para avaliação da atividade GUS, e a definição espacial da expressão do gene *Sb03g006765* na raiz. Vários esforços foram direcionados para clonagem da construção gênica do promotor *pSb07g002840::GUS*. No entanto, não obtivemos sucesso na transformação da construção em *A. tumefaciens*. Por um mecanismo ainda não elucidado, a sequência do promotor *pSb07g002840* apresenta toxicidade para a *A. tumefaciens* EH101.

Caracterização fenotípica das linhagens de sorgo contrastantes para morfologia radicular em solução nutritiva com baixo e alto P

As linhagens SC103, BTx399, BTx635 e BTx623 foram analisadas para características de morfologia radicular, massa seca total (mg) e conteúdo total de P (g) em solução nutritiva sob baixa e alta disponibilidade de P. A análise de variância (ANOVA) revelou interação significativa entre as linhagens e os níveis de P ($p_value < 0.05$) para as seguintes características: comprimento total, área de superfície radicular 1 e 2, volume total, peso seco total e conteúdo total de P (Tabela 3), indicando um comportamento diferencial das linhagens quando avaliadas em condição de baixo e alto P.

As linhagens SC103 e BTx635 apresentaram maior comprimento total e maior volume total das raízes em baixo P quando comparado com alto P. Enquanto as linhagens BTx399 e BTx623 apresentam a mesma performance, independente da condição de P (Fig. 5A-E). Esses resultados sugerem que os genótipos SC103 e BTx635 apresentam plasticidade fenotípica do sistema radicular em resposta as condições de deficiência de P. Em condição de baixa disponibilidade de P o peso seco total dos genótipos BTx399 e SC103 são superiores aos genótipos BTx635 e BTx623 (Fig. 5F). O maior acúmulo de biomassa de SC103 e BTx399 possivelmente está associada ao fato desses genótipos apresentarem maior área de superfície da raiz. Esses resultados estão de acordo com estudo prévio que caracterizou os genótipos SC103 e BTx399 como eficientes para aquisição de P, e BTx635 e BTx623 como ineficientes para aquisição de P (Silva, 2012).

Perfil de expressão dos genes *SbPSTOL1*

O perfil de expressão dos genes *Sb07g002840*, *Sb03g031690* e *Sb03g006765* foi avaliado nos genótipos contrastantes para morfologia radicular SC103, BTx399, BTx635 e BTx623. O experimento foi conduzido em solução nutritiva sob condições de baixo e de alto P. Os resultados indicam que os genes *Sb07g002840*, *Sb03g031690* e *Sb03g006765* não são específicos de raiz, já que foram detectados na parte aérea e na raiz das plântulas. No entanto, o acúmulo dos transcritos foi no mínimo duas vezes maior na raiz quando comparado à parte aérea (Fig. 6A -F). A indução da expressão pelo tratamento com baixa disponibilidade de P foi detectada apenas para os genótipos BTx399 e BTx623. No caso do BTx399, os genes *Sb07g002840* e *Sb03g031690* foram induzidos pela baixa disponibilidade de P na parte aérea e na raiz (Fig. 6A-D), e o gene *Sb03g006765* foi induzido apenas na parte aérea (Fig. 6E). A indução do gene *Sb03g006765* no genótipo BTx623 foi detectada tanto na parte aérea como na raiz (Fig. 6E). Em algumas situações os genes *SbPSTOL1* foram reprimidos pela condição de baixa disponibilidade de P, conforme observado para o gene *Sb07g002840* nos genótipos BTx635 e BTx623, e para gene *Sb03g006765*

na raiz do genótipo BTx399 (Fig. 6A-B e 6F). A expressão relativa dos transcritos *Sb07g002840*, *Sb03g031690* e *Sb03g006765* não apresentou associação direta com a maior área de superfície dos sistemas radiculares dos genótipos SC103 e BTx399 (Fig. 6B, 6D e 6F).

Localização subcelular das proteínas OsPSTOL1 e SbPSTOL1

As proteínas quinases *Sb07g002840*, *Sb03g031690*, e *Sb03g006765* diferem da proteína quinase citoplasmática OsPSTOL1 pela presença da porção extracelular composta por domínio transmembrana, e domínios de associação a parede celular. A localização subcelular foi analisada pela expressão transiente da proteína OsPSTOL1 e das proteínas SbPSTOL1 com deleção do domínio quinase [Δ K (*Sb07g002840* Δ K, *Sb03g031690* Δ K e *Sb03g006765* Δ K)] fusionadas a *enhanced green fluorescent protein* (eGFP) em células de *N. benthamiana*. Os resultados indicam que a proteína OsPSTOL1 está localizada no citoplasma (Fig. 7B). A proteína truncada *Sb07g002840* Δ K possivelmente se associa a membrana plasmática, no entanto novas análises necessitam serem conduzidas para confirmação dos resultados (Fig.7C). A porção extracelular das proteínas *Sb03g031690* e *Sb03g006765* foi detectada na membrana plasmática (Fig. 7D-E). Esses resultados são consistentes com a detecção da localização na membrana plasmática das proteínas ZmWak em milho (Zuo *et al.*, 2015), e OsDEES1 em arroz (Wang *et al.*, 2012). A associação das proteínas SbPSTOL1 à parede celular ainda não foi definida. Para isso, ensaios posteriores de plasmólise das células de *N. benthamiana* precisam ser realizados.

As análises *in silico* indicaram que as proteínas *Sb03g031690* e *Sb03g006765* apresentam domínios de associação a parede celular (Fig.1). A localização dessas proteínas na membrana plasmática é um indicativo que elas podem atuar como proteínas receptoras de estímulos externos. Conforme já descrito na literatura o domínio Gub_Wak presente em proteínas quinases receptoras liga-se covalentemente a pectinas nativas da parede celular. Após a indução do estímulo externo proteínas a jusante a proteína receptora quinase são ativadas em vias de sinalização relacionadas a resposta de expansão e diferenciação celular (Decreux *et al.*, 2006; Decreux & Messiaen, 2005; Verica *et al.*, 2003; Kohorn & Kohorn, 2012; Kohorn, 2016). Diante disso, estudos posteriores serão necessários para compreensão do complexo de proteínas envolvidas na cascata de sinalização a qual as proteínas PSTOL1 modulam a morfologia do sistema radicular.

REFERÊNCIAS

- Afzal AJ, Wood AJ, Lightfoot DA.** 2008. Plant receptor-like serine threonine kinases: roles in signaling and plant defense. *Molecular plant-microbe interactions* : MPMI **21**, 507–517.
- AL-Ghazi Y, Muller B, Pinloche S, Tranbarger TJ, Nacry P, Rossignol M, Tardieu F, Doumas P.** 2003. Temporal responses of Arabidopsis root architecture to phosphate starvation: evidence for the involvement of auxin signalling. *Plant, Cell & Environment* **26**, 1053–1066.
- Azevedo GC, Cheavegatti-Gianotto A, Negri BF, Hufnagel B, e Silva L da C, Magalhaes J V, Garcia AAF, Lana UGP, de Sousa SM, Guimaraes CT.** 2015. Multiple interval QTL mapping and searching for PSTOL1 homologs associated with root morphology, biomass accumulation and phosphorus content in maize seedlings under low-P. *BMC Plant Biology* **15**, 172.
- Bernardino KC, Pastina MM, Menezes CB, et al.** 2019. The genetic architecture of phosphorus efficiency in sorghum involves pleiotropic QTL for root morphology and grain yield under low phosphorus availability in the soil. *BMC Plant Biology* **19**, 87.
- Bustos R, Castrillo G, Linhares F, Puga MI, Rubio V, Pérez-Pérez J, Solano R, Leyva A, Paz-Ares J.** 2010. A Central Regulatory System Largely Controls Transcriptional Activation and Repression Responses to Phosphate Starvation in Arabidopsis. *PLOS Genetics* **6**, e1001102.
- Cartharius K, Frech K, Grote K, Klocke B, Haltmeier M, Klingenhoff A, Frisch M, Bayerlein M, Werner T.** 2005. MatInspector and beyond: Promoter analysis based on transcription factor binding sites. *Bioinformatics* **21**, 2933–2942.
- Decreux A, Messiaen J.** 2005. Wall-associated kinase WAK1 interacts with cell wall pectins in a calcium-induced conformation. *Plant and Cell Physiology* **46**, 268–278.
- Decreux A, Thomas A, Spies B, Basseur R, Cutsem P Van, Messiaen J.** 2006. In vitro characterization of the homogalacturonan-binding domain of the wall-associated kinase WAK1 using site-directed mutagenesis. *Phytochemistry* **67**, 1068–1079.
- De Smet I, Voss U, Jürgens G, Beckman T.** 2009. Receptor-like kinases shape the plant. *Nature cell biology* **11**, 1166–73.
- De Sousa S, Clark RT, Mendes FF, Carlos de Oliveira A, Vilaça de Vasconcelos MJ, Parentoni SN, Kochian L V, Guimarães CT, Magalhães JV.** 2012. A role for root morphology and related candidate genes in P acquisition efficiency in maize. *Functional Plant Biology* **39**, 925–935.
- D. L-SM, Shin-Han S.** 2012. Diversity, classification and function of the plant protein kinase superfamily. *Philosophical Transactions of the Royal Society B: Biological Sciences* **367**, 2619–2639.
- Devaiah BN, Nagarajan VK, Raghothama KG.** 2007. Phosphate Homeostasis and Root Development in Arabidopsis Are Synchronized by the Zinc Finger Transcription Factor ZAT6. *Plant Physiology* **145**, 147 LP-159.
- Feuillet C, Schachermayr G, Keller B.** 1997. Molecular cloning of a new receptor-like kinase gene encoded at the LrlO disease resistance locus of wheat. *The Plant Journal* **11**, 45–52.

- Frame B, Main M, Schick R, Wang K.** 2011. Genetic Transformation Using Maize Immature Zygotic Embryos BT - Plant Embryo Culture: Methods and Protocols. In: Thorpe TA,, In: Yeung EC, eds. Totowa, NJ: Humana Press, 327–341.
- Franco-Zorrilla JM, López-Vidriero I, Carrasco JL, Godoy M, Vera P, Solano R.** 2014. DNA-binding specificities of plant transcription factors and their potential to define target genes. *Proceedings of the National Academy of Sciences of the United States of America* **111**, 2367–72.
- Gamuyao R, Chin JH, Pariasca-Tanaka J, Pesaresi P, Catausan S, Dalid C, Slamet-Loedin I, Tecson-Mendoza EM, Wissuwa M, Heuer S.** 2012*b*. The protein kinase Pstol1 from traditional rice confers tolerance of phosphorus deficiency. *Nature* **488**, 535–539.
- Goodstein DM, Shu S, Howson R, et al.** 2012. Phytozome: A comparative platform for green plant genomics. *Nucleic Acids Research* **40**, 1178–1186.
- Heuer S, Lu X, Chin JH, et al.** 2009. Comparative sequence analyses of the major quantitative trait locus phosphorus uptake 1 (Pup1) reveal a complex genetic structure. *Plant Biotechnology Journal* **7**, 456–471.
- Hou X.** 2005. Involvement of a Cell Wall-Associated Kinase, WAKL4, in Arabidopsis Mineral Responses. *Plant Physiology* **139**, 1704–1716.
- Huang K-L, Ma G-J, Zhang M-L, et al.** 2018. The ARF7 and ARF19 Transcription Factors Positively Regulate *PHOSPHATE STARVATION RESPONSE1* in Arabidopsis Roots *Plant Physiology* **178**, 413-427.
- Hufnagel B, de Sousa SM, Assis L, et al.** 2014. Duplicate and conquer: multiple homologs of PHOSPHORUS-STARVATION TOLERANCE1 enhance phosphorus acquisition and sorghum performance on low-phosphorus soils. *Plant Physiology* **166**, 659–77.
- Hurni S, Scheuermann D, Krattinger SG, et al.** 2015. The maize disease resistance gene Htn1 against northern corn leaf blight encodes a wall-associated receptor-like kinase. *Proceedings of the National Academy of Sciences* **112**, 8780–8785.
- Husbands A, Bell EM, Shuai B, Smith HMS, Springer PS.** 2007. Lateral organ boundaries defines a new family of DNA-binding transcription factors and can interact with specific bHLH proteins. *Nucleic Acids Research* **35**, 6663–6671.
- Jain A, Poling MD, Karthikeyan AS, Blakeslee JJ, Peer WA, Titapiwatanakun B, Murphy AS, Raghothama KG.** 2007. Differential effects of sucrose and auxin on localized phosphate deficiency-induced modulation of different traits of root system architecture in Arabidopsis. *Plant Physiology* **144**, 232–247.
- Jefferson RA.** 1987. Assaying chimeric genes in plants: The GUS gene fusion system. *Plant Molecular Biology Reporter* **5**, 387–405.
- Jelihovschi EG, FJC and AIB.** 2014. ScottKnott: A Package for Performing the Scott-Knott Clustering Algorithm in R. *Trends in Applied and Computational Mathematics* **15**, 3–17.
- Kim T-W, Wang Z-Y.** 2010. Brassinosteroid Signal Transduction from Receptor Kinases to Transcription Factors. *Annual Review. Plant Biology* **61**, 681–704.
- Kohorn BD.** 2016. Cell wall-associated kinases and pectin perception. *Journal of Experimental Botany* **67**, 489-494.

- Kohorn BD, Kohorn SL.** 2012. The cell wall-associated kinases, WAKs, as pectin receptors. *Frontiers in Plant Science*. **3**, 88.
- Kumar S, Stecher G, Tamura K.** 2016. MEGA7: Molecular Evolutionary Genetics Analysis Version 7.0 for Bigger Datasets. *Molecular Biology and Evolution* **33**, 1870–1874.
- Lehti-Shiu MD, Zou C, Hanada K, Shiu S-HS.** 2009. Evolutionary History and Stress Regulation of Plant Receptor-Like Kinase/Pelle Genes1[W][OA]. *Plant Physiology* **150**, 12–26.
- Lim CW, Yang SH, Shin KH, Lee SC, Kim SH.** 2014. The AtLRK10L1.2, Arabidopsis ortholog of wheat LRK10, is involved in ABA-mediated signaling and drought resistance. *Plant Cell Reports* **34**, 447–455.
- López-Bucio J, Hernández-Abreu E, Sánchez-Calderón L, Pérez-Torres A, Rampey RA, Bartel B, Herrera-Estrella L.** 2005. An Auxin Transport Independent Pathway Is Involved in Phosphate Stress-Induced Root Architectural Alterations in Arabidopsis. Identification of BIG as a Mediator of Auxin in Pericycle Cell Activation. *Plant Physiology* **137**, 681–691.
- Lopez-Arredondo LD, Leyva-González MA, González-Morales SI, Lopez-Bucio J, Herrera-Estrella L.** 2014. Phosphate Nutrition: Improving Low-Phosphate Tolerance in Crops. *Annual Review of Plant Biology* **65**, 95–123.
- Lynch JP, Ho MD.** 2005. Rhizoeconomics: carbon costs of phosphorus acquisition. *Plant Soil* **269**, 45–56.
- Lynch JP.** 2011. Root phenes for enhanced soil exploration and phosphorus acquisition: tools for future crops. *Plant Physiology* **156**, 1041–1049.
- Lynch JP, Brown KM.** 2012. New roots for agriculture: exploiting the root phenome. *Philosophical Transactions of the Royal Society B: Biological Sciences* **367**, 1598–1604.
- Magnavaca R, Gardner CO, Clark RB.** 1987. Evaluation of inbred maize lines for aluminium tolerance in nutrient solution. *Genetic aspects of Plant mineral nutrition*, 255–265.
- Marschener H.** 1995. *Mineral nutritional of higher plants*. Academic Press, London.
- Mendes FF, Guimarães LJM, Souza JC, Guimarães PEO, Magalhaes J V, Garcia AAF.** 2014. Genetic architecture of phosphorus use efficiency in tropical maize cultivated in a low-P soil. *Crop Science* **54**, 1–9.
- Mendiburu FD.** 2019. agricolae: Statistical Procedures for Agricultural Research. R Package Version 1.2-3.
- Miguel MA, Postma JA, Lynch JP.** 2015. Phene synergism between root hair length and basal root growth angle for phosphorus acquisition. *Plant physiology* **167**, 1430–9.
- Nacry P, Canivenc G, Muller B, Azmi A, Van Onckelen H, Rossignol M, Dumas P.** 2005. A role for auxin redistribution in the responses of the root system architecture to phosphate starvation in Arabidopsis. *Plant physiology* **138**, 2061–74.
- Nilsson L, Müller R, Nielsen Tomh.** 2007. Increased expression of the MYB-related transcription factor, PHR1, leads to enhanced phosphate uptake in Arabidopsis thaliana. *Plant, Cell & Environment* **30**, 1499–1512.

- Niu YF, Chai RS, Jin GL, Wang H, Tang CX, Zhang YS.** 2013. Responses of root architecture development to low phosphorus availability: A review. *Annals of Botany* **112**, 391–408.
- Olsen AN, Ernst HA, Leggio LL, Skriver K.** 2005. DNA-binding specificity and molecular functions of NAC transcription factors. *Plant Science* **169**, 785–797.
- Parniske M.** 2008. Arbuscular mycorrhiza: the mother of plant root endosymbioses. *Nature reviews. Microbiology* **6**, 763–75.
- Paez-Garcia A, Motes C, Scheible W-R, Chen R, Blancaflor E, Monteros M.** 2015. Root Traits and Phenotyping Strategies for Plant Improvement. *Plants* **4**, 334–355.
- Perez-Torres C a, Lopez-Bucio J, Cruz-Ramirez a, Ibarra-Laclette E, Dharmasiri S, Estelle M, Herrera-Estrella L.** 2008. Phosphate Availability Alters Lateral Root Development in Arabidopsis by Modulating Auxin Sensitivity via a Mechanism Involving the TIR1 Auxin Receptor. *Plant Cell* **20**, 3258–3272.
- Rausch C, Bucher M.** 2002. Molecular mechanisms of phosphate transport in plants. *Planta* **216**, 23–37.
- Rubio V, Linhares F, Solano R, Martin AC, Iglesias J, Leyva A, Paz-Ares J.** 2001. A conserved MYB transcription factor involved in phosphate starvation signaling both in vascular plants and in unicellular algae. *Genes & Development* **15**, 2122–2133.
- Saghai-Marooif MA, Soliman KM, Jorgensen RA, Allard RW.** 1984. Ribosomal DNA spacer length polymorphisms in barley: Mendelian inheritance, chromosomal location, and population dynamics. *Proceedings of the National Academy of Sciences of the USA* **81**, 8014–8018.
- Sambrook, J., Fritsch, E. F., and Maniatis T.** 1989. *Molecular Cloning: A Laboratory Manual*. Cold Spring Harbor Laboratory.
- Seo PJ, Lee SB, Suh MC, Park M-J, Go YS, Park C.** 2011. The MYB96 transcription factor regulates cuticular wax biosynthesis under drought conditions in Arabidopsis. *The Plant cell* **23**, 1138–1152.
- Silva LA.** 2012. Fenotipagem para a eficiência de fósforo em linhagens de sorgo. Universidade Estadual Paulista “Júlio de Mesquita Filho”.
- Schmittgen TD, Livak KJ.** 2008. Analyzing real-time PCR data by the comparative CT method. *Nature protocols* **3**, 1101–1108.
- Shiu SH, Bleecker AB.** 2001. Receptor-like kinases from Arabidopsis form a monophyletic gene family related to animal receptor kinases. *Proceedings of the National Academy of Sciences of the USA* **98**, 19.
- Shiu S, Bleecker AB.** 2003. Expansion of the Receptor-Like Kinase / Pelle Gene Family and Receptor-Like Proteins in Arabidopsis. *Plant physiology* **132**, 530–543.

Silva LA. 2012. Fenotipagem para a eficiência de fósforo em linhagens de sorgo. Tese de Doutorado.

Sivaguru M, Ezaki B, He Z-H, Tong H, Osawa H, Baluška F, Volkmann D, Matsumoto H. 2003. Aluminum-Induced Gene Expression and Protein Localization of a Cell Wall-Associated Receptor Kinase in Arabidopsis. *Plant Physiology* **132**, 2256 -2266.

Team RC al C. 2018. R: A Language and Environment for Statistical Computing.

Verica JA, Chae L, Tong H, Ingmire P, He Z-H. 2003. Tissue-specific and developmentally regulated expression of a cluster of tandemly arrayed cell wall-associated kinase-like kinase genes in Arabidopsis. *Plant physiology* **133**, 1732–46.

Wang N, Huang H-J, Ren S-T, Li J-J, Sun Y, Sun D-Y, Zhang S-Q. 2012. The Rice Wall-Associated Receptor-Like Kinase Gene OsDEES1 Plays a Role in Female Gametophyte Development. *Plant Physiology* **160**, 696-707.

Wang J, Pei L, Jin Z, Zhang K, Zhang J. 2017. Overexpression of the protein phosphatase 2A regulatory subunit a gene ZmPP2AA1 improves low phosphate tolerance by remodeling the root system architecture of maize. *PLOS ONE* **12**, 1-23.

Winzell A, Aspeborg H, Wang Y, Ezcurra I. 2010. Conserved CA-rich motifs in gene promoters of PtMYB021-responsive secondary cell wall carbohydrate-active enzymes in Populus. *Biochemical and Biophysical Research Communications* **394**, 848–853.

Wu Q, Pagès L, Wu J. 2016. Relationships between root diameter, root length and root branching along lateral roots in adult, field-grown maize. *Annals of Botany* **117**, 379–390.

Zuo J, Lynch JP. 2004. The contribution of lateral rooting to phosphorus acquisition efficiency in maize (*Zea mays*) seedlings. *Functional Plant Biology* **31**, 949–958.

Zhou J, Jiao F, Wu Z, Li Y, Wang X, He X, Zhong W, Wu P. 2008. OsPHR2 Is Involved in Phosphate-Starvation Signaling and Excessive Phosphate Accumulation in Shoots of Plants. *Plant Physiology* **146**, 1673-1686.

Zhu J, Kaeppler SM, Lynch JP. 2005. Mapping of QTL controlling root hair length in maize (*Zea mays* L.) under phosphorus deficiency. *Plant and Soil* **270**, 299-310.

Zhu, J, Zhang C, Lynch JP. 2010. The utility of phenotypic plasticity of root hair length for phosphorus acquisition. *Functional Plant Biology* **37**, 13-322.

Zuo W, Chao Q, Zhang N, et al. 2015. A maize wall-associated kinase confers quantitative resistance to head smut. *Nature genetics* **47**, 151–157.

Tabelas

Tabela 1: Lista de oligonucleotídeos utilizados nesse trabalho

Ensaio	Gene	Código	Sequência 5' -> 3'	Direção
Confirmação dos genes	Sb07g002840	2840	AAAGGTACCATGCCACAGTCTCTTATCA	<i>Forward</i>
		2840	GTCGAATTCTTAGCTGGTCCAAAAGG	<i>Reverse</i>
	Sb03g031690	31690	AAAGGTACCATGGCCCTCTGCTCGCTA	<i>Forward</i>
		31690	GTCCTCGAGTCAAATCTGGATCACTTTTGG	<i>Reverse</i>
	Sb03g031670	31670	AAAGGTACCATGAGCGTGAACCCACCTT	<i>Forward</i>
		31670	GTCCTCGAGTCAGCTCAAGAGAACTTT	<i>Reverse</i>
	Sb03g006765	6765	GTCCCATGGATGCAACCGCTCTTGCT	<i>Forward</i>
		6765	GTCGCGGCCGCTTACAATATTTCACTGAAG	<i>Reverse</i>
Região 5'UTR	Sb07g002840	2840_externo	AGACCACGTAGGGGAAGGAT	<i>Reverse</i>
		2840_interno	AGGGTGTGGTAGTCGTCGAT	<i>Reverse</i>
	Sb03g031690	31690_externo	TGC ATG GTG GGA TAC TTG TCG	<i>Reverse</i>
		31690_interno	GTC CAC ACA GTC GAT TGC CA	<i>Reverse</i>
	Sb03g031670	31670_externo	TTGGCAGGAAATCTTCAGGT	<i>Reverse</i>
		31670_interno	TTGGCAGGAAATCTTCAGGT	<i>Reverse</i>
	Sb03g006765	6765_externo	TTGTGCGCCGTCGTAGCTGCATT	<i>Reverse</i>
		6765_interno	ACGACACTGAAGAGGCAGCCTT	<i>Reverse</i>
qRT-PCR	Sb07g002840	RTPupSbH102	CACCAGCCTCGATTTTCATACAA	<i>Forward</i>
		RTPupSbH103	AGCCGCACCGGAAGTAGAC	<i>Reverse</i>
	Sb03g031690	RTPupSb504	CGCTCCTCCTTGCTGTCTTG	<i>Forward</i>
		RTPupSb601	TGTAATCGTCGTCGGAAGGAT	<i>Reverse</i>
	Sb03g006765	RTPupSbH602	CGCCGACGATGAACATCTC	<i>Forward</i>
		RTPupSbH701	TTGGCTCTGCTGAAGACGAA	<i>Reverse</i>
	18 S	Sb18SrRNA	AATCCCTTAACGAGGATCCATTG	<i>Forward</i>
		Sb18SrRNA	CGCTATTGGAGCTGGAATTACC	<i>Reverse</i>
Região Promotora	Sb07g002840	promoter_2840	GAGGGATCCTATCATTTGATTTTTCTC	<i>Forward</i>
		promoter_2840	AAAGGATCCGGGAAAACAGTGATTG	<i>Reverse</i>
	Sb03g031690	promoter_31690	GCGGAATTCATATCACAAAGTTTAGTC	<i>Forward</i>
		promoter_31690	AAAGGATCCGGCTGAATAAGTCAG	<i>Reverse</i>
	Sb03g006765	promoter_6765_1.4	AAAGGATCCCCTCTTCGCTTATGAATGT	<i>Forward</i>
		promoter_6765_1.4	AAAGGATCCAGTGGATTGGGGATGGA	<i>Reverse</i>
Localização subcelular	OsPSTOL1	pENTR_OsPSTOL1	AAACCATGGAAATGCTGCTGTGCCAGCGC	<i>Forward</i>
		pENTR_OsPSTOL1	AAA GCGGCCGCCAGGCCTTTC	<i>Reverse</i>
	Sb07g002840	pENTR_2840	AAAGGTACCAAATGCCACAGTCTCTTATCA	<i>Forward</i>
		pENTR_2840ΔK	AAAGAATCCATGCTGGTCCAAAAGGCCT	<i>Reverse</i>
	Sb03g031690	pENTR_31690	AAAGGTACCAAATGGCCCTCTGCTCGCTA	<i>Forward</i>
		pENTR_31690ΔK	GTCCTCGAGCGTTCTTCCTTCCGTTTAAT	<i>Reverse</i>
	Sb03g006765	pENTR_6765	GTCCCATGGAAATGCAACCGCTCTTGCT	<i>Forward</i>
		pENTR_6765ΔK	AAAGCGGCCGCATTCCATGTGCTAGTAGTAC GG	<i>Reverse</i>

Tabela 2: Análise *in silico* de putativos elementos *cis* regulatórios na região promotora dos genes *PSTOL1* preditos no *software MatInspector*

Classe dos elementos <i>cis</i>	Fator de transcrição relacionado ao elemento em <i>cis</i>	Quantidade de elementos regulatórios em <i>cis</i> detectados				Função	Referências
		pOsPSTOL1	pSb07g002840	pSb03g031690	pSb03g006765		
Elementos <i>cis</i> relacionados a modificação na raiz	RAV5'	3	1	2	-	Desenvolvimento de raízes laterais	Olsen et al., 2005
	NACF (<i>NAC domain containing protein 92</i>)	7	6	2	4	Desenvolvimento de raízes laterais	Olsen et al., 2005
	LOB (<i>LOB domain factors</i>)	-	-	-	6	Formação de raízes laterais	Husbands et al., 2007
	ROOT (<i>Root hair-specific element</i>)	-	-	-	1	Específico para pelos radiculares em angiosperma	Kim, et al., 2006
	MYB96 (<i>Myb domain protein 96</i>)	-	2	2	-	Desenvolvimento de raízes laterais	Seo et al., 2011
Elementos <i>cis</i> relacionado a homeostase de P	ZFAT (<i>Zinc finger protein ZAT6</i>)	2	2	1	-	Regulação da homeostase de P e regulação da raiz	Franco-Zorrilla et al., 2014
	PHR1 (<i>Phosphate starvation response 1</i>)	8	5	2	1	Regulação da homeostase de P	Xue, G J., 2005
	MIG (<i>Myb domain of maize C1</i>)	4	3	6	2	Regulação da homeostase de P	Winzell et al., 2010

Tabela 3: Análise de variância (ANOVA) para características avaliadas em sorgo cultivado em sistema hidropônico com baixa e alta disponibilidade de P

	Grau de liberdade	Soma do quadrado médio
<i>Comprimento total das raízes (cm)</i>		
Tratamento	1	13167*
Genótipo	3	84106***
Tratamento x Genótipo	3	8382*
Resíduo	32	2104
<i>Diâmetro médio das raízes (mm)</i>		
Tratamento	1	0.0143*
Genótipo	3	0.15**
Tratamento x Genótipo	3	0.005
Resíduo	32	0.002
<i>Área de superfície de raízes muito finas (cm²)</i>		
Tratamento	1	123.77
Genótipo	3	1338.25***
Tratamento x Genótipo	3	156.86*
Resíduo	32	46.09
<i>Área de superfície de raízes finas (cm²)</i>		
Tratamento	1	445.55**
Genótipo	3	2415.57***
Tratamento x Genótipo	3	199.54**
Resíduo	32	35.83
<i>Volume total das raízes (cm³)</i>		
Tratamento	1	0.669*
Genótipo	3	6.29***
Tratamento x Genótipo	3	0.631**
Resíduo	32	0.12
<i>Peso seco total (mg)</i>		
Tratamento	1	46.68
Genótipo	3	1621.01***
Tratamento x Genótipo	3	212.56*
Resíduo	32	52.11
<i>Conteúdo total de P (g)</i>		
Tratamento	1	0.017***
Genótipo	3	0.029***
Tratamento x Genótipo	3	0.008***
Resíduo	32	9

p_value estimado * p < 0.05 ** p < 0.01 *** p < 0.001

LEGENDAS DAS FIGURAS

Figura 1: Análise filogenética das proteínas membros da superfamília RLKs/*Pelle*. A reconstrução filogenética foi realizada com a sequência de aminoácidos do domínio quinase das proteínas RLKs/*Pelle* usando o método *Maximum likelihood* (Jones-Taylor-Thornton (JTT) evolutionary model, *bootstrap* = 1000), implementado no programa Mega7.0. Apenas os valores de *bootstrap* maiores que 50% foram mostrados. As subfamílias das RLKs/*Pelle* estão destacadas com cores diferentes (direita). A legenda com os domínios proteicos preditos para cada proteína está descrita na figura (esquerda). As proteínas OsPSTOL1 e SbPSTOL1 são indicadas por letras vermelhas e azuis, respectivamente. Os grupos externos são representados pelas proteínas AtCTR1, AtMAPKKK13, GmCK2, AICK2 (AICKa2) e AtCK1 (AtCKa1). LRK10 representa as proteínas LRK10L-2.

Figura 2: Comparação entre os modelos gênicos dos genes *SbPSTOL1* na versão 1.4 e 3.1.1 do genoma de sorgo. (A) Sb07g002840, (B) Sb03g031670, (C) Sb03g031690, e (D) Sb03g006765. Os exons são representados com barras retangulares azuis, e os introns com uma linha preta entre os exons. O gene *Sb03g006765* foi confirmado a partir do sequenciamento de dois clones, as linhas cinzas representam os clones sequenciados.

Figura 3: Análise *in silico* da distribuição dos possíveis elementos *cis* regulatórios na região promotora dos genes *OsPSTOL1*, *Sb07g002840*, *Sb03g031690* e *Sb03g006765*. A sequência de 2 kpb *upstream* ao primeiro ATG de cada gene foi analisada utilizando o programa *MatInspector* com base na versão 1.4 do genoma de sorgo. Os elementos foram representados por formas geométricas. Os retângulos representam elementos relacionados a modificação na raiz. A forma circular oval representa elementos relacionados a homeostase de P. A identificação da família dos elementos *cis* regulatórios está representada em uma legenda abaixo da figura, e a função correspondente de cada uma das famílias está descrita na tabela 2.

Figura 4: Promotor pSb03g031690 direciona a expressão do gene *GUS* para as raízes laterais. (A) Figura esquemática da construção gênica utilizada para transformação de milho via *A. tumefaciens*. Análise histoquímica foi realizada para definir a localização da expressão do GUS. A localização foi investigada em plantas transgênicas regeneradas a partir de cultura de tecidos (T0). (B) Raiz primária e raízes laterais. (C) Raiz lateral. (D) Corte transversal da raiz lateral.

Figura 5: Caracterização fenotípica dos genótipos de sorgo SC103, BTx399, BTx635 e BTx623. As médias fenotípicas para as características de morfologia radicular (A) comprimento total (cm); (B) diâmetro médio (mm); (C) área de superfície de raiz 1 (cm²) classes de diâmetros de 0-1 mm,

designadas como raízes muito finas; (D) área de superfície de raiz 2 (cm²) classes de diâmetros de 1-2 mm, designadas como raízes finas; (E) volume total (cm³). As médias fenotípicas para as características de performance (F) peso seco total (mg) e (G) conteúdo total de P (g). As características foram avaliadas em plântulas crescidas por 13 dias em solução nutritiva com dois níveis de P (2,5 µM e 250µM). As barras de erro indicam o intervalo de confiança a 95% de cinco réplicas biológicas composta por três plantas. As comparações das médias dentro de cada tratamento de P foram avaliadas por *Scott Knott*. As letras indicam as diferenças estatísticas (p_values ≤0.05).

Figura 6: Perfil de expressão dos genes *SbPSTOL1*. A expressão dos genes *Sb07g002840* (A-B), *Sb03g031690* (C-D) e *Sb03g006765* (E-F) são apresentadas como expressão relativa avaliadas na parte aérea e raiz dos genótipos SC103, BTx399, BTx635 e BTx623. As plântulas foram crescidas por 13 dias em solução nutritiva com duas concentrações de P (2,5 µM e 250µM). As barras de erro indicam o intervalo de confiança a 95% de três réplicas técnicas composta por três plantas. O agrupamento das médias dentro de cada tratamento de P foram avaliadas por *Scott-Knott*. As letras indicam as diferenças estatísticas (p_values ≤0.05).

Figura 7: Localização subcelular das proteínas OsPSTOL1, *Sb07g002840*, *Sb03g031690* e *Sb03g006765* fusionadas a eGFP em células epidérmicas de *N. benthamiana*. As proteínas *Sb07g002840*, *Sb03g031690* e *Sb03g006765* foram avaliadas com deleção do domínio quinase. A fluorescência da proteína eGFP foi observada 48 horas após a agroinfiltração. (A) vetor vazio pK7FWG2. (B) OsPSTOL1::eGFP. (C) *Sb07g002840*::eGFP. (D) *Sb03g031690*::eGFP. (E) *Sb03g006765*::eGFP. As imagens foram visualizadas em microscópio de fluorescência (Zeiss).

Figura 1

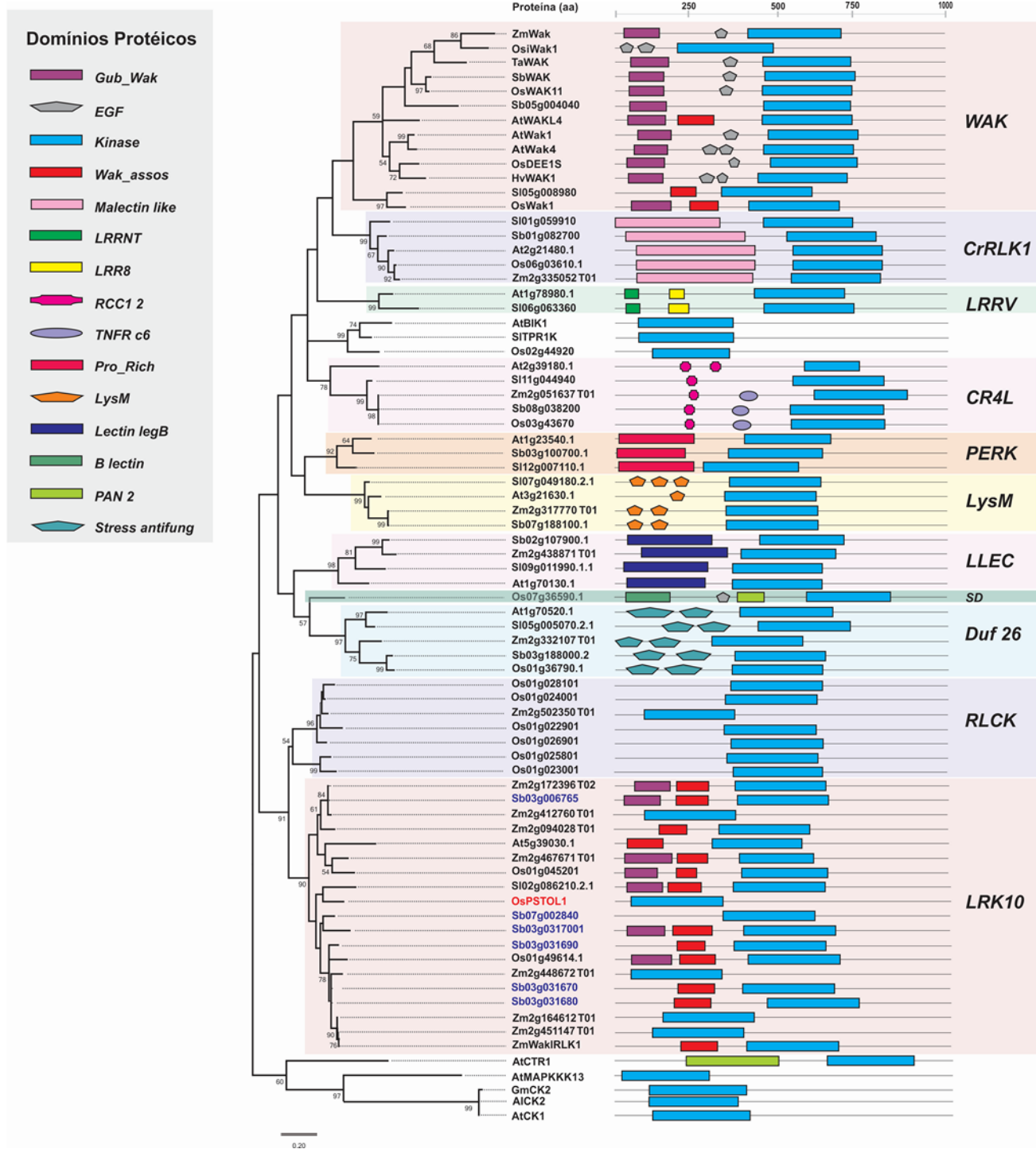


Figura 2

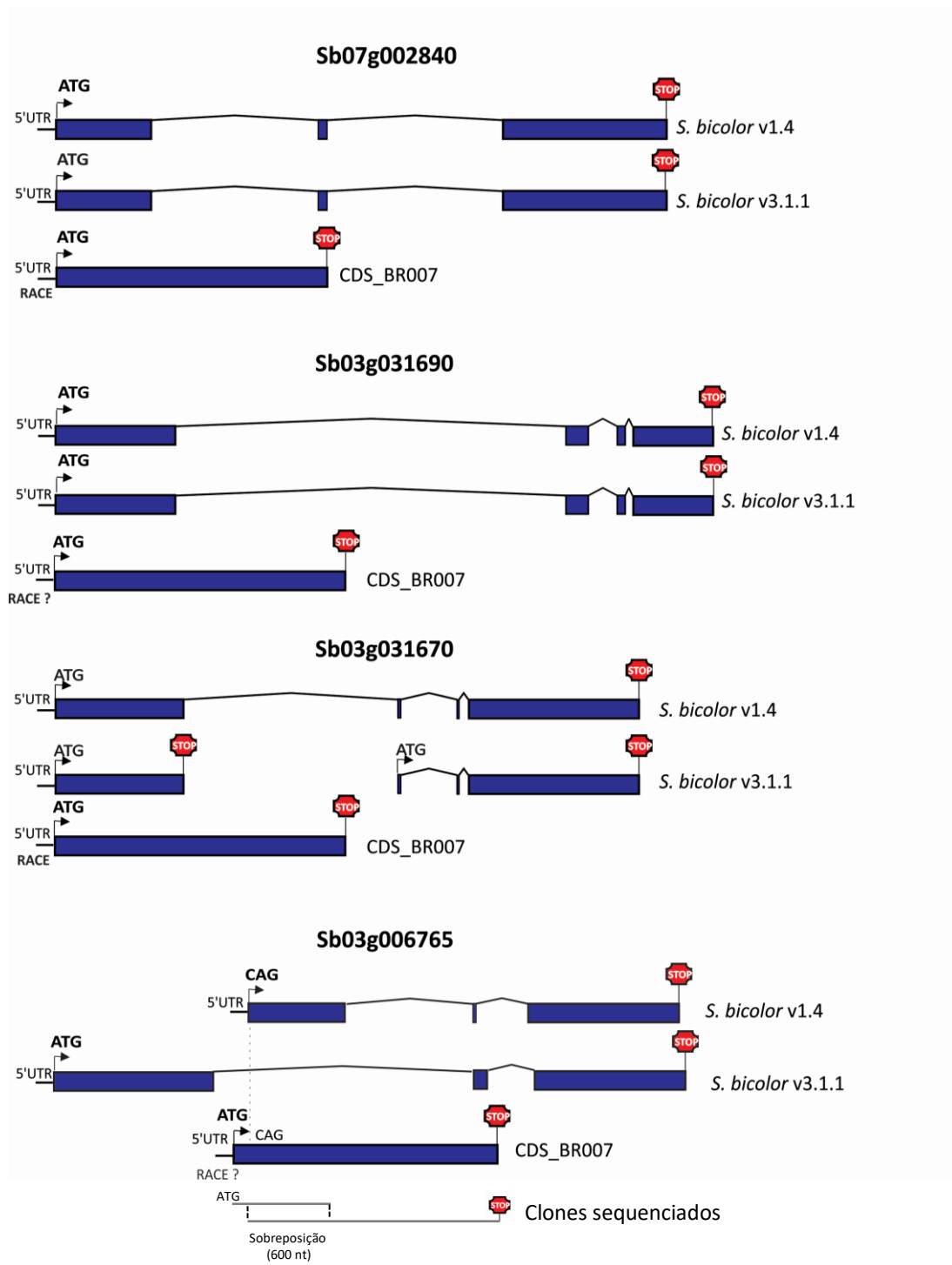
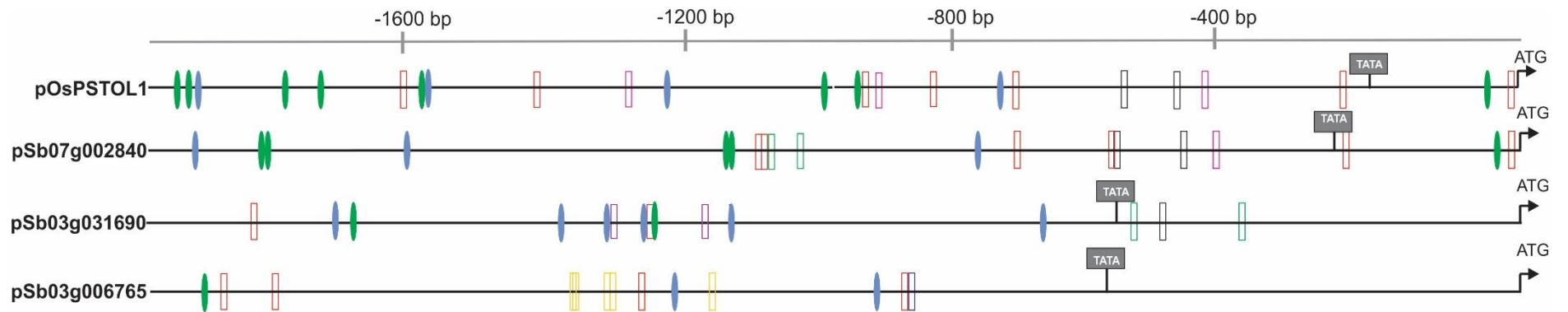


Figura 3



Legenda

Sítios para fatores de transcrição relacionados a:

Modificação no sistema radicular ⇨ ▭ RAV5' ▭ NACF, e NTMF ▭ LOB ▭ ROOT ▭ MYB96 ▭ ZFAT

Homeostase de P ⇨ ▭ PHR1 ▭ MIG

Figura 4

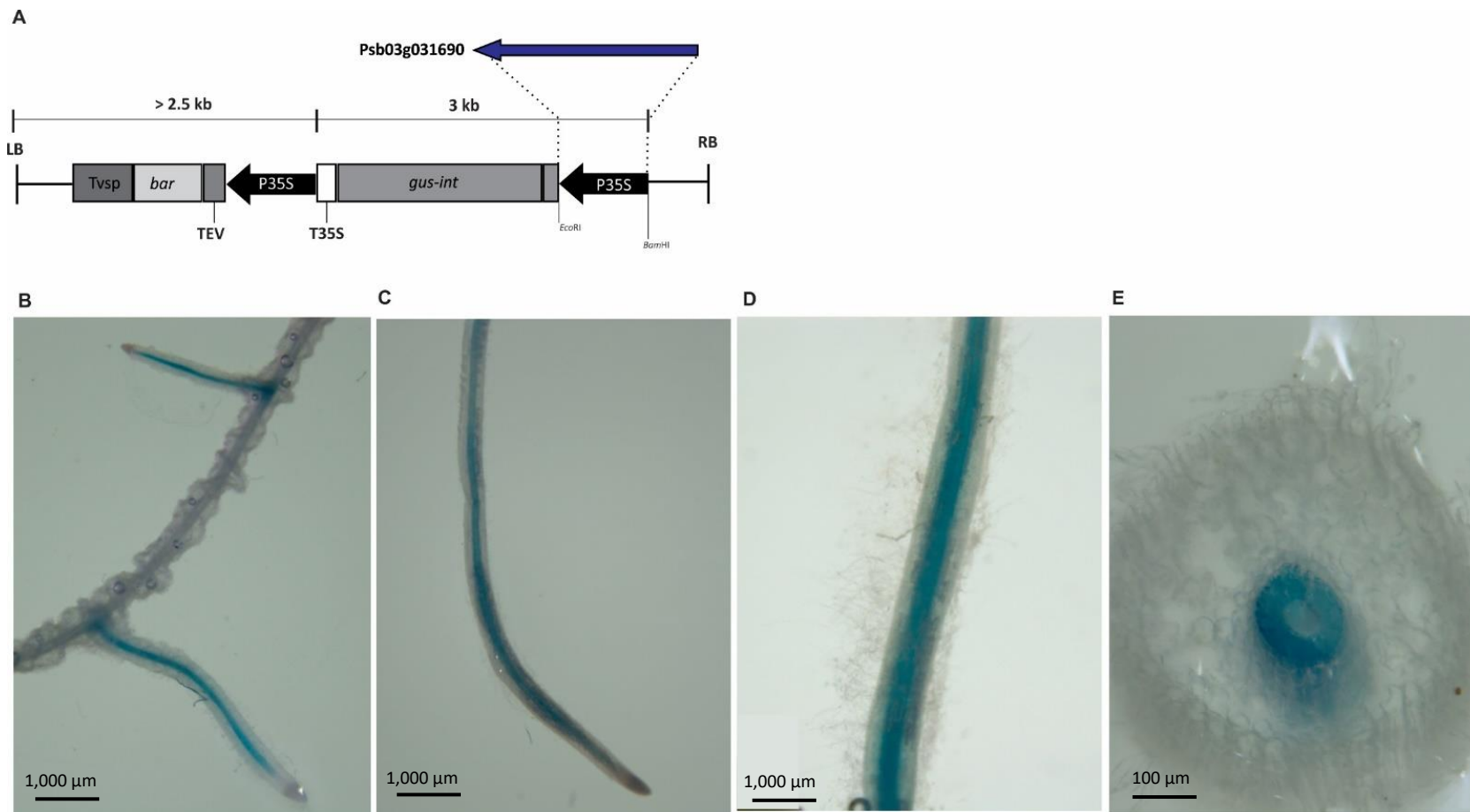


Figura 5

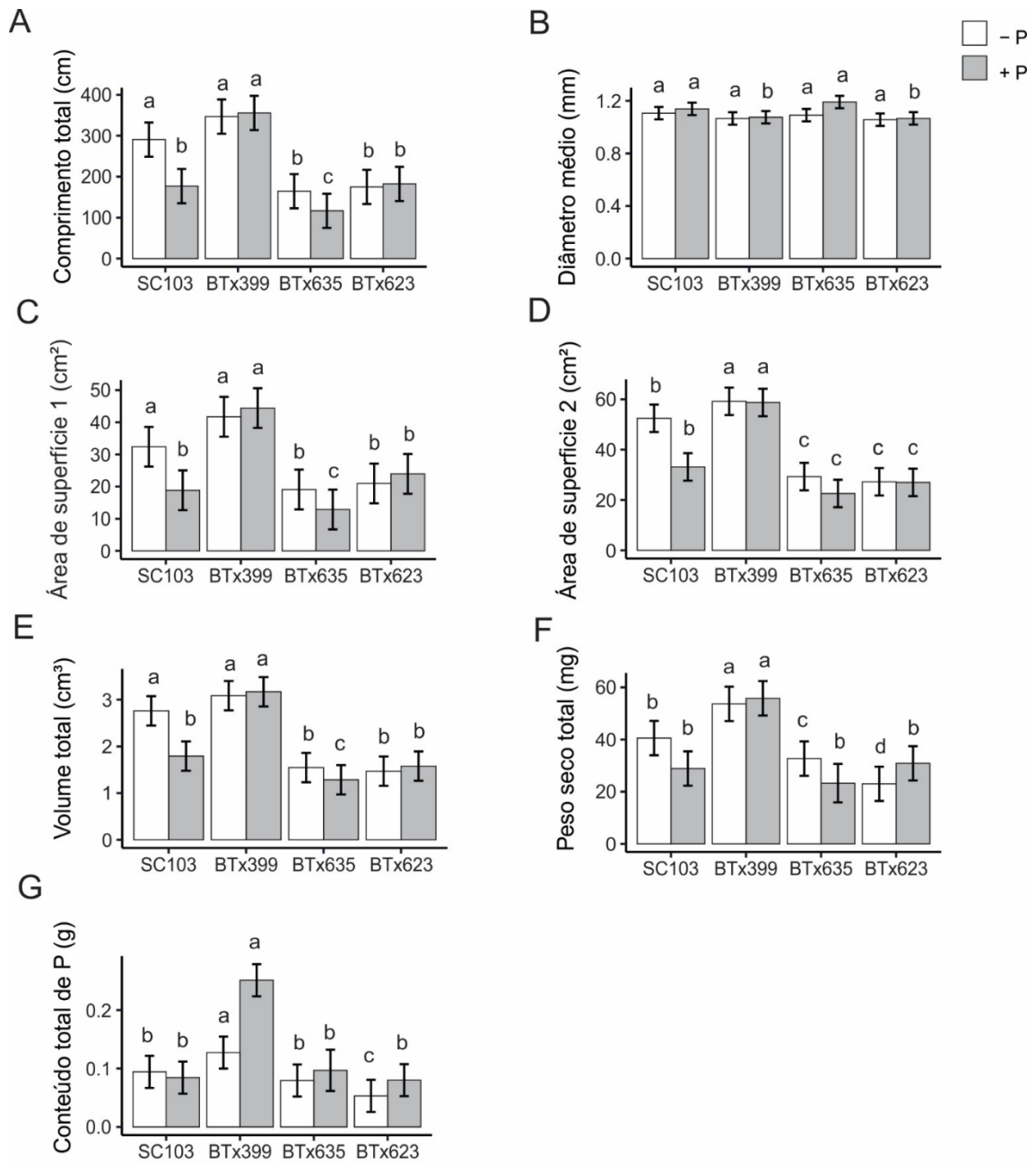


Figura 6

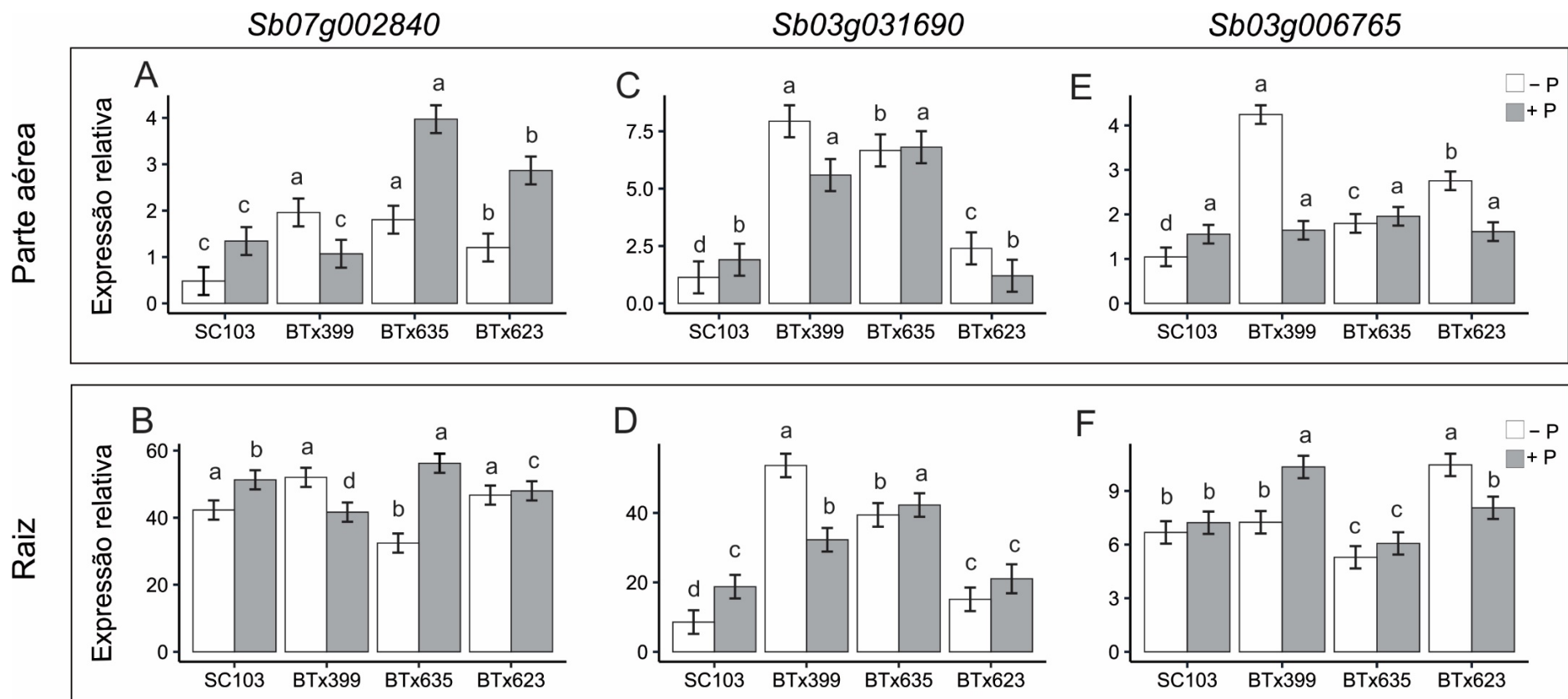
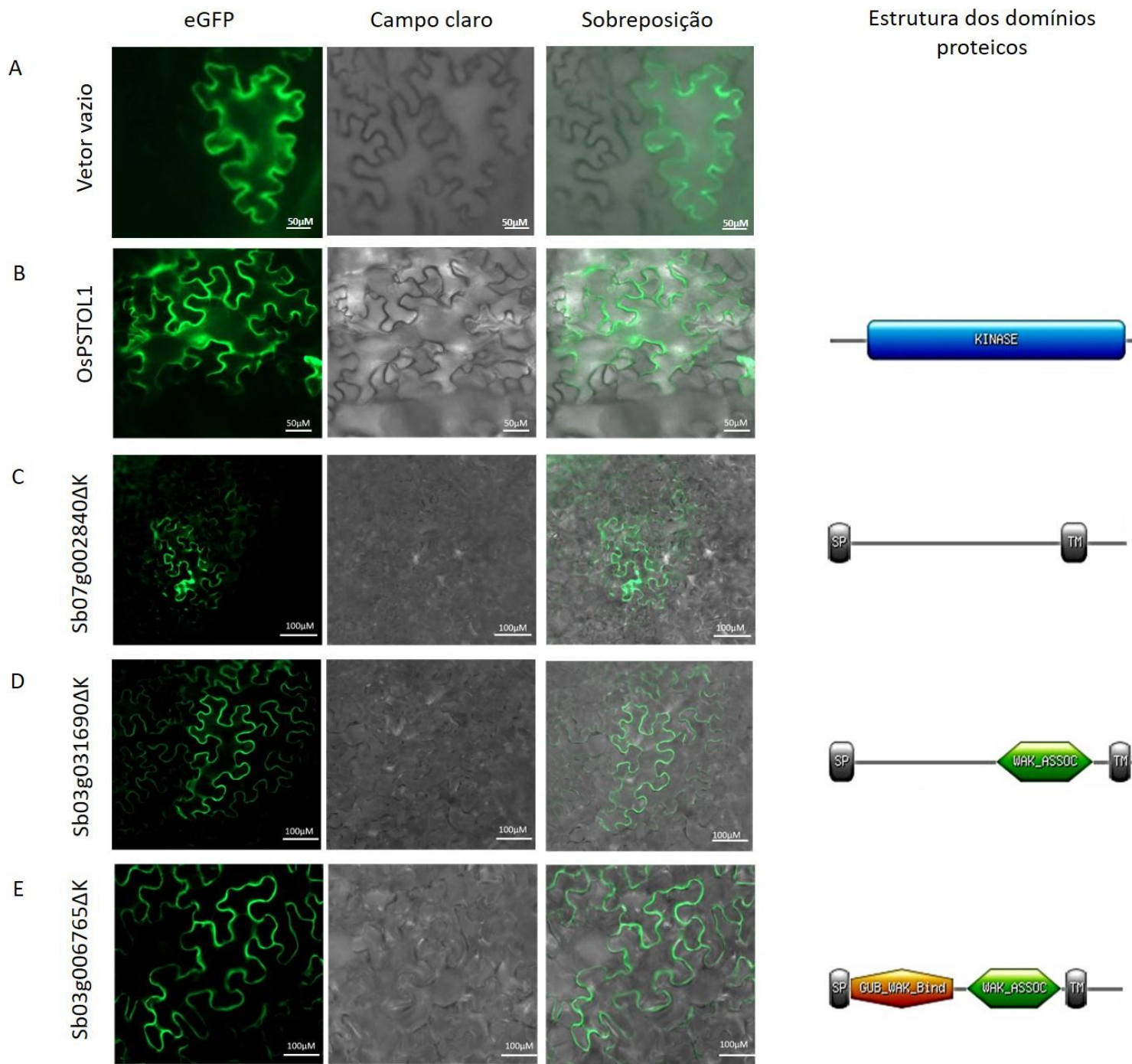


Figura 7



CONCLUSÃO GERAL E PERSPECTIVAS FUTURAS

Nesse trabalho nós estudamos o efeito da superexpressão dos genes *OsPSTOL1*, *SbPSTOL1* e *ZmPSTOL1* em plantas de milho. Os genes *OsPSTOL1* e *SbPSTOL1* foram relacionados a modulação do sistema radicular via proliferação das raízes finas, e ao aumento do acúmulo de biomassa da parte aérea de milho cultivado em solo com baixa disponibilidade de P. O melhor desempenho das plantas transgênicas em condição de estresse de P provavelmente está associado ao aumento da área de superfície do sistema radicular, conferindo assim maior exploração das camadas superficiais do solo e, conseqüentemente, maior aquisição de P. As características de morfologia radicular e acúmulo de biomassa dos eventos transgênicos *ZmPSTOL1* foram similares ao genótipo B104 não transgênico. Os genes *PSTOL1* codificam para as proteínas serina/treonina quinase classificadas na superfamília das RLKs/*Pelle*. Uma das funções das proteínas dessa superfamília está relacionada a mecanismos de desenvolvimento celular, diante disso, o próximo passo será avaliar o padrão de divisão e o alongamento celular das raízes dos eventos transgênicos de *OsPSTOL1* e *SbPSTOL1*.

O efeito dos genes *SbPSTOL1* foi também investigado na modulação do sistema radicular de sorgo. Inicialmente, nós confirmamos a relação filogenética entre as proteínas *OsPSTOL1*, *ZmPSTOL1* e *SbPSTOL1*. Ambas foram classificadas na subfamília das LRK10L-2 e derivam de um mesmo ancestral comum. Nossos resultados preliminares indicam que a região promotora dos genes *SbPSTOL1* é enriquecida com elementos *cis* regulatórios que podem atuar em modificações na morfologia radicular. Além disso, a expressão relativa dos genes *SbPSTOL1* é maior nas raízes quando comparada com a parte aérea e, no caso do gene *Sb03g0031690*, nós confirmamos que a expressão gênica é direcionada para as raízes laterais. Esses resultados sugerem que assim como o observado para as plantas de milho transgênico com superexpressão dos genes *SbPSTOL1*, em sorgo os genes *SbPSTOL1* podem estar relacionados à modulação do sistema radicular. A localização subcelular indica que as proteínas *Sb03g031690* e *Sb03g006765* localizam-se na membrana plasmática. Estudos posteriores serão necessários para verificar se as proteínas *Sb03g031690* e *Sb03g006765* estão associadas à parede celular, podendo ligar-se a fração pectina da parede celular, e atuarem em mecanismos de expansão celular. Além disso, a definição do complexo de proteínas recrutadas, juntamente com *SbPSTOL1*, é essencial para compreensão da cascata de sinalização envolvida na modulação do sistema radicular em sorgo.

ANEXO

Este anexo contém o artigo científico intitulado: “The genetic architecture of phosphorus efficiency in sorghum involves pleiotropic QTL for root morphology and grain yield under low phosphorus availability in the soil”, publicado na revista BMC Plant Biology (2019), com co-autoria de Laiane Silva Maciel.

Bernardino KC, Pastina MM, Menezes CB, de Sousa SM, **Maciel LM**, Carvalho Jr G, Guimarães CT, Barros BA, Silva LC, Carneiro PCS, Schaffert RE, Kochian LV and Magalhaes JV (2019). **The genetic architecture of phosphorus efficiency in sorghum involves pleiotropic QTL for root morphology and grain yield under low phosphorus availability in the soil.** BMC Plant Biology **19**, 87.

RESEARCH ARTICLE

Open Access



The genetic architecture of phosphorus efficiency in sorghum involves pleiotropic QTL for root morphology and grain yield under low phosphorus availability in the soil

Karine C. Bernardino^{1,2}, Maria Marta Pastina¹, Cícero B. Menezes¹, Sylvia M. de Sousa¹, Laiane S. Maciel^{1,3}, Geraldo Carvalho Jr^{1,5}, Cláudia T. Guimarães¹, Beatriz A. Barros¹, Luciano da Costa e Silva¹, Pedro C. S. Carneiro², Robert E. Schaffert¹, Leon V. Kochian⁴ and Jurandir V. Magalhães^{1,3*}

Abstract

Background: Phosphorus (P) fixation on aluminum (Al) and iron (Fe) oxides in soil clays restricts P availability for crops cultivated on highly weathered tropical soils, which are common in developing countries. Hence, P deficiency becomes a major obstacle for global food security. We used multi-trait quantitative trait loci (QTL) mapping to study the genetic architecture of P efficiency and to explore the importance of root traits on sorghum grain yield on a tropical low-P soil.

Results: P acquisition efficiency was the most important component of P efficiency, and both traits were highly correlated with grain yield under low P availability. Root surface area was positively associated with grain yield. The guinea parent, SC283, contributed 58% of all favorable alleles detected by single-trait mapping. Multi-trait mapping detected 14 grain yield and/or root morphology QTLs. Tightly linked or pleiotropic QTL underlying the surface area of fine roots (1–2 mm in diameter) and grain yield were detected at positions 1–7 megabase pairs (Mb) and 71 Mb on chromosome 3, respectively, and a root diameter/grain yield QTL was detected at 7 Mb on chromosome 7. All these QTLs were near sorghum homologs of the rice serine/threonine kinase, *OsPSTOL1*. The *SbPSTOL1* genes on chromosome 3, *Sb03g006765* at 7 Mb and *Sb03g031690* at 60 Mb were more highly expressed in SC283, which donated the favorable alleles at all QTLs found nearby *SbPSTOL1* genes. The Al tolerance gene, *SbMATE*, may also influence a grain yield QTL on chromosome 3. Another *PSTOL1*-like gene, *Sb07g02840*, appears to enhance grain yield via small increases in root diameter. Co-localization analyses suggested a role for other genes, such as a sorghum homolog of the *Arabidopsis ubiquitin-conjugating E2 enzyme, phosphate 2 (PHO2)*, on grain yield advantage conferred by the elite parent, BR007 allele.

(Continued on next page)

* Correspondence: jurandir.magalhaes@embrapa.br

¹Embrapa Milho e Sorgo, Rodovia MG 424, km 65, Caixa Postal 151, Sete Lagoas, MG 35701-970, Brazil

³Departamento de Biologia Geral, Universidade Federal de Minas Gerais, Avenida Presidente Antônio Carlos, 6627, Belo Horizonte, MG 31270-901, Brazil

Full list of author information is available at the end of the article



© The Author(s). 2019 Open Access This article is distributed under the terms of the Creative Commons Attribution 4.0 International License (<http://creativecommons.org/licenses/by/4.0/>), which permits unrestricted use, distribution, and reproduction in any medium, provided you give appropriate credit to the original author(s) and the source, provide a link to the Creative Commons license, and indicate if changes were made. The Creative Commons Public Domain Dedication waiver

(Continued from previous page)

Conclusions: Genetic determinants conferring higher root surface area and slight increases in fine root diameter may favor P uptake, thereby enhancing grain yield under low-P availability in the soil. Molecular markers for *SbPSTOL1* genes and for QTL increasing grain yield by non-root morphology-based mechanisms hold promise in breeding strategies aimed at developing sorghum cultivars adapted to low-P soils.

Keywords: Phosphorus deficiency, Phosphorus stress, Acid soils, Root system architecture

Background

Sorghum is a versatile crop that was domesticated in the tropics, in the northeastern quadrant of the African continent, possibly at least 5000 years ago [1]. Along with pearl millet, sorghum is the main staple food crop of the West African Savannah zones and in that region, guinea sorghums are broadly adapted to different stresses, including those caused by poor soil fertility [2]. In sub-Saharan Africa, two of the most important abiotic stresses that limit sorghum production are Al toxicity and low-P availability in the soil [3–5].

Both types of abiotic stresses share a common chemical basis centered on the prevalence of Al and Fe oxides in the clay fraction of highly weathered tropical soils [6]. Under low pH, Al is hydrolyzed into the ionic form, Al^{3+} , which damages plant roots, reducing crop yields [7]. Low-P availability, in turn, results from P fixation with Al and Fe oxides [8]. Plant roots absorb P from the soil solution in the orthophosphate forms, $H_2PO_4^-$ and HPO_4^{2-}

[9]. However, P fixation into soil clays impairs P diffusion from the soil solution towards the root surface, restricting uptake. Approximately half of the world agricultural lands have low-P availability [10]. Even in high input production systems, the non-renewable nature of phosphatic rock fertilizer [11] raises questions regarding the sustainability of continuously increasing rates of P fertilizer applications, which are needed to sustain crop yields. Therefore, in view of the prevalence of low-P soils in agricultural frontiers in which food production needs continuous improvement, such as in Africa, the identification of genetic factors that can be used to facilitate breeding for sorghum adaptation to low-P conditions become of utmost importance for global food security.

Aluminum tolerance in sorghum is due to the action of the Al-induced and Al-activated root citrate transporter, *SbMATE*, which underlies the aluminum tolerance locus, *Alt_{SB}*, at the terminal region of sorghum chromosome 3 [12]. Recently, the *SbMATE* allele donated by the guinea sorghum, SC283, has been shown to enhance sorghum grain yield by over 1.0 ton ha⁻¹ on an acid, Al toxic soil, with no detectable yield penalty in the absence of Al toxicity [13]. Leiser et al. [5], using *Alt_{SB}*-specific markers, also found strong associations of *SbMATE* with grain yield production, particularly in

low-P conditions in many environments in West-Africa. This suggests that *SbMATE* confers P use efficiency (PUE) in addition to Al tolerance, possibly via a joint effect of citrate mobilizing P that is fixed on the soil clays [14], and by enhancing root development in Al tolerant genotypes, increasing P uptake [15].

The ability of a plant to grow and to produce reasonable levels of grain and biomass under low-P availability, which we designate here as P use efficiency (PUE, or simply P efficiency), can be achieved via different mechanisms acting to optimize utilization of internal P or to enhance P acquisition [16]. From the crop physiology standpoint, these mechanisms may result from the modulation of P transporters, organic acid exudation, phosphatase secretion, mycorrhizae associations and alterations in root system architecture in response to low-P conditions, among other mechanisms (reviewed by López-Arredondo et al. [17]). For maize cultivated on a tropical low-P soil, P acquisition has been reported to be

more important than P internal utilization to explain differences in P use efficiency [16], which was also confirmed by QTL mapping results [18]. These studies emphasize the importance of changes in root system architecture and morphology as a mechanism favoring P acquisition (reviewed by Magalhaes et al. [19]). These modifications may involve changes in lateral root growth and angle, presence of shallow roots, in addition to enhanced proliferation of root hairs [10, 17, 20].

There is a recent body of evidence suggesting that genes modulating root morphology may result in increased P efficiency. Overexpression of the rice serine/threonine receptor-like kinase, *phosphorus starvation tolerance1* (*OsPSTOL1*, [21]) has been shown to increase grain yield in rice cultivated on a low-P soil via *OsPSTOL1*-elicited enhancement of early root growth, which favors P uptake in the developing rice plant. Subsequently, association mapping established that allelic variation at homologs of *OsPSTOL1* in sorghum, designated as *SbPSTOL1* genes, was associated with enhanced grain yield production on a low-P soil, likely via changes in root morphology, particularly root diameter and root surface area [22]. In addition, recent studies in Arabidopsis suggested a role in P efficiency for genes involved with Al tolerance, such as the

malate transporter, *ALMT1* [23] and its regulatory factor, the C₂H₂-type zinc finger, sensitive to proton rhizotoxicity 1 (AtSTOP1 [24]), in addition to the ABC-like transporter, aluminum sensitive 3 (*ALS3* [25, 26]). These genes appear to mediate an iron-dependent mechanism leading to enhancement of lateral root growth [27–31], which can possibly increase P uptake on acidic soils [15].

Using a genetic approach based on multi-trait QTL mapping, the present study aimed at unravelling the genetic architecture of P efficiency in a large sorghum recombinant inbred line population, and to establish links between the genetics and physiology of P efficiency, such as associations between root morphology, P content and sorghum grain yield on soils with low-P availability.

Results

Phenotypic analyses in the parents and RIL population

The most important trait for P efficiency within a breeding context, grain yield in the field, was assessed under low-P availability in the soil. We also estimated the relative contributions of the efficiency at which a plant acquires P from the soil (P acquisition efficiency, PAE) and also internal utilization efficiency (PUTIL), on overall P use efficiency (PUE or simply P efficiency, that encompasses both PAE and PUTIL) [16, 32]. Table 1 shows that PAE was the most important component influencing PUE for sorghum cultivated under low-P availability in the soil. Acquisition efficiency accounted for 82% of the variability in PUE, whereas the contribution of the PUTIL component was comparatively much smaller (18%). Therefore, we also assessed root morphology in hydroponics as changes in root morphology including increased root length can lead to enhanced P uptake and grain yield in soils with low-P availability. To gain insights into sorghum performance in hydroponics, we also assessed dry matter accumulation (DM) and shoot and root P content.

We observed substantial genetic variance for all traits assessed in the present study, with heritability estimates ranging from 0.3 (root diameter - RD) to 0.8 (plant height - PH, Additional file 1). Traits reflecting sorghum

performance grown on low-P growth media measured in nutrient solution (DM and P content) and in the field (grain yield - Gy) showed intermediate to high heritability estimates of between 0.4 and ~ 0.8, indicating reasonable experimental precision to detect regions of the sorghum genome associated with P efficiency. Marked transgressive segregation for grain yield in the recombinant inbred line (RIL) population, where a maximum of 4.5 ton ha⁻¹ exceeded by more than two-fold the grain yield for either parent (Additional file 1), emphasizes the rather complex, polygenic nature of P efficiency measured in sorghum cultivated under low-P availability in the soil.

We measured total root surface area (SA) of the sorghum root system and also the root surface area of roots within the diameter classes of 0–1, 1–2 and 2–4.5 mm, which are designated hereafter as very fine, fine and thicker roots, respectively. BR007 tended to exhibit greater total root surface area and had thinner roots compared to SC283 (Fig. 1a-d), which is due to the prevalence in BR007 of roots in the 0–1 mm diameter class (Fig. 1e - labeled SA1). These very fine roots comprise most of the root system in both parents but are more prevalent in BR007 (80%) compared to SC283 (73%) (Fig. 1e). However, when measured in the different root diameter classes, root surface area turned out to be heterogeneous between the parents, with SC283 showing higher surface area of both fine (SA2) and thicker (SA3) roots (Fig. 1f-g) compared to BR007. However, fine roots are still far more prevalent (~ 17%) than thicker roots (~ 1%) in the SC283 root system. Finally, the most important trait to reflect P efficiency, grain yield under low-P availability in the soil, was approximately 12% higher for the guinea race parent, SC283, compared to BR007 (Additional file 1 and Fig. 1h).

Trait associations

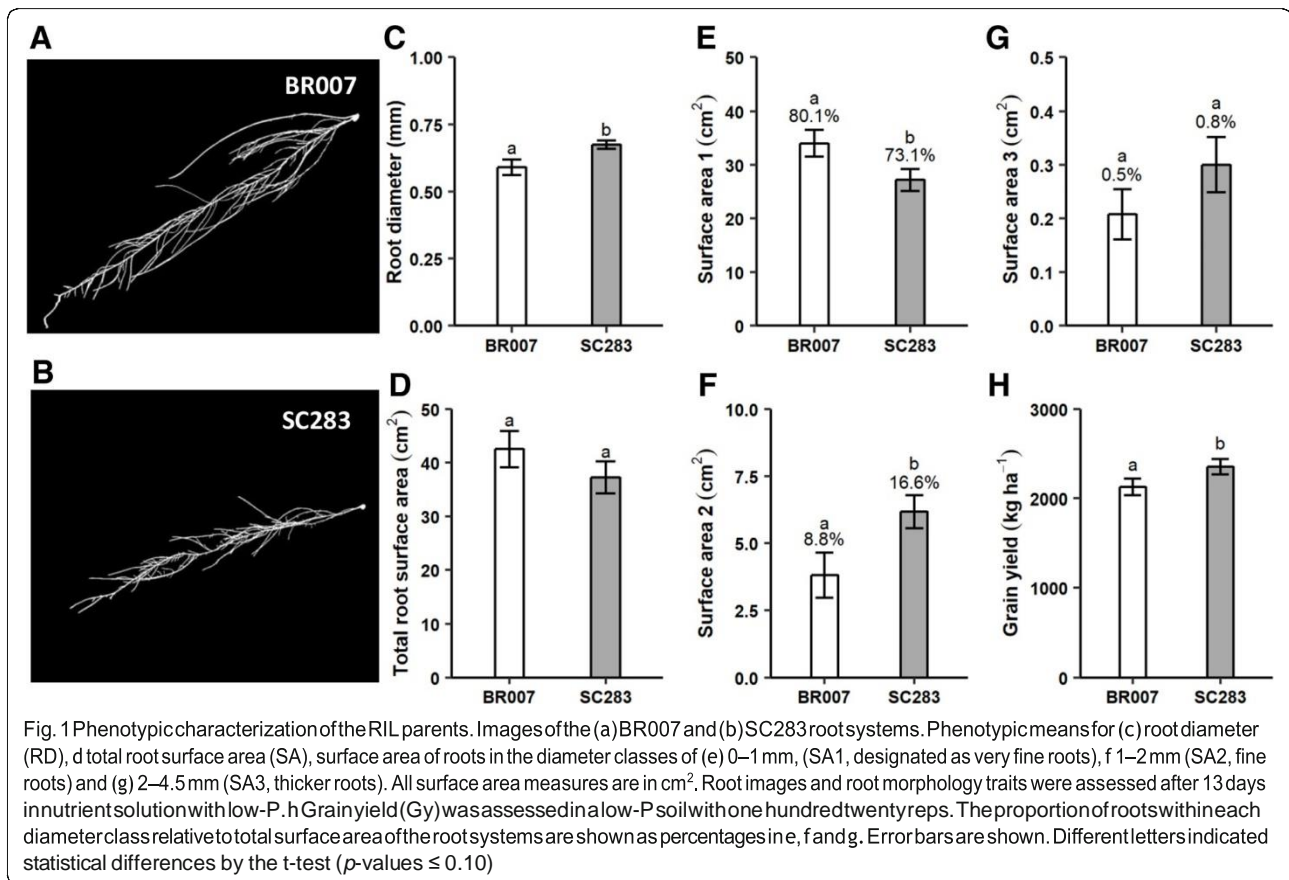
PAE and PUE were both highly correlated with grain yield ($r = 0.85$ and 0.97 , respectively; Additional file 2), which is consistent with the importance of P acquisition on P use efficiency (Table 1). PUTIL, which we found to be a minor component of PUE compared to acquisition efficiency (Table 1), was less correlated with grain yield ($r = 0.4$).

Next, we studied the association between root morphology traits and grain yield under low-P availability in the soil via a genetic correlation analysis (Fig. 2). Total root surface area was highly correlated with total root length (correlation coefficient, $r = 0.98$) and surface area of very fine roots (SA1) ($r = 0.99$). In addition, surface area of fine roots (SA2) was highly correlated with root volume 2 ($r = 1.0$). Therefore, among those traits, root surface area was used to gain insights into the role of root morphology on grain yield under low-P availability in the soil. A reduction in root diameter was in general

Table 1 Relative importance of PAE and PUTIL over PUE assessed in low-P conditions field

Trait	Correlation (r_{xy}) ^a	Standard Deviation (S)	S_x/S_y	Relative importance
PAE (x1)	0.9216	0.2285	0.8868	0.82
PUTIL (x2)	0.4763	0.0999	0.3878	0.18
PUE (y)		0.255		

^a r_{xy} : Phenotypic correlation among Phosphorus acquisition efficiency (PAE) and Phosphorus internal utilization efficiency (PUTIL) and Phosphorus use efficiency (PUE)



associated with increased total root surface area ($r = -0.46$), which was driven primarily by very fine roots (RD vs. SA1, $r = -0.53$) and, to a lesser extent, by thicker roots (RD vs. SA3, $r = -0.23$). This suggests the existence of some genetic determinants that act to increase root surface area via enhanced development of finer roots. However, the magnitude of the correlation coefficients also indicates that root surface area and root diameter are controlled to some extent independently. Surface area of fine roots was positively but weakly correlated with root diameter (RD vs. SA2, $r = 0.1$), suggesting that slight increases in root diameter between 1 and 2 mm may result in enhanced surface area. Grain yield under low-P availability in the soil was significantly correlated with the different traits reflecting surface area of fine roots ($r \cong 0.1$, p -value < 0.05), although this association tended to dissipate with thicker roots between 2 and 4.5 mm in diameter (SA3, $r = 0.08$, p -value = 0.10).

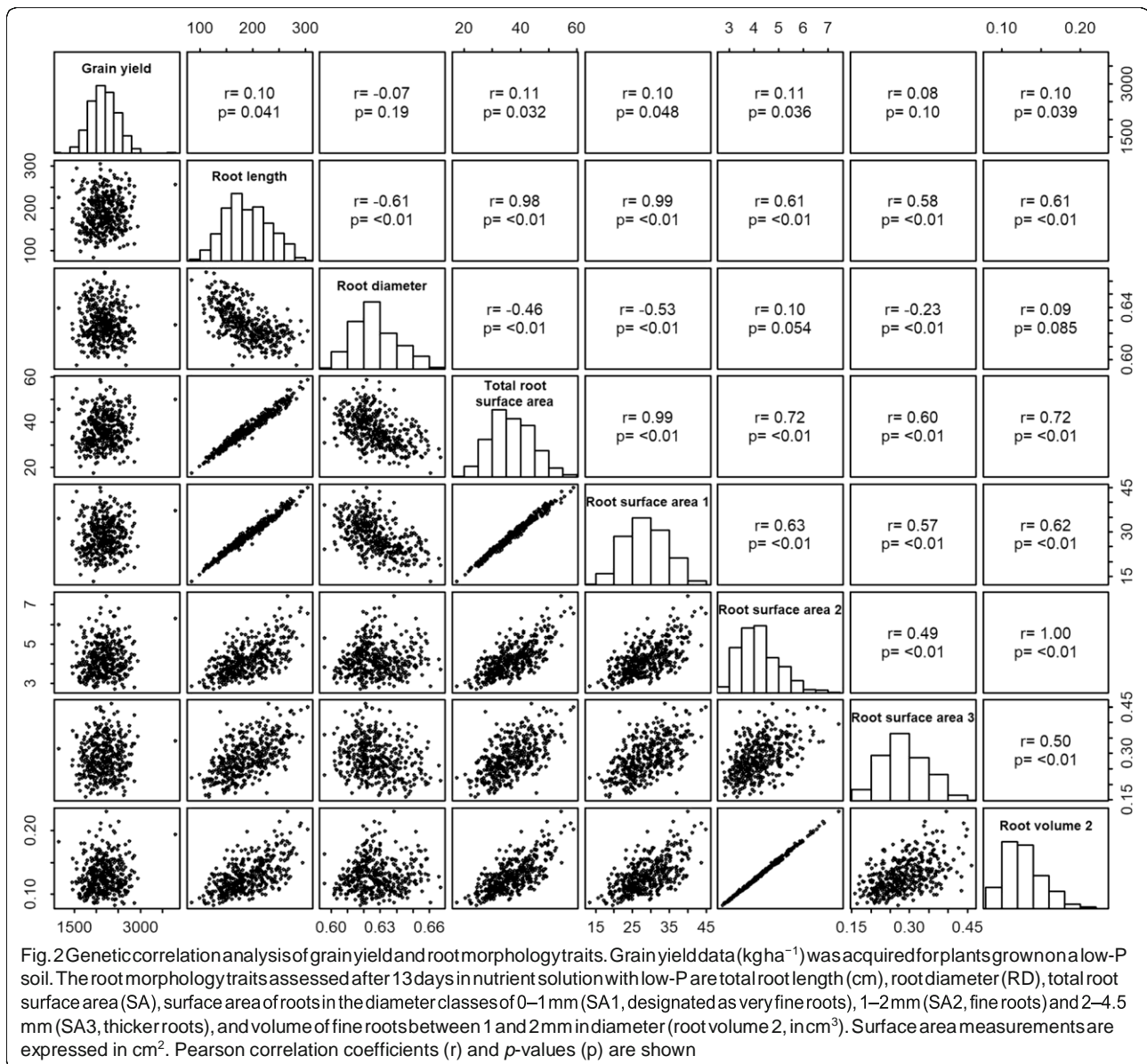
QTL mapping for root morphology and performance traits under low-P

We mapped QTLs underlying P efficiency traits and found that the majority of the QTLs, primarily for PAE (9 out of 10) and PUE (9 out of 10), but also for PUTIL (although to a lesser extent) coincided with those

detected for grain yield, with exception of the QTL on chromosome 5 for PUTIL (Additional file 3). This is consistent both with the much higher importance of PAE compared to PUTIL on PUE (Table 1) and with the strong association between grain yield and PAE/PUE (Additional file 2).

Although grain yield was the most informative trait for QTL detection, a PUTIL QTL on chromosome 5 may harbor genes underlying changes in P internal utilization and two chromosome 1 QTLs may jointly underlie PAE and PUTIL. As PUTIL was much less important than P acquisition efficiency for PUE, we thus focused primarily on the genetic mechanisms that enhance P acquisition efficiency via changes in root morphology and their role in increased grain yield on low-P soil.

We initially conducted single-trait QTL mapping with many different traits related to root morphology and sorghum performance under low-P conditions (Additional file 4). This analysis detected a total of 101 QTLs, with the favorable allele of 59 QTLs donated by the guinea parent, SC283, whereas the BR007 alleles increased phenotypic expression for 42 QTLs. Based on the correlation analyses between traits and on the single-trait QTL mapping results, we selected a subset of non-redundant and highly informative traits (i.e. traits



repeatedly associated with some QTLs) for multi-trait QTL mapping, focusing primarily on the most important P efficiency trait, namely grain yield under low-P availability in the soil (Fig. 3). P content in the grain (Pg), for example, was highly correlated with grain yield ($r = 0.92$) and we thus only included grain yield and not Pg for multi-trait QTL mapping. The final set of traits used for multi-trait QTL mapping was comprised of grain yield (Gy), surface area of fine roots in the 1–2 mm diameter class (SA2) and root diameter (RD).

For the selected traits, the majority of the QTLs detected by single-trait QTL mapping (Fig. 3a–c) were also detected by multi-trait QTL mapping (Fig. 3d). Exceptions are the QTLs for SA2 on chromosomes 5, 7 and 9 and the Gy QTL on chromosome 8 and 10, which

were not detected using multi-trait QTL mapping. Multi-trait mapping detected 14 QTLs (see Fig. 3a–c for single-trait mapping results) and revealed ten QTLs related to grain yield (Fig. 3d), within which one QTL was tightly linked to a root morphology QTL ($Gy-3\dots SA2-3$) and two were possibly pleiotropic with root morphology ($Gy/SA2-3$ and $Gy/RD-7$). For all of these QTLs, the favorable allele was donated by SC283 (Additional file 5). In contrast, the favorable alleles for five of the eight grain yield-specific QTLs were donated by BR007.

The different grain yield QTLs explained, in general, approximately 1 to 5% of the genetic variance and increased grain yield by $\sim 120 \text{ kg ha}^{-1}$ (Additional files 4 and 5), except for a Gy QTL at the end region of chromosome 9 ($Gy-9$). This QTL was detected for several different traits

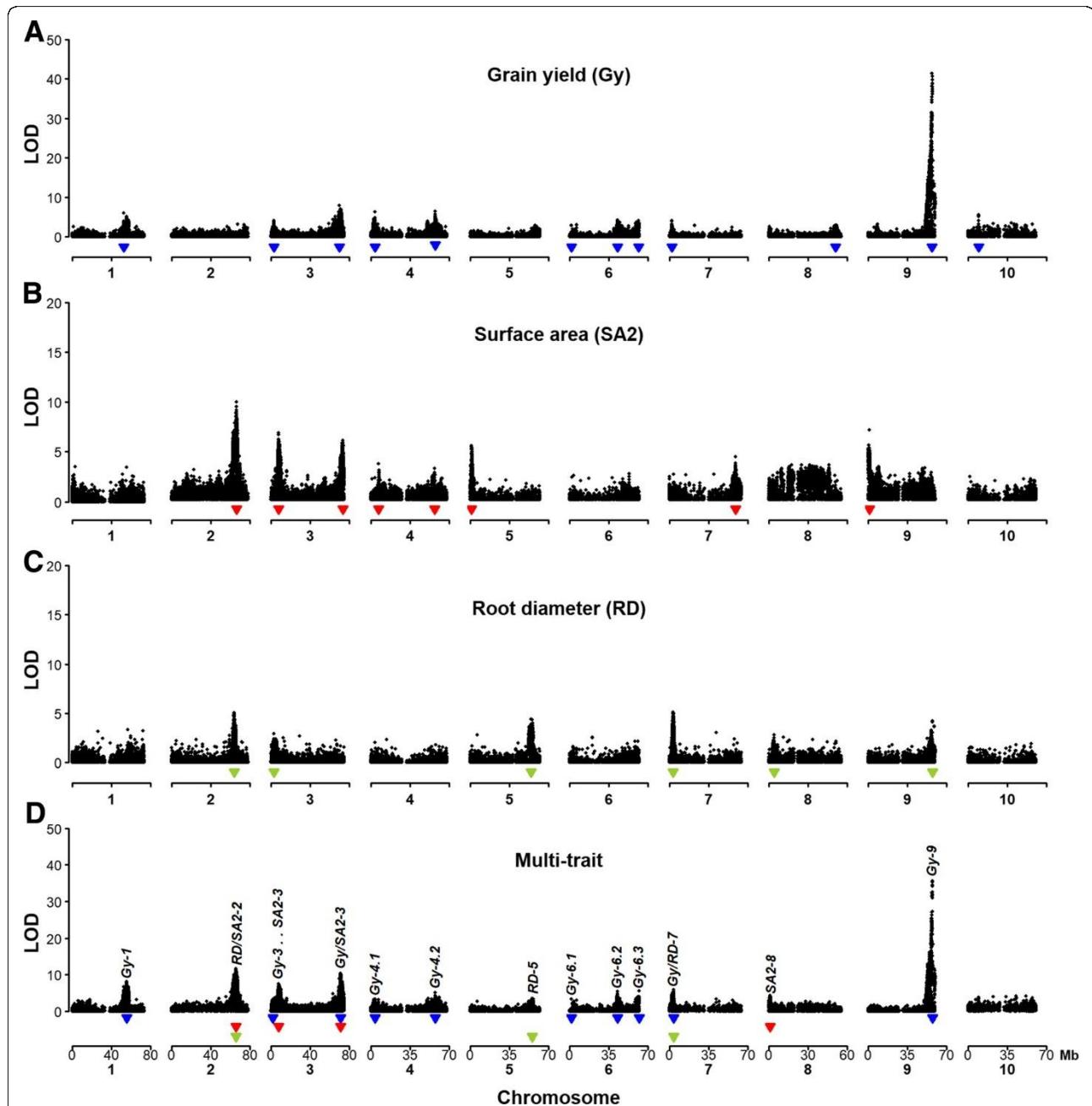


Fig. 3 Single- and multi-trait QTL mapping profiles for grain yield and root morphology traits. The final set of traits used for multi-trait QTL mapping was comprised of grain yield (Gy), surface area of fine roots in the 1–2 mm diameter class (SA2) and root diameter (RD). Grain yield (Gy) data (kg ha^{-1}) was acquired in a low-P soil. The root morphology traits assessed after 13 days in nutrient solution with low-P are root diameter (RD, mm), surface area of fine roots between 1 and 2 mm in diameter (SA2, in cm^2). QTL profiles obtained with (a–c) single- and (d) multi-trait QTL mapping are shown. QTLs were designated based on the respective traits followed by the chromosome locations, and are numbered in the case of multiple QTLs within the same chromosome. For example *Gy-6.1* is a grain yield QTL located in the beginning of chromosome 6. Tight linkage between QTL or possible pleiotropy were depicted by double dots and slashes, respectively in the QTL designations. Blue, red and green inverted triangles depict the positions of QTLs for Gy, SA2 and RD, respectively

(Additional file 4), explained the largest proportion of the genetic variance ($\sim 26\%$, Additional file 4), and was associated with the largest increase in grain yield, of $\sim 400 \text{ kg ha}^{-1}$, with the favorable allele donated by BR007.

Based on single-trait QTL analysis, all grain yield QTLs detected by multi-trait QTL mapping were co-located or were found near QTLs underlying P content and/or dry matter accumulation in hydroponics under low-P (Fig. 3, Additional file 4). The *RD/SA2-2*

QTL (Additional file 5), which was the only root morphology QTL not associated with grain yield, co-located with QTLs for root dry matter accumulation, and shoot and root P content assessed in hydroponics via single-trait analyses (Additional file 4). Multi-trait QTL mapping provided insights into possible pleiotropic QTLs underlying changes in root system morphology and grain yield in the context of genes previously shown to be associated with those traits, such as sorghum homologs of the rice serine/threonine kinase, *OsPSTOL1* [22]. The physical positions of the *SbPSTOL1* genes and that of *SbMATE*, which confers sorghum Al tolerance [33], in the context of the QTL detected by multi-trait QTL mapping, are shown in Fig. 4. The QTLs *Gy-3* and *SA2-3* were in close physical proximity, between 5.38 and 0.46 Mb, respectively, from the *PSTOL1* gene *Sb03g006765* (Fig. 4a). At the end of chromosome 3, a cluster of four *SbPSTOL1* genes were located ~ 11 Mb from the *Gy/SA2-3* QTL and this QTL was only 80 Kb from *SbMATE* (Fig. 4b). Finally, the *Gy/RD-7* QTL is located only 0.66 Mb from the *SbPSTOL1* gene, *Sb07g002840* (Fig. 4c).

Expression profile of *SbPSTOL1* genes in the parent's root systems under low-P

Multi-trait QTL mapping results indicated that the favorable alleles at QTLs either tightly linked or possibly pleiotropic with grain yield and root morphology on chromosomes 3 and 7, which were located in the vicinity of *SbPSTOL1* genes, were consistently donated by SC283. Next, we assessed the expression profile of these *SbPSTOL1* genes in roots of the RIL parents, BR007 and SC283, subjected to low-P conditions in hydroponics. *Sb03g006765*, located at the beginning of chromosome 3, and *Sb03g031690*, which is part of a *SbPSTOL1* cluster at position ~ 60 Mb on chromosome 3 [22], were both more highly expressed in the roots of the guinea parent, SC283, in the low-P growth media (Fig. 5). In contrast, expression of *Sb07g002840* was higher in BR007 roots, which donates the inferior allele at the *Gy/RD-7* QTL.

Discussion

Low-P availability in the soil is a major factor that compromises food security in many developing countries in West Africa that rely on the sorghum crop for food production [2]. West Africa is the primary domestication center of the guinea race of sorghum [34], which is used therein as a pivotal staple food in areas with low soil fertility [35]. Thus, sorghum adaptation to soils with low-P availability becomes critical for food security [5, 35].

Our QTL mapping study emphasized the complex nature of traits related to P efficiency in sorghum, with favorable alleles donated by both parents in rather equal proportions. However, the observed slight

overrepresentation of superior QTL alleles derived from the guinea race parent, SC283, may not be coincidental, reflecting local adaptation of guinea sorghums to poor soil fertility and acid soils in West Africa [2].

QTLs for root morphology coincide with grain yield QTL under low-P availability

The root system of monocotyledonous crop plants consists of one or more seminal roots that originate from the seed embryo after germination, and crown roots that emerge later from nodes along the stem [36]. Increased root surface area, which can be achieved via enhanced lateral root branching, can enhance P uptake and plant growth [37]. Among the ten grain yield QTL that were detected by multi-trait mapping, three were either tightly linked (one QTL) or possibly pleiotropic (two QTL) with root morphology traits. Those are: 1) the grain yield QTL, *Gy-3* and the QTL for surface area of fine roots, *SA2-3* at the beginning of chromosome 3, which are only ~ 6 Mb apart; 2) the pleiotropic *Gy/SA2-3* QTL at position ~ 71 Mb on chromosome 3; and 3) the *Gy/RD-7* QTL at 3.6 Mb on chromosome 7 (Fig. 3d). Thus, our multi-trait QTL mapping approach established an important role for root system morphology as an entry point for molecular breeding strategies targeting enhanced P uptake and grain yield under low-P availability in the soil.

Specific changes in root morphology are likely important for P efficiency

The grain yield QTLs that are possibly determined by changes in root surface area seem to be more specific to roots between 1 and 2 mm (*SA2*) in diameter than to the very fine roots between 0 and 1 mm (*SA1*) or thicker roots (2–4.5 mm, *SA3*). Via single-trait mapping, a QTL for *SA2* (and not for other root diameter classes) was found at the beginning of chromosome 3, tightly linked to a *Gy* QTL, whereas the grain yield/surface area QTL at the end of chromosome 3 was near *SA2* and *SA3* QTL. A total surface area (*SA*) QTL was also found at the end of chromosome 3, but this is expected as total surface area, which is highly correlated with *SA1*, largely represents the sum of surface area of roots in all diameter classes. Importantly, eight QTLs in total were detected for surface area of fine roots via single-trait mapping, whereas only four and two QTLs were detected for total surface area (that is highly correlated with surface area of very fine roots, $r = 0.99$) and for surface area of thicker roots, respectively. Very thick roots are not expected to play a major role in nutrient uptake, as plant species with a majority of fine roots in their root systems tend to optimize the ratio between root surface area available for uptake and root weight, reflecting a reduced carbon cost for root biomass formation [38].

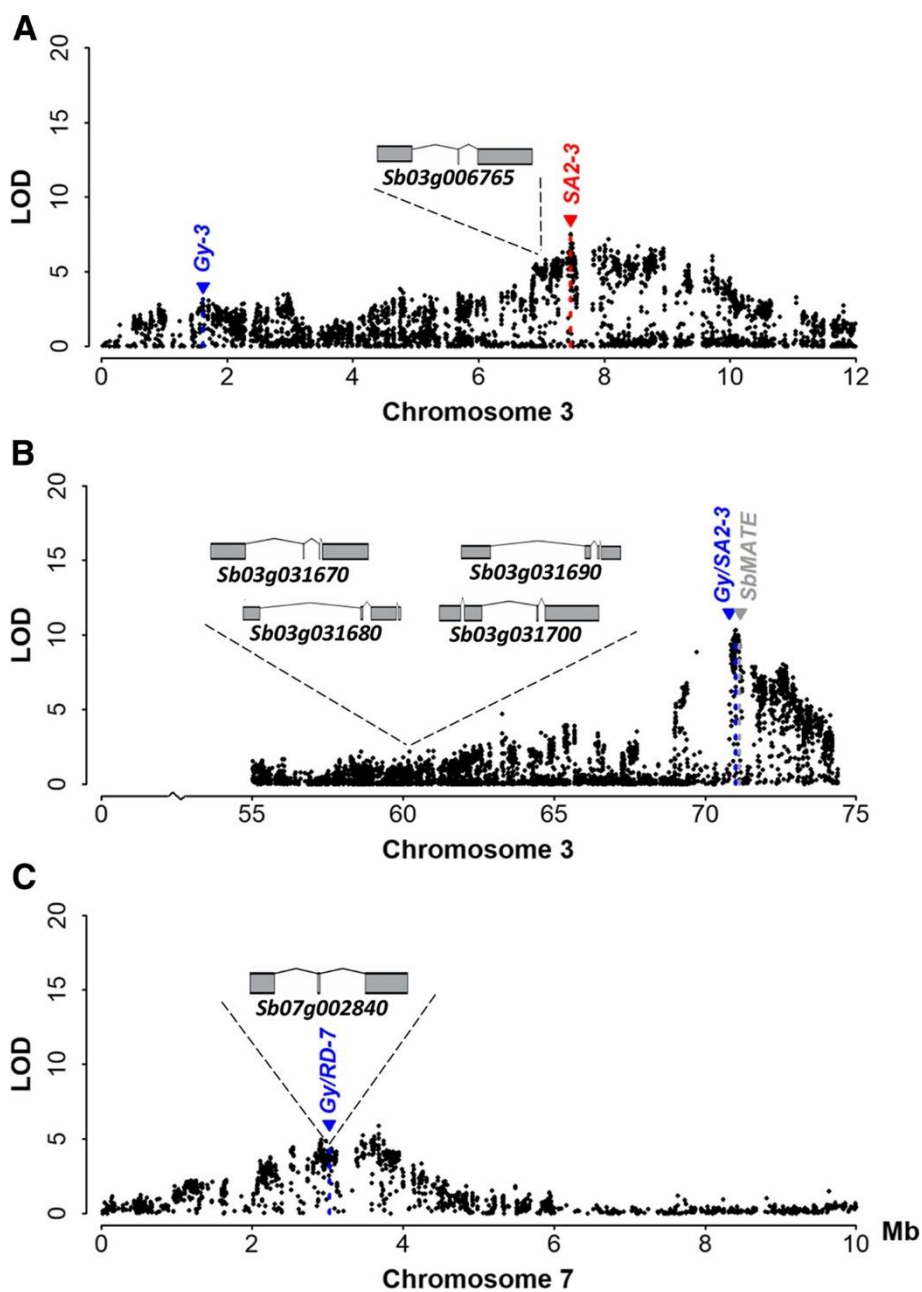


Fig. 4 Physical positions of *SbPSTOL1* genes in the context of the QTL regions detected by multi-trait QTL mapping (Fig. 3d). The root morphology traits assessed after 13 days in nutrient solution with low-P are root diameter (RD, mm) and surface area of fine roots between 1 and 2 mm in diameter (SA2, in cm²). Possible pleiotropy between Gy (grain yield), SA2 and RD QTL, when detected, were depicted by slashes in the QTL designations. Physical positions and gene models for the *SbPSTOL1* genes (<https://phytozome.jgi.doe.gov/>, v1.4 of the sorghum genome), a *Sb03g006765*, b the *SbPSTOL1* cluster including *Sb03g031690* and (c) *Sb07g002840* are shown

It is generally thought that the finer the roots, the better the root system can mine the soil for diffusion-limited nutrients, like the phosphate anion on tropical soils. However, although fine roots are the key factor for uptake, particularly for nutrients with very low mobility in tropical soils such as P, our QTL

data interestingly suggest there is a trade-off between decreased root diameter and enhanced P uptake. This can be expected as decreased root diameter, beyond a given threshold may, for example, limit root penetration through the soil [38] and, possibly, lead to less root longevity [39].

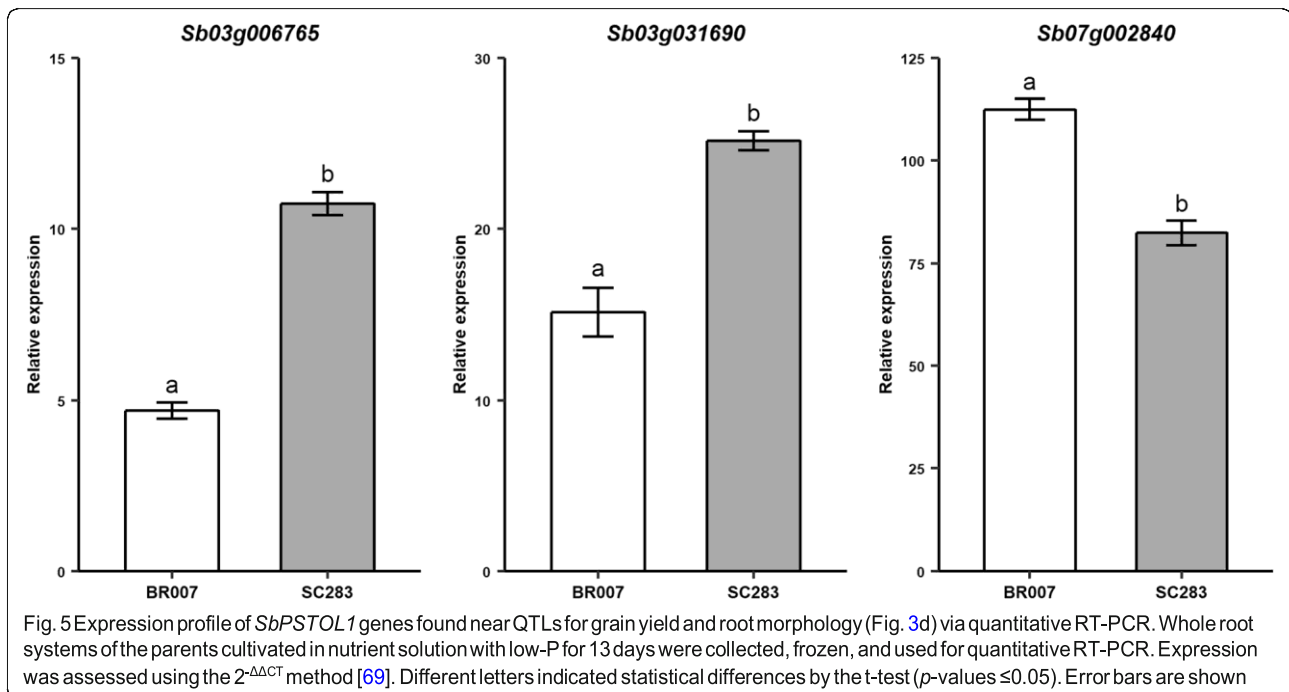


Fig. 5 Expression profile of *SbPSTOL1* genes found near QTLs for grain yield and root morphology (Fig. 3d) via quantitative RT-PCR. Whole root systems of the parents cultivated in nutrient solution with low-P for 13 days were collected, frozen, and used for quantitative RT-PCR. Expression was assessed using the $2^{-\Delta\Delta CT}$ method [69]. Different letters indicated statistical differences by the t-test (p -values ≤ 0.05). Error bars are shown

SbPSTOL1 genes possibly underlie QTLs for root morphology and grain yield

All three root morphology QTL that were found to be either tightly linked or pleiotropic with grain yield are located in the vicinity of sorghum homologs of the rice serine/threonine kinase, *OsPSTOL1*, which was previously found to enhance early root growth and grain yield in rice under low-P availability [21].

Based on multi-trait mapping, two QTLs underlying grain yield and root surface area, *Gy-3* and *SA2-3*, were found on chromosome 3 at positions 1.6 and 7.4 Mb, respectively. Those QTLs are only ~ 6 Mb apart and are physically very close to the *SbPSTOL1* gene, *Sb03g006765*, at position 7 Mb. A possible pleiotropic QTL, simultaneously underlying *SA2* and *Gy* (*Gy/SA2-3*), was found approximately ~ 11 Mb from a *SbPSTOL1* cluster at position ~ 60 Mb on chromosome 3. The favorable alleles both at the *SA2* and *Gy* QTLs near *Sb03g006765* and at the possible *Gy/SA2-3* pleiotropic QTL at position 71 Mb are derived from the guinea parent, SC283. Although BR007 tended to show greater root surface area compared to SC283, this is due to the prevalence in BR007 of very fine roots, between 0 and 1 mm in diameter (Fig. 1). Compared to BR007, SC283, which donates the positive alleles for the *Gy* and *SA2* QTLs in the vicinity of *SbPSTOL1* genes, has about twice the proportion of fine roots between 1 and 2 mm in diameter, whose surface area gives rise to both *SA2* QTL on chromosome 3. Finally, both *Sb03g006765* and *Sb03g031690* (that is part of a *SbPSTOL1* cluster at position ~ 60 Mb), exhibited significantly higher expression in response to low-P growth

conditions specifically in SC283 roots, when compared to BR007, which is in agreement with SC283 donating *SbPSTOL1* alleles that enhance the surface area of fine roots at the respective chromosome 3 QTL.

Previously, single nucleotide polymorphism (SNP) loci within the *SbPSTOL1* gene *Sb03g006765*, and in the *SbPSTOL1* genes present in the gene cluster at position ~ 60 Mb, were associated both with variation in root surface area and sorghum performance under low-P [22]. This suggests that the grain yield QTL on chromosome 3 results, at least in part, from enhanced surface area conferred by *SbPSTOL1* genes. However, the major Al tolerance gene, *SbMATE*, is located at position 71 Mb on the same chromosome, and thus is closer to the pleio-tropic *Gy/SA2-3* QTL in the region (Fig. 4). *SbMATE* has been shown to contribute to grain yield under low-P conditions, possibly via citrate-based enhanced mobilization of P that is bound to the soil clays [5], or simply as an indirect effect of enhanced root development under Al toxicity in the subsoil [15]. Thus, we cannot rule out that *SbMATE* is responsible for some of the yield advantage that gives rise to the grain yield QTL at the end of sorghum chromosome 3.

We previously reported that allelic variation at the *SbPSTOL1* gene, *Sb07g002840*, influences root diameter, biomass accumulation and P uptake, although associations with grain yield were not found using a sorghum association panel [22]. A pleiotropic QTL underlying both *Gy* and *RD* was found only ~ 0.6 Mb away from *Sb07g002840*, and the favorable allele for this *Gy/RD-7* QTL was donated by SC283. It is interesting to

note that SC283 exhibits overall a larger root diameter compared to BR007, which is in agreement with the SC283 origin of the favorable allele at the *Gy/RD-7* QTL. In barley subjected to low-P conditions, based on the effects of co-localized QTLs, larger root diameter was related to higher grain yield [40], which is consistent with our results with *Sb07g002840*. A positive relationship has been reported between the size of the apical meristem (reflected by the apical diameter) and important characteristics such as the elongation rate, growth duration and gravitropism [38], which could lead to enhanced performance under low-P conditions. It is thus possible that the slight increases in root diameter elicited by *Sb07g002840* lead to an increase in the surface area of laterals that are still fine, generating more physically robust roots without substantial carbon cost. Hence, these roots would be more efficient to optimize P mining in the soil, leading to enhanced P uptake and grain yield under soil low-P availability. Unlike the *SbPSTOL1* genes on chromosome 3, root *Sb07g002840* expression is lower in SC283 compared to BR007. This could suggest an allele-specific repressor effect of *Sb07g002840* on root diameter, with lower expression of the SC283 allele of *Sb07g002840*, leading to a slight increase in root diameter.

Syntenic analysis in sorghum and maize supports a role for *PSTOL1* genes in root morphology and reveals other genes possibly involved in P efficiency

We compared the positions of the grain yield QTL detected in sorghum by multi-trait QTL mapping with QTLs related to root morphology and P efficiency reported in the closely related species, maize. The summary shown in Additional file 6 was based primarily on a QTL mapping study that included the same traits used in our sorghum RIL population [41] and in a comprehensive meta-analysis of QTLs related to low-P tolerance in maize, which defined 23 consensus QTL (*cQTL*, [42]).

The maize root morphology QTLs, *qMulti3.04*, *qRL8.05* and *qRD4.05*, harbor maize homologs of *Sb03g006765*, *Sb03g031690*, and *Sb07g002840*, respectively (the *SbPSTOL1* genes at chromosomes 3 and 7 that are near grain and root morphology QTLs, Fig. 4), in regions that are syntenic between maize and sorghum (Additional file 6). Consistent with our findings that *Sb07g002840* influences root diameter, *qRD4.05* is also associated with changes in root diameter in maize. Four homologs of *OsPSTOL1* were found in maize *cQTL3-1* at bin 3.04 [42], which overlaps with *qMulti3.04* [41] that is associated with multiple root morphology traits. In this region, the maize *PSTOL1*-like gene, *GRMZM2G412760*, is closely related to *Sb03g006765*. In conjunction with the presence of a functional *PSTOL1*

protein in rice (*OsPSTOL1*, [21]), this suggests that the *PSTOL1* function in modulating root morphology is rather ancient, predating the divergence between maize, sorghum and rice.

This analysis also suggests possible functions for grain yield QTL that are apparently unrelated to root morphology in sorghum. Previously, we detected a major QTL for plant height and flowering time at the end region of sorghum chromosome 9 [43], which coincides with the QTL underlying multiple traits that was found in the present study. The ubiquitin-conjugating enzyme UBC24, encoded by *phosphate2* (*PHO2*), which is a major player in P homeostasis and plant responses to P deficiency [44], has been recently implicated in tolerance to low-P in maize [45]. We found a highly similar *PHO2* homolog at position ~ 57 Mb on sorghum chromosome 9, which closely overlaps with multiple QTLs related to root morphology and many other traits, including grain yield (Additional file 4 and Fig. 3). *GRMZM2G381709*, a maize homolog of *PHO2*, is also located in a syntenic position of the maize genome, near a cQTL (*cQTL6-2*) for low-P tolerance in maize defined by meta-analysis (Additional file 6).

Sorghum homologs of the auxin transporters, PIN1 and PIN6, are found near the grain yield QTL at position ~ 58 Mb on sorghum chromosome 4 (Fig. 3). A related PIN protein in maize is found near another QTL for tolerance to low-P conditions in maize, *cQTL5-5* (Additional file 6). *PIN* genes that encode auxin transporters have been implicated in root architecture changes involving lateral roots under low-P in wheat [46] and may play a significant role in sorghum and maize P efficiency. On chromosome 6, a sorghum homolog of the Al tolerance gene, *ALMT1*, which encodes a root malate efflux transporter and has been recently reported to modulate root growth in response to low-P [30], is found at position ~ 44 Mb, thus near the grain yield QTL at position 42.5 Mb (Fig. 3 and Additional file 4). In maize, the consensus QTL, *cQTL10-1* [42], is also found near a maize homolog of *ALMT1*, suggesting a role for *ALMT1* on P efficiency in both maize and sorghum. As with *SbMATE*, it is also possible that root malate release via *ALMT1* is involved in solubilizing P that is fixed on the surface of Fe and Al oxide minerals in the soil, making them bioavailable for root uptake.

Conclusions

Phosphorus acquisition efficiency was the major component of P efficiency for sorghum cultivated under low-P availability in the soil and grain yield was highly correlated with both traits. Although our findings emphasize root system morphology as a major target for molecular approaches aimed at developing P efficient sorghum cultivars, other distinct mechanisms may also play a

significant role in sorghum performance on low-P soils via enhanced P acquisition. The molecular determinants of such mechanisms, along with *SbPSTOL1* genes, should power novel, gene-based molecular breeding strategies to enhance food security in tropical regions with low-P availability.

Methods

Genetic material

A population composed of 396 recombinant inbred lines (RILs, $F_{10:11}$), derived from a cross between the sorghum lines, BR007 and SC283, was developed by single-seed descent [47] at Embrapa Maize and Sorghum (Sete Lagoas - MG, Brazil). Both BR007 (Redbina-type) and SC283 (sorghum converted guinea) were introduced into the Embrapa breeding program in 1972 from the Purdue Breeding Program (West Lafayette - IN, US). BR007 is Al sensitive whereas SC283 is highly tolerant to Al toxicity [33]. Previous studies indicated that, while SC283 has higher grain yield in a soil with low-P availability compared to BR007, the grain yield increase in BR007 in response to adequate P supply is in turn higher than in SC283 [48].

Phenotyping for low-P in field conditions

Four field experiments were conducted at the experimental station of Embrapa Maize and Sorghum in Sete Lagoas, State of Minas Gerais, Brazil, during the summer season of 2012–2013. The experimental site is a clay and highly weathered tropical soil, with low fertility in natural conditions, low pH, Al toxicity and low-P. Soil P (Mehlich 1) varied from 1 to 6 ppm between 0 and 20 cm of soil depth, and from 1 to 4 ppm at the sub-superficial soil layer (20–40 cm). The minimum and maximum content of available P in the soil (Psoil) was 5.88 kg ha^{-1} and 19.79 kg ha^{-1} .

Each experiment was arranged as a 12×10 alpha lattice design, with three complete replicates and ten incomplete blocks per replicate. Each block contained 12 plots, within which ten RILs (regular treatments) and the two parents (common checks) were allocated. Each plot consisted of a three-meter row, with 0.45 m between rows and 8 plants m^{-2} . Fertilization consisted of 150 kg ha^{-1} of 20–00–20 (NPK) at sowing and 200 kg ha^{-1} of urea applied 30 days after sowing.

Grain yield (Gy, kg ha^{-1}), flowering time (FT, days), plant height (PH, cm), phosphorus content in the plant (leaves and stems - Pp, kg ha^{-1}) and phosphorus content in the grain (Pg, kg ha^{-1}) were evaluated. For P measurements, samples of plant tissues and grains were collected in each plot, weighted and then dried at 65°C to constant weight. Dry plant tissues and grains were then weighted, grounded and homogenized. Twenty gram

subsamples were used to determine P concentration and total P content (Pt), using inductively-coupled argon plasma emission spectrometry.

The phosphorus efficiency indexes were calculated according to the methodology proposed by Moll et al. [32], where: 1) phosphorus use efficiency (PUE) is equal to the product between phosphorus acquisition efficiency (PAE) and phosphorus internal utilization efficiency (PUTIL); 2) PAE is the total phosphorus content (Pt = Pp, P content in the plant + Pg, P content in the grain) divided by P content available in the soil; 3) PUTIL is Gy divided by Pt.

Root system phenotyping in low-P conditions

Root morphology traits were assessed in nutrient solution as described by de Sousa et al. [49] and Hufnagel et al. [22], using a randomized block design with three replicates. Seeds were surface-sterilized using sodium hypochlorite (5%), washed with distilled water and placed in moistened paper rolls. After 4 days, uniform seedlings were transferred to moistened blotting papers and placed into paper pouches ($24 \times 33 \times 0.02 \text{ cm}$) as described by Hund et al. [50].

Each experimental unit consisted of one pouch, with three plants per pouch, whose bottom (3 cm) was immersed in containers filled with 5 l of the nutrient solution described in [51], with pH 5.65 and a P concentration of $2.5 \mu\text{M}$. The containers were kept in a growth chamber with 27°C day and 20°C night temperatures and a 12-h photoperiod, under continuous aeration for 13 days.

After 13 days, root images were acquired using a digital camera Nikon D300S SLR. Images were then analyzed using both the RootReader2D (<http://www.plantmineralnutrition.net/software/rootreader2d/>) and WinRhizo (<http://www.regent.qc.ca/>) software. The following traits were measured: root length (RL - cm); root diameter (RD - mm); total root surface area (SA - cm^2); surface area of very fine roots between 0 and 1 mm in diameter (SA1 - cm^2); surface area of fine roots between 1 and 2 mm in diameter (SA2 - cm^2); surface area of thicker roots between 2 and 4.5 mm in diameter (SA3 - cm^2); root volume (RV - cm^3) and volume of fine roots between 1 and 2 mm in diameter (V2 - cm^3). Shoot dry matter (SDM) and root dry matter (RDM), phosphorus content in the shoot (Ps) and phosphorus content in the root (Pr) (in grams) were also measured.

Phenotypic analyses

Traits assessed in field and hydroponic experiments were analyzed using mixed models. For field experiments, the following model was used:

$$y_{ijkl} = \mu + E_j + R_{k\delta_{j\delta}} + B_{l(kj)} + G_i + \epsilon_{ijkl}$$

y_{ijkl} is the phenotypic value of individual i in the block l of the k^{th} replicate, within the experiment j ; μ is the overall mean; and G_i is the genetic effect of individual i , which can be defined as:

$$G_i = g_i + t_i + n_g + n_c$$

g_i is the random effect of RIL i , n_g is the total number of RILs; t_i is the fixed effect of check i ; and n_c is the total number of checks; E_j is the fixed effect of the j^{th} experiment ($j = 1, \dots, 4$); $R_{k(j)}$ is the fixed effect of replicate k ($k = 1, \dots, 3$) in experiment j ; $B_{l(kj)}$ is the random effect of block l ($l = 1, \dots, 10$) in the replicate k , within the experiment j ; and $\epsilon = (\epsilon_{1111}, \epsilon_{2111}, \dots, \epsilon_{IJKL})'$ is a $N_{obs} \times 1$ residual random vector assumed to be normally distributed with mean zero and variance σ^2 , in which N_{obs} is the total number of observations.

The model used for analyzing the hydroponic experiments was:

$$y_{ij} = \mu + B_j + g_i + \epsilon_{ij}$$

where y_{ij} is the phenotypic value of the RIL i ($i = 1, \dots,$

n_g) in the block j ; μ is the overall mean; g_i is the random genetic effect of RIL i ; B_j is the fixed effect of block j ($j = 1, \dots, 3$); and $\epsilon = (\epsilon_{11}, \epsilon_{21}, \dots, \epsilon_{IJ})'$ is a $N_{obs} \times 1$ residual random vector assumed to be normally distributed with mean zero and variance σ^2 . Fixed and random effects were tested using the Wald statistics [52] and the likelihood ratio test (LRT, [53]) respectively, considering a 5% significance level (α).

For both statistical models, the genetic effect of RIL was first taken as random for estimating the genetic variance component (σ^2) via restricted maximum likelihood (REML), and the heritability coefficient of each trait. The effect of RIL was then considered as fixed for estimating the adjusted means using best linear unbiased estimators (BLUEs). All the mixed models analyses were performed using the GenStat software (v.17.1.0) [54].

Trait heritabilities were estimated as proposed by Cullis et al. [55], called generalized heritabilities, using:

$$h^2 = 1 - \frac{vBLUP}{2\sigma_g^2}$$

where $vBLUP$ is the average variance of the difference between two best linear unbiased predictions (BLUPs). Person's correlation coefficients [56] were estimated based on the adjusted means of genotypes for traits assessed in the field and in the hydroponic experiments, using the

SNP markers

Genomic DNA was isolated from approximately 500 mg of leaf tissue (eight plants per accession, i.e. RILs and their parents) as described by Saghai-Marooof et al. [59]. DNA samples were genotyped by sequencing according to Elshire et al. [60]. Reads were aligned to the version 1.4 of sorghum reference genome using Burrows-Wheeler

performed using the GBS pipeline [62] implemented in the TASSEL software [63]. Missing genotypes were

imputed using the NPUTE software [64]. Then, SNP data were filtered for 40% of minor allele frequency (MAF).

QTL mapping

The final set of traits used for multi-trait QTL mapping was comprised of grain yield (Gy), surface area of fine roots in the 1–2 mm diameter class (SA2) and root diameter (RD). Multi-trait QTL mapping analysis was performed according to the procedures described in Silva et al. [65] implemented in R. For that, a multi-locus QTL mapping procedure was considered, using the Haley & Knott regression [66] and the following linear model:

$$y_{it} = \mu_t + a_{tr}x_{ir} + \epsilon_{it}$$

package *Hmrc* [57] in R [58] where y_{it} is the adjusted mean of RIL i ($i = 1, \dots, n_g$) for trait t ($t = 1, \dots, T$); μ_t is the intercept for each trait; a_{tr} is the r^{th} QTL main effect on trait t ; x_{ir} represents the genotype of RIL i for the SNP marker r ($r = 1, \dots, n_M$), being n_M the total number of markers; x_{ir} assumed values equal to 0 or 2 for RILs with homozygous genotypes for the allele donated by BR007B or SC283, respectively; and $\epsilon_i = (\epsilon_{1i}, \epsilon_{2i}, \dots, \epsilon_{Ti})'$ is a $T \times 1$ random vector assumed to be independent and identically distributed according to a multivariate normal distribution with mean vector zero and positive definite symmetric variance-covariance matrix Σ_ϵ , i.e. $\epsilon_i \sim MVN(0, \Sigma_\epsilon)$. Single-trait QTL mapping analyses were performed for each trait, using the above model ($t = 1$ gives an univariate regression model).

Multiple QTL models were built based on a F-selection procedure, testing the significance of a putative QTL main effect at each SNP position along the genome. Significance of QTLs main effects were tested using the Score Statistic [67], considering a 10% significance level (α). According to simulations performed by Silva et al. [65], this significance level maximized the QTL detection power and kept the false discovery rate (i.e. the proportion of spurious QTLs) within an acceptable level.

QTL positions were refined after the inclusion of every new QTL in the model, until no more significant QTL main effects were found. Finally, non-significant QTL effects

Quantitative analysis of *SbPSTOL1* gene expression

Sorghum seedlings were grown in a modified Magnavaca nutrient solution [51] containing a low-P concentration (2.5 μ M P), as described in the section *Root system phenotyping in low-P conditions*. The experiment was set up in randomized block design with three replicates and three seedlings per experimental unit (paper pouch), giving a total of nine biological replicates per genotype. After 13 days in nutrient solution, the expression profiles of the *SbPSTOL1*-like genes (*Sb03g006765*, *Sb03g031690*, and *Sb07g002840*) were assessed in the roots of the RIL parents, BR007 and SC283. Total RNA was isolated from bulked root tissues (nine roots per bulk), using the SV Total RNA Isolation System kit (Promega Corporation, Madison, WI, USA), according to the manufacturer's instructions. Total RNA (1 μ g) was used for cDNA synthesis using the High Capacity cDNA R Transcription kit (Applied Biosystems, Foster City, CA, USA). Transcripts were quantified by quantitative real-time PCR (qPCR-RT), using SYBR Green technology with the ABI Prism 7500 Fast System (Applied Biosystems, Foster City, CA, USA).

Transcript relative quantification was performed with 20 ng cDNA samples and 0.02 ng for the endogenous constitutive control (18 s rRNA). Primers were designed for *SbPSTOL1* and 18 s rRNA sorghum genes using the PrimerQuest tool (<https://www.idtdna.com/PrimerQuest/>) (Additional file 7). Calculation of relative gene expressions were performed using the $2^{-\Delta\Delta CT}$ method [69], with three technical replicates.

Additional files

Additional file 1: Descriptive statistics and variance components for traits assessed in low-P conditions. (field and hydroponics). (DOCX 27 kb)

Additional file 2: Correlations and *p*-values among all traits assessed in low-P conditions. (field and hydroponics). (DOCX 30 kb)

Additional file 3: Single-trait QTL mapping profiles for grain yield (Gy), phosphorus use efficiency (PUE), phosphorus acquisition efficiency (PAE) and phosphorus internal utilization efficiency (PUTIL). Blue, light blue, pink and yellow inverted triangles depict the positions of QTLs for Gy, PUE, PAE and PUTIL respectively. (TIF 127 kb)

Additional file 4: Detailed information and confidence interval of the QTLs detected by single-trait QTL mapping. (Sheets "Single-trait values" and "Confidence Interval"). (XLSX 33 kb)

Additional file 5: Detailed information of the QTLs detected by multi-trait QTL mapping. (DOCX 24 kb)

Additional file 6: Synteny between sorghum, Arabidopsis and maize for the main QTLs detected in this study. (XLSX 55 kb)

Additional file 7: Primers used for qPCR-RT assays. (DOCX 14 kb)

Abbreviations

Al: Aluminum; *ALMT1*: Aluminum-activated malate transporter in wheat; *ALS3*: Aluminum sensitive 3 (ABC-like transporter); *Alt_{5B}*: Aluminum tolerance locus in *Sorghum bicolor*; *AtSTOP1*: Sensitive to proton rhizotoxicity in Arabidopsis; BLUE: Best linear unbiased estimation; BLUP: Best linear unbiased predictions; BWA: Burrows-wheeler aligner program; DM: Dry matter; E2: Ubiquitin-conjugating enzyme; FT: Flowering time; GBS: Genotyping by sequencing; Gy: Grain yield; LRT: Likelihood rate test; MAF: Minimum allele frequency; Mb: Mega base pairs; *OsPSTOL1*: Phosphorus starvation tolerance 1 in rice; P: Phosphorus; PAE: Phosphorus use efficiency; Pg: Phosphorus content in grain; PH: Plant height; PHO2: Phosphate 2; Pp: Phosphorus content in the plant (leaves and stem); Pr: Phosphorus content in root tissues; Ps: Phosphorus content in the shoot; Psoil: Phosphorus content available in the soil; Pt: Total phosphorus content; PUE: Phosphorus use efficiency; PUTIL: Phosphorus internal utilization efficiency; QTL: Quantitative trait locus; r: Correlation coefficient; RD: Root diameter; RDM: Root dry matter; REML: Restricted maximum likelihood; RIL: Recombinant inbred line; RL: Root length; RV: Root volume; SA: Total root surface area; SA1: Surface area of very fine roots between 0 and 1 mm in diameter; SA2: Surface area of fine roots between 1 and 2 mm in diameter; SA3: Surface area of thicker roots between 2 and 4.5 mm in diameter; *SbMATE*: Multidrug and toxic compound extrusion in *Sorghum bicolor*; *SbPSTOL1*: Phosphorus starvation tolerance 1 in *Sorghum bicolor*; SDM: Shoot dry matter; SNP: Single nucleotide polymorphism; SRL: Specific root length; UBC24: Ubiquitin-conjugating 24 enzyme; V2: Volume of fine roots between 1 and 2 mm in diameter

Acknowledgements

We thank all staff and trainees of Embrapa Maize and Sorghum that indirectly collaborated in the execution of this work.

Funding

We acknowledge grants from the CGIAR Generation Challenge Program, the Embrapa Macroprogram, the Fundação de Amparo a Pesquisa do Estado de Minas Gerais (FAPEMIG) and the National Council for Scientific and Technological Development (CNPq). The funding body had no role in the design of the study and collection, analysis, and interpretation of data and in writing the manuscript.

Availability of data and materials

The datasets used and/or analyzed during the current study are available from the corresponding author on reasonable request.

Authors' contributions

Conceived, supervised the study, contributed to manuscript writing and revision: JVM. Performed experiments, analyzed the data and contributed to manuscript writing: KCB. Contributed to sorghum phenotyping: CBM, SMS, GCJ, RES. Designed the statistical framework, contributed to data analysis and interpretation: MMP, LCS. Conducted expression profiling: LSM and BAB. Synteny analyses and manuscript revision: LVK and CTG. Revised the paper: PCSC. All authors read and approved the final manuscript.

Ethics approval and consent to participate

Not applicable.

Consent for publication

Not applicable.

Competing interests

The authors declare that they have no competing interests.

Publisher's Note

Springer Nature remains neutral with regard to jurisdictional claims in published maps and institutional affiliations.

Author details

¹Embrapa Milho e Sorgo, Rodovia MG 424, km 65, Caixa Postal 151, Sete Lagoas, MG 35701-970, Brazil. ²Universidade Federal de Viçosa, Avenida Peter Henry Rolfs, s/n, Viçosa, MG 36570-900, Brazil. ³Departamento de Biologia Geral, Universidade Federal de Minas Gerais, Avenida Presidente Antônio Carlos, 6627, Belo Horizonte, MG 31270-901, Brazil. ⁴Global Institute for Food

Security, University of Saskatchewan, Saskatoon, SK S7N 4J8, Canada. ⁵Present Address: Helix Sementes, Rua Arnaldo Luiz de Oliveira, 75, Setor D, Bela Vista, Patos de Minas, MG 38703-240, Brazil.

Received: 22 October 2018 Accepted: 19 February 2019

Published online: 28 February 2019

References

- De Wet MJM, Harlan JR. The origin and domestication of *Sorghum bicolor*. Econ Bot. 1971;25:128–35 Springer.
- Weltzien E, Rattunde H, Clerget B, Siart S, Toure A, Sagnard F. Sorghum diversity and adaptation to drought in West Africa. In: Jarvis D, Mar I, Sears L, editors. Enhancing use Crop Genet Divers to Manag abiotic Stress Agric Prod Syst; 2006. p. 31–8.
- Doumbia MD, Hossner LR, Onken AB. Variablesorghum growth in acid soils of subhumid west africa. Arid Soil Res Rehabil. 1993;7:335–46.
- Doumbia MD, Hossner LR, Onken AB. Sorghum growth in acid soils of West Africa: variations in soil chemical properties. Arid Soil Res Rehabil. 1998;12:179–90.
- Leiser WL, Rattunde H, Weltzien E, Cisse N, Abdou M, Diallo A, et al. Two in one sweep: aluminum tolerance and grain yield in P-limited soils are associated to the same genomic region in west African Sorghum. BMC Plant Biol. 2014;14:206.
- Shaw JN. Iron and aluminum oxide characterization for highly-weathered Alabama ultisols. Commun Soil Sci Plant Anal. 2001;32:49–64.
- Kochian LV. Cellular mechanisms of aluminum toxicity and resistance in plants. Annu Rev Plant Biol. 1995;46:237–60.
- Marschner H. Mineral nutrition of higher plants. 2nd ed; 1995.
- Vance CP, Uhde-Stone C, Allan DL. Phosphorus acquisition and use: critical adaptations by plants for securing a nonrenewable resource. New Phytol. 2003;157:423–47.
- Lynch JP. Root phenes for enhanced soil exploration and phosphorus acquisition: tools for future crops. Plant Physiol. 2011;156:1041–9.
- Hammond JP, Broadley MR, White PJ. Genetic responses to phosphorus deficiency. Ann Bot. 2004;94:323–32.
- Magalhaes JV, Liu J, Guimarães CT, Lana UGP, Alves VMC, Wang Y-H, et al. A gene in the multidrug and toxic compound extrusion (MATE) family confers aluminum tolerance in sorghum. Nat Genet. 2007;39:1156–61.
- Carvalho G, Schaffert RE, Malosetti M, Viana JHM, Menezes CB, Silva LA, et al. Back to acid soil fields: The citrate transporter SbMATE is a major asset for sustainable grain yield for sorghum cultivated on acid soils. G3; Genes/Genomes/Genetics. 2016;6:475–84.
- Drouillon M, Merckx R. The role of citric acid as a phosphorus mobilization mechanism in highly P-fixing soils. Gayana Bot. 2003;60:55–62.
- Magalhaes JV, Piñeros MA, Maciel LS, Kochian LV. Emerging pleiotropic mechanisms underlying aluminum resistance and phosphorus acquisition on acidic soils. Front Plant Sci. Frontiers. 2018;9:1–12.
- Parentoni SN, De Souza Júnior CL. Phosphorus acquisition and internal utilization efficiency in tropical maize genotypes. Pesqui Agropecu Bras. 2008;43:893–901.
- López-Arredondo DL, Leyva-González MA, González-Morales SI, López-Bucio J, Herrera-Estrella L. Phosphate nutrition: improving low-phosphate tolerance in crops. Annu Rev Plant Biol. 2014;65:95–123.
- Mendes FF, Guimarães LJM, Souza JC, Guimarães PEO, Magalhaes JV, Garcia AAF, et al. Genetic architecture of phosphorus use efficiency in tropical maize cultivated in a low-P soil. Crop Sci. 2014;54:1530–8.
- Magalhaes JV, de Sousa SM, Guimaraes CT, Kochian LV. Chapter 7 - The role of root morphology and architecture in phosphorus acquisition: physiological, genetic, and molecular basis. In: Plant Macronutr Use Effic. London: Elsevier Inc; 2017. p.123–47.
- Ho MD, Rosas JC, Brown KM, Lynch JP. Root architectural tradeoffs for water and phosphorus acquisition. Funct Plant Biol. 2005;32:737–48.
- Gamuyao R, Chin JH, Pariasca-Tanaka J, Pesaresi P, Catausan S, Dalid C, et al. The protein kinase Pstol1 from traditional rice confers tolerance of phosphorus deficiency. Nature. 2012;488:535–9 Nature Publishing Group.
- Hufnagel B, de Sousa SM, Assis L, Guimaraes CT, Leiser W, Azevedo GC, et al. Duplicate and conquer: multiple homologs of PHOSPHORUS-STARVATION TOLERANCE1 enhance phosphorus acquisition and sorghum performance on low-phosphorus soils. Plant Physiol. 2014;166:659–77.
- Sasaki T, Yamamoto Y, Ezaki B, Katsuhara M, Ahn SJ, Ryan PR, et al. A wheat gene encoding an aluminum-activated malate transporter. Plant J. 2004;37:645–53.
- Iuchi S, Koyama H, Iuchi A, Kobayashi Y, Kitabayashi S, Kobayashi Y, et al. Zinc finger protein STOP1 is critical for proton tolerance in Arabidopsis and coregulates a key gene in aluminum tolerance. Proc Natl Acad Sci U S A. 2007;104:9900–5.
- Larsen PB, Tai C, Kochian LV, Howell SH. Arabidopsis mutants with increased sensitivity to aluminum. Plant Physiol. 1996;110:743–51.
- Larsen PB, Geisler MJB, Jones CA, Williams KM, Cancel JD. ALS3 encodes a phloem-localized ABC transporter-like protein that is required for aluminum tolerance in Arabidopsis. Plant J. 2005;41:353–63.
- Belal R, Tang R, Li Y, Mabrouk Y, Badr E, Luan S. An ABC transporter complex encoded by aluminum sensitive 3 and NAP3 is required for phosphate deficiency responses in Arabidopsis. Biochem Biophys Res Commun. 2015;463:18–23 Elsevier Ltd.
- Dong J, Piñeros MA, Li X, Yang H, Liu Y, Murphy AS, et al. An Arabidopsis ABC transporter mediates phosphate deficiency-induced remodeling of root architecture by modulating iron homeostasis in roots. Mol Plant. 2017;10:244–59.
- Balzergue C, Dartevielle T, Godon C, Laugier E, Meisrimler C, Teulon JM, et al. Low phosphate activates STOP1-ALMT1 to rapidly inhibit root cell elongation. Nat Commun. 2017;8:1–16.
- Mora-Macías J, Ojeda-Rivera JO, Gutiérrez-Alanís D, Yong-Villalobos L, Oropeza-Aburto A, Raya-González J, et al. Malate-dependent Fe accumulation is a critical checkpoint in the root developmental response to low phosphate. Proc Natl Acad Sci. 2017;114:E3563–72.
- Müller J, Toev T, Heisters M, Teller J, Moore KL, Hause G, et al. Iron-dependent callose deposition adjusts root meristem maintenance to phosphate availability. Dev Cell. 2015;33:216–30.
- Moll RH, Kamprath EJ, Jackson WA. Analysis and interpretation of factors which contribute to efficiency of nitrogen utilization. Agron Journal. 1982; 74:562–4.
- Magalhaes JV, Garvin DF, Wang Y, Sorrells ME, Klein PE, Schaffert RE, et al. Comparative mapping of a major aluminum tolerance gene in sorghum and other species in the Poaceae. Genetics. 2004;167:1905–14.
- De Wet MJM. Special paper: systematics and evolution of sorghum sect. Sorghum (Gramineae). Am J Bot. 1978;65:477–84 Wiley Online Library.
- Leiser WL, Rattunde HF, Piepho H-P, Weltzien E, Diallo A, Melchinger AE, et al. Selection strategy for sorghum targeting phosphorus-limited environments in West Africa: analysis of multi-environment experiments. Crop Sci. 2012;52:2517–27 The Crop Science Society of America, Inc.
- Uga Y, Assaranurak I, Kitomi Y, Larson BG, Craft EJ, Shaff JE, et al. Genomic regions responsible for seminal and crown root lengths identified by 2D & 3D root system image analysis. BMC Genomics. 2018;19:273 BioMed Central.
- Zhu J, Lynch JP. The contribution of lateral rooting to phosphorus acquisition efficiency in maize (*Zea mays*) seedlings. Funct Plant Biol CSIRO. 2004;31:949–58.
- Wu Q, Pagès L, Wu J. Relationships between root diameter, root length and root branching along lateral roots in adult, field-grown maize. Ann Bot. 2016;117:379–90 Oxford University Press.
- Eissenstat DM. Costs and benefits of constructing roots of small diameter. J Plant Nutr. 1992;15:763–82 Taylor & Francis.
- Gong X, McDonald G. QTL mapping of root traits in phosphorus-deficient soils reveals important genomic regions for improving NDVI and grain yield in barley. Theor Appl Genet. 2017;130:1885–902 Springer.
- Azevedo GC, Cheavegatti-Gianotto A, Negri BF, Hufnagel B, Silva Lda C, Magalhaes JV, et al. Multiple interval QTL mapping and searching for PSTOL1 homologs associated with root morphology, biomass accumulation and phosphorus content in maize seedlings under low-P. BMC Plant Biol. 2015;15:172.
- Zhang H, Uddin MS, Zou C, Xie C, Xu Y, Li W-X. Meta-analysis and candidate gene mining of low-phosphorus tolerance in maize. J Integr Plant Biol. 2014;56:262–70 Wiley Online Library.
- Sabadin PK, Malosetti M, Boer MP, Tardin FD, Santos FG, Guimarães CT, et al. Studying the genetic basis of drought tolerance in sorghum by managed stress trials and adjustments for phenological and plant height differences. Theor Appl Genet. 2012;124:1389–402.
- Liu T-Y, Huang T-K, Tseng C-Y, Lai Y-S, Lin S-I, Lin W-Y, et al. PHO2-dependent degradation of pho1 modulates phosphate homeostasis in Arabidopsis. Plant Cell. 2012;24:2168–83.
- Du Q, Wang K, Zou C, Xu C, Li W-X. The PILNCR1-miR399 regulatory module is important for low phosphate tolerance in maize. Plant Physiol. Am Soc Plant Biol. 2018;177:1743–53.

46. Talboys PJ, Healey JR, Withers PJA, Jones DL. Phosphate depletion modulates auxin transport in *Triticum aestivum* leading to altered root branching. *J Exp Bot*. 2014;65:5023–32 Oxford University Press UK.
47. Johnson HW, Bernard RL. Soybean genetics and breeding. *Adv Agron*. 1962; 14:149–221.
48. Schaffert RE, Alves VMC, Pitta GVE, Bahia AFC, Santos FG. Genetic variability in sorghum for P efficiency and responsiveness. In: Horst WJ, Schenk MK, Bürkert A, Claassen N, Flessa H, Frommer WB, et al., editors. *Plant Nutr Dev Plant Soil Sci*. Dordrecht: Springer; 2001. p. 72–3.
49. Morais De Sousa S, Clark RT, Mendes FF, Carlos De Oliveira A, Vilaça De Vasconcelos MJ, Parentoni SN, et al. A role for root morphology and related candidate genes in P acquisition efficiency in maize. *Funct Plant Biol*. 2012;39:925–35.
50. Hund A, Trachsel S, Stamp P. Growth of axile and lateral roots of maize: I development of a phenotyping platform. *Plant Soil*. 2009;325:335–49.
51. Magnavaca R, Gardner COE, Clark RB. Inheritance of aluminum tolerance in maize. In: Gabelman WH, Loughman BC, editors. *Genet Asp Plant Miner Nutr Dev Plant Soil Sci*. Dordrecht: Springer; 1987. p. 201–12.
52. Wald A. Tests of statistical hypotheses concerning several parameters when the number of observations is large. *Trans Am Math Soc*. 1943;54:426–82.
53. Neyman J, Pearson ES. On the use and interpretation of certain test criteria for purposes of statistical inference: part I. *Biometrika*. 1928;20A:175–240.
54. VSN International. *GenStat for Windows*. 17th ed. Hemel Hempstead: VSN International; 2014. Available from: GenStat.co.uk
55. Cullis BR, Smith AB, Coombes NE. On the design of early generation variety trials with correlated data. *J Agric Biol Environ Stat*. 2006;11:381–93.
56. Pearson K. Mathematical contributions to the theory of evolution. III. Regression, heredity, and Panmixia. *Philos Trans R Soc London Ser a, Contain Pap a Math or Phys Character*. 1895;187:253–318.
57. Harrell Jr FE. With contributions from Charles Dupont and many others. *Hmisc: Harrell Miscellaneous*. 2015. R package version 3.17–4.
58. Team RC. R: a language and environment for statistical computing. Vienna: R Foundation for Statistical Computing; 2016. Available from: <https://www.r-project.org/>
59. Saghai-Marouf MA, Soliman KM, Jorgensen RA, Allard RW. Ribosomal DNA spacer-length polymorphisms in barley: mendelian inheritance, chromosomal location, and population dynamics. *Proc Natl Acad Sci*. 1984; 81:8014–8.
60. Elshire RJ, Glaubitz JC, Sun Q, Poland JA, Kawamoto K, Buckler ES, et al. A robust, simple genotyping-by-sequencing (GBS) approach for high diversity species. *PLoS One*. 2011;6:1–10.
61. Li H, Durbin R. Fast and accurate short read alignment with burrows--wheeler transform. *Bioinformatics*. 2009;25:1754–60 Oxford University Press.
62. Glaubitz JC, Casstevens TM, Lu F, Harriman J, Elshire RJ, Sun Q, et al. TASSEL-GBS: A high capacity genotyping by sequencing analysis pipeline. *PLoS One*. 2014;9:e90346.
63. Bradbury PJ, Zhang Z, Kroon DE, Casstevens TM, Ramdoss Y, Buckler ES. TASSEL: software for association mapping of complex traits in diverse samples. *Bioinformatics*. 2007;23:2633–5.
64. Roberts A, McMillan L, Wang W, Parker J, Rusyn I, Threadgill D. Inferring missing genotypes in large SNP panels using fast nearest-neighbor searches over sliding windows. *Bioinformatics*. 2007;23:401–7.
65. Silva LDCE, Wang S, Zeng Z-B. Multiple trait multiple interval mapping of quantitative trait loci from inbred line crosses. *BMC Genet*. 2012;13:67.
66. Haley CS, Knott SA. A simple regression method for mapping quantitative trait loci in line crosses using flanking markers. *Heredity (Edinb)*. 1992;69:315–24.
67. Zou F, Fine JP, Hu J, Lin DY. An efficient resampling method for assessing genome-wide statistical significance in mapping quantitative trait loci. *Genetics*. 2004;168:2307–16.
68. Zellner A. An efficient method of estimating seemingly unrelated regressions and tests for aggregation bias. *J Am Stat Assoc*. 1962;57:348–68 Taylor & Francis.
69. Schmittgen TD, Livak KJ. Analyzing real-time PCR data by the comparative CT method. *Nat Protoc*. 2008;3:1101–8.

Ready to submit your research? Choose BMC and benefit from:

- fast, convenient online submission
- thorough peer review by experienced researchers in your field
- rapid publication on acceptance
- support for research data, including large and complex data types
- gold Open Access which fosters wider collaboration and increased citations
- maximum visibility for your research: over 100M website views per year

At BMC, research is always in progress.

Learn more biomedcentral.com/submissions

